«ELECTRICAL ENGINEERING & ELECTROMECHANICS»

SCIENTIFIC & PRACTICAL JOURNAL
Journal was founded in 2002
Founders:
National Technical University «Kharkiv Polytechnic Institute» (Kharkiv, Ukraine)
State Institution «Institute of Technical Problems of Magnetism of the NAS of Ukraine» (Kharkiv, Ukraine)

ISSUE 4/2017

TABLE OF CONTENTS

Editorial office address: Dept. of Electrical Apparatus, NTU «KhPI», Kyrpychova Str., 2, Kharkiv, 61002, Ukraine
phones: +380 57 7076281, +380 67 3594696, **e-mail:** a.m.grechko@gmail.com (**Grechko O.M.)**

ISSN (print) 2074-272X
ISSN (online) 2309-3404

Printed 30.08.2017. Format 60 x 90 ⅛. Paper – offset. Laser printing. Edition 200 copies. Order no.66/172-04-2017.
Printed by Printing house «Madrid Ltd» (11, Maksymilianivska Str., Kharkiv, 61024, Ukraine)

UDC 621.3: 537.8: 910.4 **doi: 10.20998/2074-272X.2017.4.01**

M.I. Baranov

AN ANTHOLOGY OF THE DISTINGUISHED ACHIEVEMENTS IN SCIENCE AND TECHNIQUE. PART 39: NOBEL PRIZE LAUREATES IN PHYSICS FOR 2011-2015

Purpose. Implementation of brief analytical review of the distinguished scientific achievements of the world scientists-physicists, awarded the Nobel Prize on physics for the period 2011-2015. Methodology. Scientific methods of collection, analysis and analytical treatment of scientific and technical information of world level in area of astrophysics, physics of elementary particles, physics of high energies, of modern theoretical and experimental physics. Results. The brief analytical review of the scientific openings and distinguished achievements of scientists-physicists is resulted in area of modern physical and technical problems which were marked the Nobel Prizes on physics for the period 2011-2015. Originality. Systematization is executed with exposition in the short concentrated form of the known scientific and technical materials, devoted opening of acceleration of expansion of Universe, creation of breach technologies of manipulation the quantum systems, theoretical discovery of mechanism of origin of mass of under-atomic particles, invention of effective power sources of light − blue light-emitting diodes and opening of neutrino oscillations. Practical value. Popularization and deepening of scientific and technical knowledges for students, engineers and technical specialists and research workers in area of modern theoretical and experimental physics, extending their scientific range of interests and cooperation in further development of scientific and technical progress in human society. References 17, figures 14.

Key words: **modern physics, distinguished achievements, speed-up expansion of Universe, technologies of manipulation of the quantum systems, mechanism of origin of the masses of under-atomic particles, energy saving sources of light, blue light-emitting diodes, neutrino oscillations**..

Приведен краткий аналитический обзор выдающихся научных достижений ученых мира, отмеченных Нобелевской премией по физике за период 2011-2015 гг. В число таких достижений вошли открытие ускорения расширения Вселенной, создание прорывных технологий манипулирования квантовыми системами, теоретическое обнаружение механизма происхождения массы субатомных частиц, изобретение энергоэффективных источников света − синих светодиодов и открытие нейтринных осцилляций. Библ. 17, рис. 14.

Ключевые слова: **современная физика, достижения, ускоренное расширение Вселенной, технологии манипулирования квантовыми системами, механизм происхождения массы субатомных частиц, энергосберегающие источники света, синие светодиоды, нейтринные осцилляции.**

Introduction. Physics in the will of the famous Swedish engineer-inventor and businessman Alfred Nobel (1833-1896) was mentioned in the first of five fields of scientific knowledge and social movements (physics, chemistry, medicine, literature and the struggle for peace between nations), which should In the near future to establish awards for outstanding scientific research, revolutionary inventions, a major contribution to the culture and development of human society [1]. Note that the first Nobel Prize in physics was awarded to the German Wilhelm Roentgen (1845-1923) in 1901 *«for the discovery of X-rays»* [2]. From 1901 to 2011, the Nobel Prize in physics was awarded to 190 scientists around the world. At the same time, 58 times the Prize was awarded to two or three researchers simultaneously (according to the existing position in the authors' team of applicants there should be no more than three scientists) [1]. American John Bardin (1908-1991) has so far been the only scientist awarded in this group of scientists Nobel Prize in Physics twice - in 1956 *(«for the study of semiconductors and the discovery of transistor effect»*) and in 1972 *(«for the development of the theory of superconductivity»*) [2, 3]. Women scientists became Nobel Prize Laureates in physics only twice - the Frenchwoman of Polish descent Maria Sklodowska-Curie (1867-1934) in 1903 (*«for the study of the phenomenon of radioactivity»*) and the American Maria Geppert-Mayer (1906-1972) in 1963 (*«for the creation of a shell model of the nucleus»*) [2].

1. The discovery of the acceleration of the expansion of the Universe. The Laureates of the Nobel Prize for Physics in 2011 were the Americans Saul Perlmutter (Fig. 1), Adam Riess (Fig. 2) and Brian Schmidt (Fig. 3) *«for the discovery of the acceleration of the expansion of the Universe by observing distant supernovas»* [1]. Their fundamental conclusion about the accelerated expansion of the universe with time was obtained in the course of very fine and accurate observations of supernova stars conducted by S. Perlmutter from the University of California (Berkeley, USA), A. Riess from the Space Telescope Science Institute (Baltimore, USA) and B. Schmidt from the famous Mount Stromlo Observatory at the Australian National University [1].

Fig. 1. Prominent American physicist-astronomer Saul Perlmutter, born in 1959, Nobel Prize Laureate in physics for 2011

S. Perlmutter, A. Riess and B. Schmidt carried out their many years astronomical observations using exclusively supernovae of type I*a* located in the distant galaxies of our Universe. For these observations, they used several large telescopes, including a 3.6-meter telescope type NTT (New Technology Telescope) and a 8.2-meter telescope type VLT from the world-famous South American observatory La Silla (ESO, Chile) [1]. Fig. 4 shows a series of photos of the 1995K supernova made by the Laureates on April 3, 1995, using a 3.6-meter NTT telescope [1]. Based on the analysis of such images, they made a scientific discovery, awarded such a high Prize.

Fig. 2. Prominent American physicist-astronomer
Adam G. Riess, born in 1969,
Nobel Prize Laureate in physics for 2011

Fig. 3. Prominent Australian-American physicist-astronomer
Brian P. Schmidt, born in 1967,
Nobel Prize Laureate in physics for 2011

It is believed that the accelerated expansion of the universe is due to the presence of «dark» energy («black holes») in it [1, 4]. The origin of this energy in outer space and its nature for scientists are still deeply mysterious phenomena. In the scientific world, it is common to believe that this discovery, accomplished by astronomical physicists, is one of the few recent truly great scientific discoveries in physics and astronomy [1]. It can have serious worldview significance for mankind. Here we should note that the fundamental discovery made earlier on the basis of astronomical observations by the famous American astronomer Edwin Powell Hubble (1889-1953) about the expansion of the universe remained practically beyond the «field of vision» of the Nobel Committee at the Royal Swedish Academy of Sciences [1]. An interesting fact is that E.P. Hubble once led the movement of numerous scientists for the establishment of the Nobel Prize in astronomy. It should be noted that this movement did not have much success, but it apparently influenced the members of the Nobel Committee in a certain way, who nevertheless made the decision that the world's astronomers could receive the Nobel Prize in physics [1, 2].

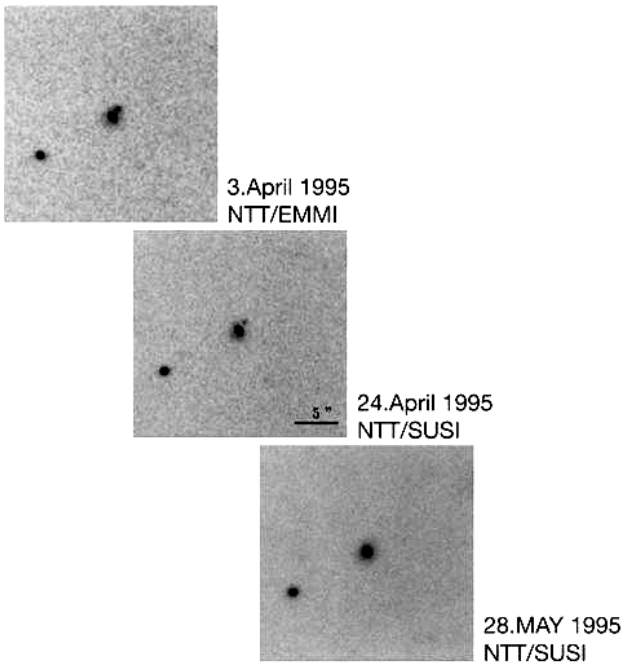

Fig. 4. A series of astronomical images of a very distant supernova in our Universe, which has an international registration number 1995K [1]

Recall that for 111 years of awarding the Nobel Prizes (for the period 1901-2011), astronomical scientists were awarded 11 times this prestigious award [1].

2. The discovery of a method for measuring microparticles and quantum systems without destroying them. Nobel Prize winners in physics in 2012 were Frenchman Serge Haroche (Fig. 5) and American David Wineland (Fig. 6) working in the field of quantum physics, *«for the advanced discoveries of experimental methods that make it possible to measure individual quantum systems»* [5]. S. Haroche and D. Wineland laid the scientific basis for a new generation of experiments in quantum physics that allow «to directly observe individual quantum particles without destroying them.» S. Haroche and D. Vineland carried out their quantum experiments independently of each other. These scientists managed to develop original physic-engineering solutions for manipulating individual quantum microparticles without destroying their quantum-mechanical nature. Many experimental physicists believed that such studies were simply impossible. The American physicist used the method of ion «traps», manipulating ions with the help of

quasiparticles-photons (quanta of an electromagnetic field or light that do not have a rest mass [6]). His French counterpart, on the other hand, measured the quanta of light, directing the flow of atoms of matter through a photon «trap» [5].

D. Wineland taught specialists to trap microparticles that carry an electric charge (for example, atoms and ions), and also to monitor and measure their state with the help of light quanta [5].

Fig. 5.Prominent French experimental physicist
Serge Haroche, born in 1944,
Nobel Prize Laureate in physics for 2012

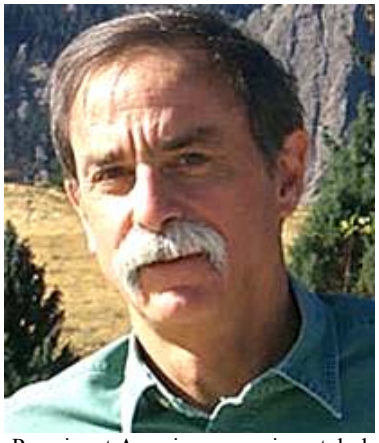

Fig. 6. Prominent American experimental physicist
David J. Wineland, born in 1944,
Nobel Prize Laureate in physics for 2012

S. Haroche developed an opposite scientific approach that allows you to understand the physical wonders of the quantum world. He came up with a way to control and measure the properties of «captured» photons with the help of atoms trapped in the «trap» [5]. In this case, S. Haroche and his colleagues used «Rydberg» atoms in their experiments, which are more than a thousand times larger than ordinary atoms of matter [6]. They sent them to a photon «trap» with a strictly defined rate, causing them to communicate with the microwave photons (quanta of light) present there. Because of this interaction, the quantum energy state of the «Rydberg» atoms themselves, named after the famous Swedish physicist J.R. Rydberg (1854-1919) [2, 7], while changing. Measurement of the state of these atoms occurred at the output of the specified «trap». As a result, physicists received information about photons trapped in the trap, without destroying them. Like everything, at first glance, it's easy! And behind this apparent simplicity lies the many years of painstaking work of many physicists, connected with high-precision measurements at the atomic level. The described method, as it turned out, can be used to calculate the number of photons trapped in the trap. Subsequently, the physics laureates, based on these achievements, have learned to track changes in the quantum state of an individual photon in real time [5, 8]. Thanks to their research, it became possible to create in the future superhigh-precision clocks and superfast high-speed quantum computers. If a quantum computer with a large volume of information qubits is created in the foreseeable future, its computing power is expected to be truly enormous, which will lead to a real information and technological breakthrough in the world.

3. Theoretical detection of the mechanism of origin of the mass of subatomic particles. The Nobel Prize in physics for 2013 was awarded to two theoretical physicists, the Belgian Francois Englert (Fig. 7) and the British Peter Higgs (Fig. 8) [9].

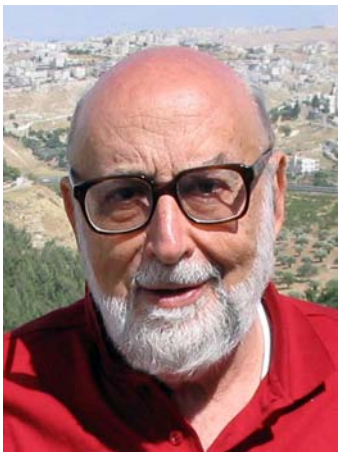

Fig. 7. Prominent Belgian theoretical physicist
Francois Englert, born in 1932,
Nobel Prize Laureate in physics for 2013

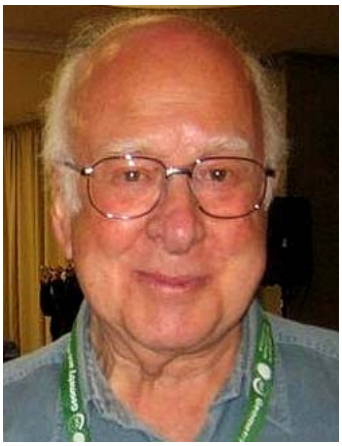

Fig. 8. Prominent British theoretical physicist
Peter Higgs, born in 1929,
Nobel Prize Laureate in physics for 2013

This Prize F. Engert and P. Higgs were awarded *«for the theoretical detection of the mechanism that helps to understand the origin of the mass of subatomic particles,*

recently confirmed by the discovery of the predicted elementary particle in experiments on the ATLAS and CMS detectors of the Large Hadron Collider at CERN» [9]. It is important to note that these physicists were given this prestigious and highly paid (USD 1.2 million for two [5]) Prize not for the prediction of the «Higgs» boson experimentally discovered in 2012 at the largest accelerating electrophysical installation in the world - Large Hadron Collider (LHC) at the European Center for Nuclear Research (CERN), located near Geneva (Switzerland) [3], but for the very «Higgs» mechanism, whose «echo» is the «Higgs» boson. The history of constructing theories of weak and strong interactions of microparticles in the field of elementary particle physics and high-energy physics is quite complex, requires special consideration and is not particularly interesting for us now. Undoubtedly, it is interesting in terms of the scientific priority for not one dozen theoretical physicists who have put their heads and hands on the creation of such theories and the development of a «Higgs» mechanism (for example, R. Braut, Ch. Yang, R. Mills, G. Guralnik, K. Hagen, T. Kibble and others) [9].

The role of the boson, first mentioned explicitly (in the form of a new massive spinless particle) in the theoretical work of P. Higgs (1964), as a convenient «echo» for the experimental mechanism of interaction in the microworld, was truly realized by physicists only in 1970th years [9]. Here to him (this boson), as well as to the very mechanism of interaction of elementary particles for ever, and a convenient and brief, but not quite fair epithet «Higgs». It was after the theory of electroweak interactions was constructed that relied, among other things, on this mechanism, and also after it was shown that this theory is renormalizable (self-consistent and suitable for calculations) and there arose a mass interest among physicists towards properties and to Search for the Higgs boson [9].

Theoretical physicists began to calculate the processes of birth and decay of this boson, and experimental physicists began to search for it in nuclear reaction products at all the largest colliders in the world (for example, in Europe at the electron-positron LEP accelerator with energy up to 104 GeV at CERN and in the USA at a giant proton-antiproton accelerator «Tevatron» with an energy of up to 1 TeV at the E. Fermi National Laboratory for Nuclear Research [3]). There were years of observations, and no one could find the required boson. The overwhelming majority of the world's leading physicists based on accumulated scientific data by the beginning of the 21st century convinced themselves that the Higgs boson should exist. They lacked the final touch - the direct discovery of the «Higgs» boson in the experiment. And now, at the super-powerful proton collider LHC at CERN, actually launched in 2009, the Higgs boson in 2012 was experimentally discovered. This important scientific event happened almost 50 years after the theoretical discovery of this elementary particle [9].

What is the essence of the «Higgs» mechanism and why does the «Higgs» boson answer the microcosm? According to [9], the «Higgs» mechanism for relativistic theories of the interaction of elementary particles is based on the idea that when a massless scalar particle «contacts» a massless carrier of interaction, a carrier particle with mass (some unknown massive boson) is born. To approach historical truth in the issue of the birth in physics of elementary particles of this idea, formulated by P. Higgs only in 1964, we note that in 1963 prominent American physicist, Nobel Prize Laureate in physics for 1936 («*for the discovery in cosmic rays of the positron»* [2]) Karl Anderson (1905-1991), published a similar idea with reference to the nonrelativistic theory of the interaction of microparticles [9]. Therefore, the author of the above-mentioned scientific idea, which later became the basis of the «Higgs» mechanism of particle interaction, probably should be considered the US physicist K. Anderson.

As for the possible liability for the inexperienced reader of the Higgs boson for the mass of all the particles in our Universe, it is immediately necessary to say unambiguously that this boson does not give anybody and nothing in nature [9]. It turns out that the mass of particles is given by a «Higgs» field. The «Higgs» boson is only a microscopic «ripple» and a kind of energy perturbation of this «Higgs» field [9]. In addition, the Higgs field gives mass only to electrons, muons and some other heavy particles [6, 9]. The mass of protons and neutrons that make up the nuclei of all chemical elements from the periodic system of elements of D.I. Mendeleyev [3, 6] and the mass numbers A determining them and, correspondingly, up to 99 %, the mass of any substance, determine completely different physical mechanisms [9]. In this connection, the «Higgs» field corresponds approximately to 1 % of the mass of the surrounding matter [9]. The «black holes» present in space, as well as the undiscovered particles of «dark» matter [4] and, possibly, neutrinos also receive their mass due to other physical sources [9]. At present, in physics of elementary particles on the universal level of communication between scientists, it is considered that the «Higgs» boson is nothing, and the «Higgs» field is everything [9]. It is not yet possible to obtain and investigate this field without the boson in question. Therefore, the «Higgs» boson should help mankind to know the properties and origin of the «Higgs» field. And for this, numerous experiments are required at the Large Hadron Collider LHC, accompanied by the birth and decay of the Higgs boson. Statistical processing of the results obtained in these processes should «shed» light on its nature and the nature of the «Higgs» field. At present, physicists believe that the «Higgs» field does not generate gravity associated with the total energy of the physical body. The «Higgs» field can translate some of the energy of the physical body into rest energy (in its mass). However, it does not influence the gravitational interaction of bodies [9].

4. The invention of blue LEDs – energy-saving light sources. In 2014, three Japanese experimental physicists, Isamu Akasaki (Fig. 9), Hiroshi Amano (Fig. 10) and Shuji Nakamura (Fig. 11) received the Nobel Prize in physics *«for the creation of a new energy efficient and environmentally friendly light source - blue light-emitting diodes"* [10-13]. Note that before 1990, world manufacturers of LEDs could only produce red, yellow and green diodes. It is known that only a combination of

blue, green and red colors can give a pure white color. Therefore, the current problem in the physics and technology of semiconductors for the world's leading manufacturers of LED products was the one that was associated with the invention of light-emitting diodes giving a bright blue color [10].

Fig. 9. Prominent Japanese experimental physicist Isamu Akasaki, born in 1929, Nobel Prize Laureate in physics for 2014

Fig. 10. Prominent Japanese experimental physicist Hiroshi Amano, born in 1960, Nobel Prize Laureate in physics for 2014

Fig. 11. Prominent Japanese experimental physicist Shuji Nakamura, born in 1954, Nobel Prize Laureate in physics for 2014

Fundamental and applied physical and technical investigations of I. Akasaki, H. Amano and Sh. Nakamura showed that one of the promising semiconductor compounds on the basis of which it is possible to create such light emitters can be gallium nitride GaN [10-13]. In the early 1990s, these Japanese physicists based on GaN gallium nitride created both double-layered and multilayer heterostructures with *p-n* junctions of conductivity that provide the creation and industrial production of blue-light-emitting diodes [10-13]. This scientific and technical event was a major breakthrough in the field of world light technologies.

In 1993, Nichia Chemical Industries Corporation (NCI) (Tokushima, Japan) was the first in the world to start the industrial production of blue LEDs [10]. These LEDs made it possible to manufacture new energy-saving white sources. The invention of I. Akasaki, H. Amano and Sh. Nakamura of blue LEDs, which are necessary for obtaining all shades of light in LED devices, was a real technological revolution for outdoor LED video screens [10].

Sh. Nakamura became famous not only for the invention of blue LEDs of high brightness, but also for the NCI Corporation in 2005 win in a lawsuit to pay him a fee based on the results of the introduction of his patents worth about 9 million USD (the largest Japanese bonus!) [13].

5. Discovery of neutrino oscillations. The Nobel Prize in physics for the year 2015 was awarded to two experimental physicists: Canadian Arthur Bruce McDonald (Fig. 12) and Japanese Takaaki Kajita (Fig. 13) *«for the discovery of neutrino oscillations, which shows that neutrinos have a mass»* [14]. These scientists led the two leading scientific groups SNO (Sudbury Neutrino Observatory, Canada) and Super-Kamiokande (Japan), engaged in the study of the easiest, most mysterious and subtle instrumentation detectors - neutrinos [6, 7]. These particles, which interact extremely weakly with matter, belong to leptons [6]. They arise in the beta decay of atomic nuclei and the decays of elementary particles and are characterized by spin $S_\nu=\pm1/2$ [6, 7]. Their measurements have shown that neutrinos come in three varieties: electronic ν_e, muonic ν_μ and tau-neutrino ν_τ [6, 14].

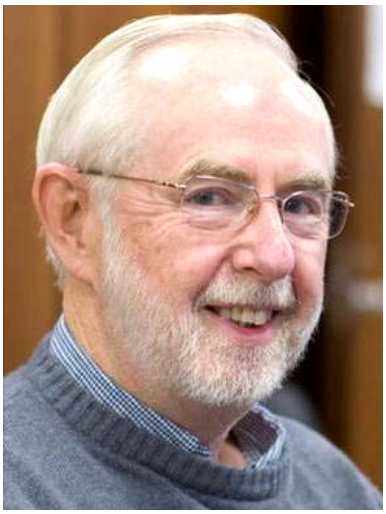

Fig. 12. Prominent Canadian experimental physicist Arthur Bruce McDonald, born in 1943, Nobel Prize Laureate in physics for 2015

Fig. 13. Prominent Japanese experimental physicist Takaaki Kajita, born in 1959, Nobel Prize Laureate in physics for 2015

Moreover, these three kinds of neutrinos are not separated from each other in the microworld and, accordingly, in the macrocosm. They are able to mutually oscillate - spontaneously turn «on the fly» into each other. It was for the proof of the reality of this physical effect (neutrino oscillations) that the Nobel Prize for the past year was awarded to these scientist-physicists. Experimental demonstration of this fact in the field of elementary particle physics and measurement of parameters of neutrino oscillations using cosmic rays contributed to the active development of neutrino physics and the progress in this scientific area of our knowledge. Mutual transformations of neutrinos in the Earth's atmosphere (Fig. 14) are due to their very small masses at distances of a few (tens of) kilometers - a purely quantum effect [14, 15]. Note that the main milestones in the field of neutrino physics prior to the studies we are considering are A.B. McDonald and T. Kajita became [2, 14]: achievements awarded the Nobel Prize in physics for 1988 (*«for the discovery of muon neutrinos»*), for 1995 *(«for the discovery of electronic neutrinos"*) and for 2002 («*for the discovery of solar neutrinos»*). Despite this, before the discovery of A.B. McDonald and T. Kajita, neither neutrino masses nor their oscillation parameters were known to physicists [2].

Fig. 14 schematically shows the processes of «birth» during the passage of high-energy cosmic rays (mainly the proton flux *p*) through the earth's atmosphere of pions (π), muons (μ), electrons (e), muonic ν_μ and electronic ν_e neutrinos, measured Deeply located underground in the mines by detectors (detector) [14]. In the course of the measurements, it was established that after the course of the series shown in Fig. 14 decays to the Earth neutrinos penetrate in the ratio $\nu_\mu/\nu_e \approx 1.2/1$.

Estimated calculation data, performed by theoretical physicists in 1991, indicated that for the reduced ratio of muonic ν_μ and electronic ν_e neutrinos, an equality of the form $\nu_\mu/\nu_e \approx 2/1$ [14-16].

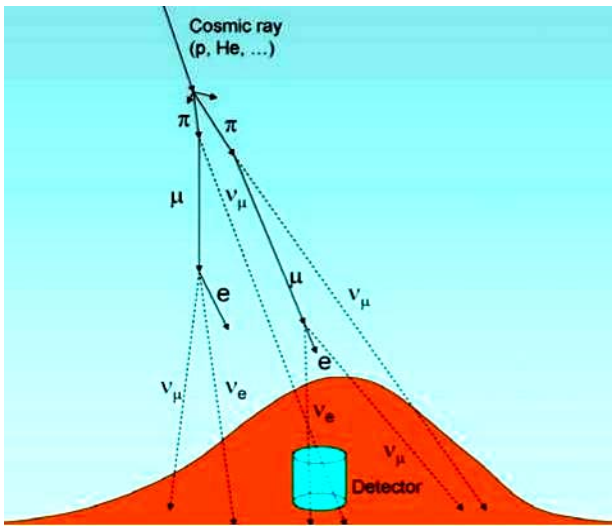

Fig. 14. Schematic representation of the processes of «birth» of muonic and electronic neutrinos in the Earth's atmosphere [12]

The reason for the discrepancies in the ν_μ/ν_e ratio for physicists was at that time unknown and incomprehensible. In 1998, at an international conference on astrophysics, T. Kajita, on behalf of the collaboration of Japanese scientists Super-Kamiokande, a report was made, from the results of which it emerged that in underground neutrino detectors from above (from the nearest Earth's surface) and from below (from a remote opposite terrestrial surface) Numerous quantities of muonic neutrinos ν_μ arrive at the Earth. The neutrino detector Super-Kamiokande was a large underground cistern located in an old mine inside the mountain and filled with ultrapure ordinary water [16]. The internal walls of the detector were completely covered with sensitive photomultipliers, which registered light flashes from nuclear events that flowed inside its working substance-water. The energy cosmic neutrino (with an energy of the order of 100 MeV) of the electron or muonic variety, colliding with the atomic nucleus of water, turns into an electron e or a muon μ that flies forward at a high speed and emits light due to the Vavilov-Cherenkov effect [6, 14-16]. Due to this, the neutrino detector Super-Kamiokande not only detected a neutrino bombarding it, but also determined their sort, energy and direction of arrival to the Earth. Recall that the substance of our planet for neutrinos is almost completely «transparent» [14]. Therefore, on the basis of the experimental data obtained by Japanese physicists, an important conclusion was drawn that on a thousand-kilometer path through the solid crust, semi-liquid mantle and liquid core of the Earth [17], an essential part of the muon neutrinos ν_μ penetrating our planet from the opposite location of the side detectors Turn into other types of neutrinos [14]. Moreover, not in the electronic neutrinos ν_e measured by the detectors, but in the unmetered by them, the tau-neutrino ν_τ. Analogous results in the part of neutrino oscillations (with respect to electronic ν_e, muon ν_μ and tau-neutrino ν_τ coming from the Sun) in the period 2001-2002 were obtained by the collaboration of Canadian scientists SNO with the help of underground neutrino detectors of elementary particles, the capacitances of which were filled with heavy water,

whose nuclei (deuterons) contained a weakly bound system of proton and neutron [14, 15]. At the energy of several neutrons of SNO neutrons acting on the detectors, the deuterons of their heavy water decay into protons and neutrons. By highlighting gamma quanta in neutrino detectors that accompany the capture of deuterium nuclei by the produced neutrons, physicists have judged the nuclear transformations taking place in them. So physicists from the Super-Kamiokande and SNO collaborations obtained irrefutable experimental evidence in favor of the existence of neutrino oscillations [14]. These experimental results also confirmed the validity of the «solar model» developed by theoretical physicists, describing the thermonuclear reactions that are taking place inside our luminaries and the «born» fluxes of solar neutrinos that pervade space and penetrate outer space and the planet Earth.

REFERENCES

1. Available at: http://www.biguniverse.ru/posts/nobelevskaya-premiya-po-fizike-2011 (accessed 12 June 2013). (Rus).

2. Khramov Yu.A. *Istoriia fiziki* [History of Physics]. Kiev, Feniks Publ., 2006. 1176 p. (Rus).

3. Baranov M.I. *Antologiia vydaiushchikhsia dostizhenii v nauke i tekhnike: Monografiia v 2-kh tomakh. Tom 1.* [An anthology of outstanding achievements in science and technology: Monographs in 2 vols. Vol.1]. Kharkov, NTMT Publ., 2011. 311 p. (Rus).

4. Baranov M.I. *Antologiia vydaiushchikhsia dostizhenii v nauke i tekhnike: Monografiia v 2-kh tomakh. Tom 2.* [An anthology of outstanding achievements in science and technology: Monographs in 2 vols. Vol.2]. Kharkov, NTMT Publ., 2013. 333 p. (Rus).

5. Available at: http://news.21.by/other-news/2012/10/09/635932.html (accessed 11 May 2013). (Rus).

6. Kuz'michev V.E. *Zakony i formuly fiziki* [Laws and formulas of physics]. Kiev, Naukova Dumka Publ., 1989. 864 p. (Rus).

7. *Bol'shoj illjustrirovannyj slovar' inostrannyh slov* [Large illustrated dictionary of foreign words]. Moscow, Russkie slovari Publ., 2004. 957 p. (Rus).

8. Available at: http://www.newizv.ru/lenta/2012-10-09/171050-francuz-i-amerikanec-stali-laureatami-nobelevskoj-premii-po-fizike.html (accessed 22 May 2013). (Rus).

9. Available at: http://physiclib.ru/news/item/f00/s04/n0000439/index.shtml (accessed 12 September 2014). (Rus).

10. Available at: http://rian.com.ua/dossier/20141009/358062370.html (accessed 23 March 2013). (Rus).

11. Available at: https://en.wikipedia.org/wiki/Isamu_Akasaki (accessed 10 May 2010).

12. Available at: https://en.wikipedia.org/wiki/Hiroshi_Amano (accessed 10 April 2012).

13. Available at: https://en.wikipedia.org/wiki/Shuji_Nakamura (accessed 11 May 2010).

14. Available at: http://www.nanometer.ru/2015/10/09/nobelevskaa_premia_465746.html (accessed 03 October 2013). (Rus).

15. Available at: https://en.wikipedia.org/wiki/Arthur_B._McDonald (accessed 12 January 2013).

16. Available at: https://en.wikipedia.org/wiki/Takaaki_Kajita (accessed 21 July 2012).

17. Baranov M.I. *Izbrannye voprosy elektrofiziki. Tom 3: Teorija i praktika elektrofizicheskih zadach* [Selected topics of Electrophysics. Vol. 3: Theory and practice of electrophysics tasks]. Kharkiv, Tochka Publ., 2014. 400 p. (Rus).

Received 11.02.2016

M.I. Baranov, Doctor of Technical Science, Chief Researcher,
Scientific-&-Research Planning-&-Design Institute «Molniya»
National Technical University «Kharkiv Polytechnic Institute»,
47, Shevchenko Str., Kharkiv, 61013, Ukraine,
phone +38 057 7076841, e-mail: eft@kpi.kharkov.ua

How to cite this article:

Baranov M.I. An anthology of the distinguished achievements in science and technique. Part 39: Nobel Prize Laureates in Physics for 2011-2015. *Electrical engineering & electromechanics*, 2017, no.4, pp. 3-9. **doi: 10.20998/2074-272X.2017.4.01.**

UDC 621.3 (09)+621.3 (477) **doi: 10.20998/2074-272X.2017.4.02**

V.B. Klepikov, O.Ye. Tverytnykova

PROFESSOR P.P. KOPNIAIEV – SCIENTIST, PUBLIC PERSON, ESTABLISHER OF HIGHER ELECTRICAL ENGINEERING EDUCATION (to the 150th anniversary of his birth)

Purpose. *To carry out complete historical and scientific analysis of Professor P.P. Kopniaiev's activities and establish his role and place of achievements in the formation of the basic concepts and directions of the theory of electrical engineering and its practical application in the development of higher education in Ukraine.* ***Methodology.*** *We have applied general scientific methods of logic and classification, analysis and synthesis and special historical methods – historical-comparative, problem-chronological, synchronic and diachronic.* ***Results.*** *On the basis of generalization of a wide range of sources of central, regional and personal archives, the principles and content of scientific-pedagogical, organizational and public activities of P.P. Kopniaiev were revealed and the classification of the scientific work according to the main directions of his research was conducted.* ***Originality.*** *Complex analysis of P.P. Kopniaiev's scientific-pedagogical, organizational and public activities were carried out in the field of higher electrical engineering education and industrial development in Ukraine, and his scientific achievements were classified according to the main directions.* ***Practical value.*** *Factual information, generalizations and conclusions can be applied in the teaching of humanitarian and engineering disciplines in higher education, in particular in the development of the lecture courses and textbooks used in educational activities, as well as in the preparation of general and scientific works on the history of science and technology.* References 16, figures 4.

Key words: **electrical engineering science, higher education, Professor P.P. Kopniaiev, Kharkiv Polytechnic Institute.**

Раскрыто процесс зарождения системы высшего электротехнической образования в Украине в конце XIX в. начала XX в. Обоснованно вклад профессора П.П. Копняева в основание научной электротехнической школы Украины. Раскрыто организационную деятельность ученого в создании электротехнического факультета Харьковского политехнического институт и первого в Украине специализированного высшего учебного заведения электротехнического профиля. Доказано, что восемь основных электротехнических направлений научных исследований, начатых П.П. Копняевым, получили развитие и стали в последующие годы отдельной научной школой или научным направлением. Библ. 16, рис. 4.

Ключевые слова: **электротехническая наука, высшее образование, профессор П.П. Копняев, Харьковский политехнический институт.**

Introduction. As evidenced by the experience of world and domestic science and education, a decisive role in their progress was played by prominent personalities. The formation of electrical engineering and the system of higher electrical engineering education in Ukraine is closely linked with the activities of talented electrical engineer, the organizer of science and education, Professor P.P. Kopniaiev. In different years, the scientist held the posts of Dean of the Mechanical Department, the Faculty of Electrical Engineering, the Rector of the Kharkiv Technological Institute (KhTI), the chairman of the All-Ukrainian Electrical Engineering Section and the All-Ukrainian Association of Engineers. P.P. Kopniaiev is the author of the first fundamental textbooks and manuals. He insisted on widespread implementation of his own developments and research results of his students, which enabled the development of the electrical engineering industry in Ukraine. It is precisely with his name that the establishment of the Department of Electrical Engineering, the Faculty of Electrical Engineering and the first specialized educational institution in Ukraine - the Kharkiv Electrical Engineering Institute - is directly connected. Scientific and organizational activities of P.P. Kopniaiev was fragmented in the publications of the students of the scientist and published before the anniversary of the Electrical Engineering Faculty of NTU «KhPI» [1, 2]. Investigations [3, 4] are dedicated to the personality of Professor P.P. Kopniaiev [3, 4].

The goal of the paper is on the base of scientific literature and processing sources, primarily archival documents, to supplement the information on scientific and educational activities and biography of the famous Ukrainian electrical engineer - P.P. Kopniaiev.

The origin of electrical engineering research in Ukraine. The system of higher electrical engineering education began to be formed at the leading Universities of Ukraine in the late 19th and early 20th centuries. In Lviv Polytechnic, the beginning of electrical engineering studies is associated with the activities of Professors F. Strzheletsky and K. Olearsky. The interest in the new industry was revealed by talented engineer and scientist R. Gostkovsky. His scientific works concern the issues of electric motors, DC generators, the use of electric energy for rail transport, and so on. Further research in the field of electrical engineering was continued by Professor F. Dobzhinsky. He carried out electrical measurements, electric machines, the theory of electric circuits, and so on. As a separate educational discipline, electrical engineering was introduced into the curriculum of the Lviv Polytechnic in 1887. And in 1890 a Department of Electrical Engineering was established, headed by Professor R. Dzeslevsky, a graduate of the Technical Academy of Lviv. The expansion of the electrical engineering direction of the Lviv Polytechnic is associated with Professor S. Frise and Professor G.Z. Sokolnitsky initiated introduction of electrical engineering in Western Ukraine.

Electrical engineering at the KPI was taught by well-known scientists: Professors M.A. Artemiev,

A.V. Krukovsky, A.A. Skomorokhov, S.M. Usaty, A.A. Sokolov. At the initiative of A.V. Krukovsky an electrical laboratory was created. Professor M.A. Artemiev had a wealth of practical experience, which allowed him to become the Head of the Department of Electrical Engineering created in the KPI in 1900 and begin teaching this discipline. In 1918, in order to expand the training of engineers of new specialties, at the KPI Electrical Engineering Faculty with branches of electric power stations, electric traction and communications technology was created, but in fact nothing has changed. As before, the issue of electrical engineers was conducted in one specialization at Mechanical Department. The number of students who completed the Diploma Works on electrical engineering was five to six per year. Since 1921 the general course of electrical engineering has been expanded. Several new disciplines were introduced, including the introduction to electrical engineering, the encyclopedia of electrical engineering, the theoretical foundations of electrical engineering and the basics of the theory of alternating currents.

In 1921, the Electrical Engineering Department of the reorganized Ekaterinoslav Polytechnic Institute was attached to the Mechanical Engineering Faculty of the Ekaterinoslav Mining School. It was headed by Professor of electrical engineering G. E. Evreinov He began research in the field of electrification of mining enterprises, theoretical foundations of electrical engineering and became the founder of electromechanical specialty at the Institute. In Odessa, the Higher Courses of Telegraph Mechanics were opened in 1900. In subsequent years, the Courses were expanded and in 1923 the Odessa Electrical Engineering College of High Currents was organized. The educational institution trained communication engineers, the training period was four years. In 1929 the Electrical Engineering College was reorganized into the Faculty of Electrical Engineering of the Odessa Polytechnic Institute [3, pp. 36-40].

The organization of the physical office has become the impetus for the establishment of electrical engineering research in the Kharkiv Practical Technological Institute. On August 5, 1885 at the suggestion of V.L. Kirpichov, as Assistant Professor of physics, Associate Professor of the Kharkiv University O.K. Pogorelko was appointed by the Ministry of Public Education. Expanding the teaching of electrical engineering in the KhTI belongs to a talented electrical engineer, scientist and Professor M.P. Klobukov [4, p. 12].

Activities of P.P. Kopniaiev from to establish the Electrical Engineering Faculty and the Electrical Engineering Institute. After graduation in 1898 P.P. Kopniaiev (Fig. 1) was invited to the Kharkiv Technological Institute. All subsequent life of the scientist, with the exception of forced departure to St. Petersburg in 1905-1907, is connected with Kharkiv, with KhTI, where he was formed as a leading scientist in the field of electrical engineering and as the founder of electrical engineering education in Ukraine.

Fig. 1. Pavlo Petrovich Kopniaiev

Scientific and pedagogical activity of P.P. Kopniaiev started in KhTI at the time when the situation with the electrical engineering direction was unresolved. Educational discipline «General Electrical Engineering» was taught to students of Mechanical Department in volume of two hours per week, diploma projects on electrical specialization were not performed. There were no scientific studies either. Professor P.P. Kopniaiev immediately began reorganizing the teaching of disciplines of the electrical engineering profile. At his initiative, the number of lecture hours was increased. For the first time in the curriculum special courses were included covering various sections of electrical engineering, and, most importantly, a load was assigned for graduation design. All this created favorable conditions for the first issue, which took place already in 1900 and consisted of five specialists specializing in electrical engineering. Extension of the teaching of electrical engineering disciplines, the introduction of new electrical engineering directions, the use of new techniques, the formation of independent electrical engineering disciplines required the creation of textbooks, manuals, methodological literature. Published in 1893-1894 by the lithographic method, the textbook on general electrical engineering by M.P. Klobukov was the only textbook in Ukraine, had a small set and a number of shortcomings. Summing up the accumulated material, during 1900-1902, P.P. Kopniaiev prepared a two-part textbook for publication, which contains a full course of general electrical engineering. They became the first in Ukraine textbooks on the basics of electrical engineering. Manuals by P.P. Kopniaiev were marked by a sequence of teaching, accompanied by examples, which gave the opportunity to apply theoretical foundations for practical activities in the field of electrical engineering [5, sheets 1-2].

Creation of the Department of Electrical Engineering contributed to the expansion of the subjects of diploma projects in electrical engineering specialization and to increase the number of lectures to three hours in the first year and two - in the second. For example, in 1904/1905 academic year twenty five topics

were worked out. It became obligatory to attend laboratory and practical classes. The term of the course in electrical engineering was completed when the exam was completed. P.P. Kopniaiev is the initiator of the introduction of new teaching methods. He submitted a request to the Institute's academic committee to allow students, in parallel with listening to lectures, to carry out laboratory work and independent projects. Before these innovations, students listened first the course of lectures, were tested and only then became practical work. After several meetings, the innovator-scientist was allowed the introduction of a new learning system [6, sheet 1].

Even at the beginning of his pedagogical activity at the Technological Institute P.P. Kopniaiev developed a project for the organization of an independent Electrical Engineering Faculty (EF). In 1907, 1912, 1914, the scientist made new attempts at its organization. On November 26, 1920, on the basis of the decision of the People's Committee of Professional Education of Ukraine, a commission under the leadership of P.P. Kopniaiev was created. The commission consisted of: lecturers of KhTI V.O. Izyurov, secretary of the commission V.M. Kyyanitsia, responsible for the construction of the laboratories Engineer V.A. Radzig and the representative of the Council of Students F.A. Stupel. The purpose of the commission was to organize an independent Electrical Engineering Faculty, to create new curricula, to supply new modern equipment. Electrical Engineering Faculty was opened on January 21, 1921. Professor P.P. Kopniaiev was appointed as Dean [2].

It should be noted that the first Electrical Engineering Faculty in Ukraine was opened at the KPI in 1918. But in fact the issue of electrical engineers was conducted only in one specialization. Diploma projects in electrical engineering 5-6 students per year performed.

The opening of the Faculty of Electrical Engineering in KhTI was very important for the development of industry in the South of Russia. P.P. Kopniaiev at the creation of the Faculty, predicting the huge demand for specialists in new electrical engineering specializations, offered accelerated releases - training for four years by separate curricula [57, p. 169].

The Faculty consisted of four Departments: «Electric Machines», «Electrical Equipment», «General Electrical Engineering», «Electric Traction». The Faculty was taught courses on the electrical equipment of factories and plants, electrification of mining industry, electric networks and lines, electric stations and city trams. The term of study was five years, industrial practice became an obligatory element of training, to the teaching of leading disciplines factory engineers were involved. The study of special courses was carried out in the measuring and electromechanical laboratories. On the proposal of Professor P.P. Kopniaiev setting up a high voltage laboratory began. Under the project of the scientist the purpose of the new laboratory was not only the educational process, but also scientific work. In the laboratory it was planned to conduct technical tests of high-voltage insulators and other insulating materials, research of high voltage lines. Accumulated by P.P. Kopniaiev during the previous years experience of training specialists contributed to the fact that already in the first year of the existence of the Faculty there was a release of highly skilled specialists. Graduate projects were carried out on the following topics: city electric tram; electrical supply of cities, district stations, electric installations for mines, equipment of electromechanical plant [7, sheets 2-4].

The Professors and lecturers of the Faculty included four Professors: O.O. Potebnya, V.M. Khrushchev, S.O. Teys and P.P. Kopniaiev and ten lecturers, including O.B. Bron, V.M. Kyyanitsia, O.Ya. Berger, M.F. Perevozsky The generalization of archival materials allows us to assert that the basis of the staff of the Faculty was graduates of the Mechanical Faculty of the KhTI, students of P.P. Kopniaiev [8, sheets 1-27; 9, sheets 1-2; 1].

The fruitful work of the scientist to create the Faculty of Electrical Engineering provided the grounds for the organization in 1930 of the first specialized technical institution of the electrical engineering profile in Ukraine - the Kharkiv Electrical Engineering Institute. The Institute has developed a scientific and technical school in the field of electrical engineering, where three main functions - educational, research and innovation - were presented. Fundamental and applied scientific researches were conducted, based on a powerful laboratory base, and corresponded to a high scientific level. There was a close connection with production, the results of research were implemented and had economic, social significance. During this period, the first steps were taken to establish international cooperation. Scientists worked on topical issues and realized scientific developments, received world recognition.

During the 1930-1934, the teaching staff of the Institute was strengthened by highly qualified specialists. At the suggestion of P.P. Kopniaiev and V.M. Khrushchev to the posts of faculty members of the Departments experts from production, research staff of research institutions, were invited. It contributed to improving the teaching of fundamental and practical disciplines, improving the quality of teaching specialized courses and disciplines in technology of processes, strengthening the links between research Departments and production, the development of new scientific directions and the beginning of reform in the Institute of scientific electrical engineering school, strengthening the teaching potential (Fig. 2) [10, sheets 1-3].

The presence of a powerful scientific potential contributed to optimizing the structure of the Institute. The development of electrical engineering in this period took place quite rapidly, which required the creation of new Faculties with differential specialties for the training of specialists in a narrow specialization and curriculum, which differed in content. Thanks to the base, which was formed in the previous years at the Faculty of Electrical Engineering by Professor P.P. Kopniaiev, training of specialists at the Electrical Enginering Institute took place in the following directions: electrical machines, electrical apparatus, electric traction, central power stations, transmission and distribution of electric energy. So, Professor P.P. Kopniaiev was initiated and supported by his students such areas of scientific activity as fundamental and applied research in the fields of high

voltage technology and transmission of electric energy at a distance (V.M. Khrushchev, S.M. Fertik); theory and practice of electric machines (G.I. Shturman, O.Ya. Berger); electrical apparatus (B.F. Vashura, O.B. Bron); power engineering and electric power stations (A.L. Matveev); electric drive (T.P. Gubenko, A.L. Aronov); theoretical bases of electrical engineering (O.P. Sukachev); electrical measurements (O.Kh. Khinkulov); electric traction (O.O. Potebnya).

Fig. 2. The first issue of electrical engineers of the Kharkiv Electrical Engineering Institute

Research activity of P.P. Kopniaiev. The results of the initial research investigations of the scientist were published in 1896 and immediately attracted the attention of the scholars of Europe. In the work the scientist theoretically substantiated the proposed method of analogy, emphasized the unity of laws, which are essential for a particular group of phenomena, and proved that in this regard the laws have the same mathematical formulation. Unfortunately, the proposed model has not found a decent use. Meanwhile, the work of P.P. Kopniaiev in the conditions of that time was of great importance. He was the first Russian scientist, and in 1898 he laid the scientific foundations of the method of analogy in electrical engineering. This method has become widespread in modern conditions, has given us the opportunity to solve complex research problems [11].

The first specialization, which gradually began to differentiate into the discipline, became the course «Electric Machines». The machines of direct current prevailed in the installations of that time. The formation of a new course required academic literature for students and for the training of scientific staff. The analysis carried out by the author allows us to assert that the existing scientific works on the theory of electric machines of Russian and foreign scientists at that time did not meet the basic requirements for the content of discipline. The basic literature for the study of discipline at that time was the textbooks of the scientists of the German scientific school, which were considered the most experienced specialists in the field of electrical machines. But their works began to be translated only after 1908.

In 1904, based on the materials of his own research P.P. Kopniaiev published a work devoted to questions of theory, design, research of electric machines of direct current [12]. The textbook systematized the experimental material accumulated by the author for his years in the KhTI and during internship in foreign electrical engineering high schools. The decisive factor in this work was that the scientist developed new methodological approaches to teaching the material. Without exaggeration, it should be noted that the work of P.P. Kopniaiev became the basis for the training of electrical engineers. The principles of the presentation in this section differed from other authors. The scientist considered the properties of various types of electric motors and made a complete classification of their common properties.

Next, P.P. Kopniaiev began to systematize his own teaching aids for the comprehensive training of electrical engineers. A certain group of scientific works was united by the author on the theme of the community and was a cycle of five fundamental volumes: the basis of electrical engineering, electrical measurements, DC dynamos, AC machines and transformers and electrical installations. The last volume covered the materials of disciplines, which the scientist taught in KhTI - electrical networks and electric stations. The author presents a classification and methodology for calculating wires, taking into account economic factors, their own original method of calculating illumination. He proposed several formulas for calculating the force of light (illumination) and the required component. This method had the advantage over the works of German scholars who received the result, based on empirical data or offered rather cumbersome calculations. Later, the German scientist O. Bloch created a technique similar to the P.P. Kopniaiev's one. In the second section, the author presented a development of the question of the probable increase in the load of power plants for the next decade. It was not yet elaborated and a very important issue of the operation of power plants. As the further development of power engineering showed, the scientist advanced his time with his work. In the last section P.P. Kopniaiev gives the methods of calculations of complex electric networks. Summarizing the methods known at that time, he analyzes each of them in detail, emphasizing the disadvantages and advantages.

Professor P. P. Kopniaiev made a significant contribution to the development of the direction of electric traction in Ukraine by his work on tram traction. In 1911 he, using his own experience, developed a technical project of the city electric tram in Mariupol. Based on work on traction mechanics by A.I. Lipets and D.M. Lebedev, the scientist proposed a graphical method for determining energy consumption, depending on the path profile and the tram car movement analytical equation. Unlike its predecessors, the graphical method of P.P. Kopniaiev, based on mathematical reasoning, determined the characteristics of velocity, current, time and energy consumption (that is, the corresponding graphs were constructed). Thus, there was a complete set of characteristics of the car, which determined the velocity, run time, current and the amount of electric energy consumed by the car, depending on the profile of the path. Further work was aimed at improving the methodology for calculating tram traction without graphic constructions. The result was the development of an

analytical method, which did not depend on the graphic. This technique, proposed by P.P. Kopniaiev, it was necessary to apply in fact, in aggregate, two methods for obtaining accurate results of calculations. Technical advantage of methods of calculating tram traction of P.P. Kopniaiev was fully confirmed during the tests on existing trams [13, 14].

The scientific heritage of the scientist is more than fifty works and covers the main directions of development of electrical engineering at the beginning of the twentieth century. Scientific work of a scientist can be classified into six main groups. The first group consists of works from general electrical engineering, which for a long time were the basic material for the training of specialists. The second group consists of fundamental works on the theory of electric machines of constant and alternating current. Studies on metrology and electrical measurements cover the third group of scientific works. The fourth group includes the work of the scientist on electric traction problems. Works on the calculations of electrical networks should be classified in the fifth group. And the last group consists of works on electric installations.

Public activities. Together with the teaching and scientific work P.P. Kopniaiev skillfully combined public activity. During 1907-1908 he was elected head of the commission for the organization of the first South-Russian electrical engineering exhibition in Kharkiv. The purpose of the exhibition was to popularize the achievements of electrical engineering and the introduction of electrical engineering achievements in the industry, in particular, mining and agriculture. He is a permanent member of the All-Russian Electrical Engineering Congresses (Fig. 3), worked for twenty years in the leadership of the Southern Russian Society of Technologists and edited the «Proceedings» published by the society; Acting Chairman of the Electrical Engineering Section of the All-Ukrainian Association of Engineers in Kharkiv; he was a member of the International Electrical Engineering Commission. The activity of the scientist in this direction was very important for the formation of the system of training engineers and scientific workers in Ukraine, the development of the electric economy in the city of Kharkiv. In 1916 he was elected Dean of the Faculty of Mechanics. During 1919-1920, he served as Rector of KhTI [15, sheets 22; 16, sheets 1-3].

Fig. 3. Presidium of the First All-Ukrainian Energy Congress, Kharkiv, 1929

Conclusions. Certainly, Professor P.P. Kopniaiev was the founder of higher electrical engineering education and a scientific school in the field of electrical engineering in Ukraine. In the person of the scientist, the talent of the researcher, the professionalism of the educator and the natural organizational abilities are organically combined. The decisive feature of his scientific and pedagogical activity was innovation. Analysis of scientific heritage and coverage of achievements of Professor P.P. Kopniaiev suggests that he has the features of a scientific leader. So, in the 1920's in the Kharkiv Technological Institute by P.P. Kopniaiev a foundation was created for the development of the scientific and technical school of electrical engineering in the years to come.

The traditions of the founder of electrical engineering education and science are stored at NTU «KhPI». From four Departments of the Electrical Engineering Faculty created by P.P. Kopniaiev in 1921, they conduct their pedigree scientific and pedagogical collectives of about 20 Departments of four Faculties of the NTU «KhPI».

On January 21, 2011, the National Technical University «Kharkiv Polytechnic Institute» held a solemn meeting of the Academic Council devoted to the 90th anniversary of the establishment of the Faculty of Electrical Engineering and the opening of the monument to the founder of the Faculty Professor P.P. Kopniaiev.

The meeting was attended by the grandson of P.P. Kopniaiev - Professor of the M.V. Lomonosov Moscow State University, Head of the sector of the M. Keldysh Institute of Applied Mathematics, Doctor of Physical and Mathematical Sciences, professor O.D. Briuno, as well as Professor, Doctor of Physical and Mathematical Sciences G.S. Rofe-Beketov. His grandfather, Academician of architecture O.M. Beketov, together with P.P. Kopniaiev at one time headed the commission for the construction of the Electrical Engineering Building for a new Faculty (Fig. 4).

Fig. 4. O.D. Briuno and G.S. Rofe-Beketov (21.01.2011)

REFERENCES

1. Belkind L.D. *Sbornik, posvyashchennyy pamyati zasluzhennogo professora Pavla Petrovicha Kopnyaeva* [Collection dedicated to the memory of the Honored Professor Pavel Petrovich Kopnyaev]. Kharkov, 1955. 135 p. (Rus).

2. Tovazhnyanskyy L.L., Tverytnykova O.Ye. Electrotechnical faculty of Kharkiv Technology Institute. Origins of development. *Energy saving. Power engineering. Energy audit*, 2011, no.4(86), pp. 66-74. (Ukr).

3. Tverytnykova O.Ye. *Zarodzhennia i rozvytok naukovo-tekhnichnoi shkoly Profesora P.P. Kopniaieva. Monohrafiia* [The origin and development of the scientific and technical school of Professor P.P. Kopniaiev. Monograph]. Kharkiv, NTU «KhPI» Publ., 2010. 212 p. (Ukr).

4. Kameneva V.A. *Pavel Petrovich Kopnyaev* [P.P. Kopniaiev]. M. – L, Gosenergoizdat Publ., 1959. 96 p. (Rus).

5. *Instytut arkhivoznavstva Natsionalnoi biblioteky Ukrainy im. V.I. Vernadskoho NAN Ukrainy. Fond Instytutu elektrodynamiky NAN Ukrainy 263* [Institute of Archival Studies of the National Library of Ukraine named after V.I. Vernadskyi National Academy of Sciences of Ukraine. Fund of the Institute of Electrodynamics of NAS of Ukraine 263]. Desc. 2. iss. 171, 94 p. (Ukr).

6. *Instytut arkhivoznavstva Natsionalnoi biblioteky Ukrainy im. V.I. Vernadskoho NAN Ukrainy. Fond IED NAN Ukrainy 263* [Institute of Archival Studies of the National Library of Ukraine named after V.I. Vernadskyi National Academy of Sciences of Ukraine. Fund of IER Foundation of the NAS of Ukraine 263]. Desc. 2. iss. 172, 114 p. (Ukr).

7. *Derzhavnyi arkhiv Kharkivskoi oblasti (DAKhO). Fond R-1682 Kharkivskoho politekhnichnoho instytutu* [State Archives of Kharkiv Region. Fund R-1682 of Kharkiv Polytechnic Institute]. Desc. 1. iss. 83, 14 p. (Ukr).

8. *Derzhavnyi arkhiv Kharkivskoi oblasti (DAKhO). Fond R-1682 Kharkivskoho politekhnichnoho instytutu* [State Archives of Kharkiv Region. Fund R-1682 of Kharkiv Polytechnic Institute]. Desc. 1. iss. 295, 27 p. (Ukr).

9. *Arkhiv natsionalnoho tekhnichnoho universytetu «Kharkivskyi politekhnichnyi instytut»* [Archive of National Technical University «Kharkiv Polytechnic Institute»]. F.R, 1682. iss. 11, 10 p. (Ukr).

10. *Derzhavnyi arkhiv Kharkivskoi oblasti (DAKhO). Fond 5404 Kharkivskoho elektrotekhnichnoho instytutu* [State Archives of Kharkiv Region. Fund 5404 of Kharkiv Electrotechnical Institute]. Desc. 2. iss. 59, 15 p. (Ukr).

11. Kopnyaev P.P. The analogy between the phenomena of electricity and hydraulics. *Electricity*, 1898, no.11-12, pp. 159-166. (Rus).

12. Kopnyaev P.P. *Dinamo-mashiny postoyannogo toka. Ih teoriya, ispytanie, konstruktsiya i raschet (s otdelnym atlasom chertezhey)* [Dynamo machines of direct current. Their theory, test, design and calculation (with a separate atlas of drawings]. Kharkov, Adolf Darre Publ., 1904. 290 p. (Rus).

13. Kopnyaev P.P. Analytical calculation of tram traction. *Electricity*, 1915, no 2. (Rus).

14. Kopnyaev P.P. Graphic calculation of tram traction. *Electricity*, 1914, no.2. . (Rus).

15. *Derzhavnyi arkhiv Kharkivskoi oblasti (DAKhO). Fond 770 Kharkivskoho tekhnolohichnoho instytutu* [State Archives of Kharkiv Region. Fund 770 of Kharkov Technology Institute]. Desc. 1. iss. 630, 61 p. (Ukr).

16. *Derzhavnyi arkhiv Kharkivskoi oblasti (DAKhO). Fond R-1682 Kharkivskoho politekhnichnoho instytutu* [State Archives of Kharkiv Region. Fund R-1682 of Kharkiv Polytechnic Institute]. Desc. 1. iss. 35, 11 p. (Ukr).

Received 29.06.2017

V.B. Klepikov[1], *Doctor of Technical Science, Professor,*
O.Ye. Tverytnykova[1], *Candidate of Historical Science, Associate Professor,*
[1] National Technical University «Kharkiv Polytechnic Institute», 2, Kyrpychova Str., Kharkiv, 61002, Ukraine,
phone +38 057 7076226,
e-mail: klepikov@kpi.kharkov.ua, tveekhpi@ukr.net

How to cite this article:
Klepikov V.B., Tverytnykova O.Ye. Professor P.P. Kopniaiev – scientist, public person, establisher of higher electrical engineering education (to the 150th anniversary of his birth). *Electrical engineering & electromechanics*, 2017, no.4, pp. 10-15. **doi: 10.20998/2074-272X.2017.4.02.**

UDC 621.316.9 **doi: 10.20998/2074-272X.2017.4.03**

V.G. Dan'ko, E.V. Goncharov, I.V. Poliakov

ANALYSIS OF THE OPERATION PECULIARITIES OF THE SUPERCONDUCTING INDUCTIVE CURRENT LIMITER WITH ADDITIONAL SUPERCONDUCTING SCREEN

Purpose. ***The inductances of magnetic system of a current limiter for the nominal operating mode were determined. The aspects of functioning and a design of a superconducting short-circuit current limiter of inductive type with a superconductive main and additional screens, and superconductive winding, which are placed in a general cryostat on a ferromagnetic core, which ensures an improvement of magnetic field dissipation and in energy efficiency are observed.*** ***Methodology.*** ***The analysis of distribution of magnetic field of the short-circuit current limiter of inductive type with superconducting high-temperature coil and superconducting main and additional screens, using mathematical modeling by the finite element method in math software package FEMM for different modes of operation is carried out.*** ***Results.*** ***The calculations of magnetic field dissipation in operational modes are carried out.*** ***Originality.*** ***The investigations aimed to analyze the influence of distribution of the magnetic field in inductive short-circuit current limiter with superconducting additional screen on its operation modes. First calculation of the distribution of magnetic fields in different modes of operation for the short-circuit current limiter in the area between high-temperature superconducting screens.*** ***Practical value.*** ***The advantage of additional screen of superconducting short-circuit current limiter is to improve screening from dissipation of the magnetic fields of the magnetic system and reducing the power losses at nominal mode. Using the proposed methodology will identify options acceptable to the current limiter mode of operation.*** References 15, tables 3, figures 6.

Key words: **current limiter, high-temperature superconductor, superconducting screen, inductance, magnetic field, ferromagnetic core**.

Проведен анализ режимов работы и конструктивной схемы сверхпроводящего ограничителя тока короткого замыкания индуктивного типа с дополнительным сверхпроводящим экраном. Проведено математическое моделирование магнитной системы ограничителя тока методом конечных элементов в программной среде FEMM. Проведен расчет распределения магнитных полей в различных режимах срабатывания ограничителя тока короткого замыкания на участке между основным и дополнительным экранами, что позволяет определить параметры ограничителя тока. Библ. 15, табл. 3, рис. 6.

Ключевые слова: **ограничитель тока, высокотемпературный сверхпроводник, сверхпроводящий экран, индуктивность, магнитное поле, магнитопровод**.

Introduction. The development of the electric power industry is characterized by an increase in the generation of electricity, the development of increased capacities, the creation of high-power power systems. Thus, there were prerequisites for the development of electric power on a new technological basis of high-temperature superconductivity.

A superconducting high-temperature short-circuit current limiter is an alternative to the use of conventional current-limiting reactors. According to the structural features, two main concepts of the superconducting current limiter can be distinguished: resistive and inductive, and other circuitry based on them [1, 2].

The resistive design of the superconducting current limiter, based on the nonlinearity of the superconductor's resistance, can use massive elements or coils [3]. In the case of superconducting coils utilization as superconducting elements, they are connected so that the full inductance of the limiter is minimal [4]. The main disadvantage of a resistive superconducting current limiter is significant heat dissipation and overheating at short circuits.

In the inductive construction, which is considered in the work of Yonsei University, the magnetic coupling between the superconducting element and the winding is carried out through the three-rod magnet [5]. Also, for example, in the work of the ABB Company a three-phase current limiter (1.2 MVA) with a cylindrical screen of 16 rings of superconducting ceramics Bi-2212 has been designed, which was tested and operated during the year [6]. The operation of an inductive current limiter is due to the presence of magnetic scattering fields, which can negatively affect the use of a metal cryostat and increase power losses.

Reducing the effect of magnetic scattering fields can be achieved by using an additional superconducting screen.

But the features of the inductive current limiter, using an additional superconducting screen, have not been investigated.

The goal and definition of the research. The goal of the paper is to investigate the features of the short circuit current limiter with an additional superconducting screen. The purpose of the work is to analyze the modes of operation with the definition of the distribution of magnetic fields in the current limiter.

The general view of the design scheme of the current limiter with the additional superconducting screen and the circuit for switching on the phase of the mains with the load is given in Fig. 1 [7].

The short-circuit current limiter is located in the cryostat *1* with the current conductors *2* on the middle rod of the ferromagnetic core of the magnetic circuit *3*. From the inner wall of the cryostat to the outer axially the main superconducting screen *4*, the outer superconducting

screen *5*, the superconducting coil *6* between them are located. The cryostat is filled with liquid nitrogen for cooling the winding and screens to the superconducting state (77 K) [8].

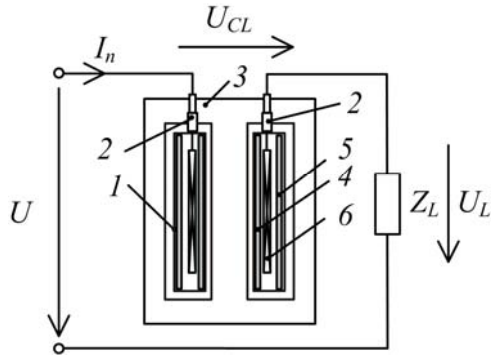

Fig. 1. Design scheme of the current limiter

The winding *6* is connected in series with the load, and in the nominal mode through it the load current I_n flows. The superconducting screen *4* shields the middle magnet circuit rod from the magnetic field that is created by the winding *6*.

Inductance of the superconducting current limiter winding at nominal mode [9]:

$$L_{sc} = \frac{\Psi}{I_n} = \mu_a w^2 \frac{2\pi r_{mid} b}{3h_{coil}},$$

where Ψ is the winding flux linkage; I_n is the rated current; r_{mid} is the average winding radius; b is the winding width; h_{coil} is the winding height; w is the winding number of turns; μ_a is the absolute magnetic permeability [10].

Let us consider how the voltage drop U_{CL} on the current limiter affects the load voltage decrease U_L in relation to the voltage of the electrical network U. The use of high-temperature superconductors for the windings of the current limiter reduces their resistance to practically purely inductive ($R \to 0$). That is, the voltage on the current limiter U_{CL} outstrips the current I_n by ~ 90º (Fig. 2).

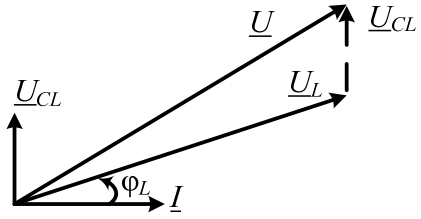

Fig. 2. Vector diagram of the electric circuit with superconducting current limiter

According to the vector diagram $\underline{U} = \underline{U}_L + \underline{U}_{CL} = \underline{U}_L + k_{CL}\underline{U}_L$, where k_{CL} is the correlation coefficient U_{CL} with load voltage U_L.

From the vector diagram, the load voltage

$$U_L = \frac{U}{\sqrt{\left(k_{CL} + \sqrt{1-\cos^2\varphi_L}\right) + \cos^2\varphi_L}},$$

where φ_L is the angle of the phase shift of the nature of the load.

In industrial regions of Ukraine, cosφ is within the range of 0.9-0.95, therefore the voltage on the current limiter should be limited to $0.05U_L$, laying the appropriate design parameters of the current limiter [11]. With cos$\varphi \approx 0.97$, one can accept k_{CL} = (0.1-0.15). The results of the calculation of the relationship between the load voltage U_L and the voltage of the electrical network U, depending on k_{CL} and cosφ_L are shown in Table 1.

Table 1

U_L as a part of U

k_{CL}	cosφ_L			
	0.85	0.9	0.95	1.0
0.05	0.973 U	0.977 U	0.983 U	0.999 U
0.1	0.947 U	0.954 U	0.965 U	0.995 U
0.15	0.92 U	0.931 U	0.946 U	0.99 U

From Table 1 it is evident that with an active load of the electric network, the superconducting current limiter, even with a significant drop in the voltage on it, practically does not affect the voltage decrease on the load.

Calculation of the magnetic field distribution. The calculation of the distribution of the magnetic field in the nominal mode of the current limiter operation using the finite element method in the FEMM mathematical software package [12] was carried out.

To calculate the magnetic field, a calculation geometric model of the magnetic system of the current limiter was built with the parameters given in Table 2 [13].

Table 2

Current limiter parameters

Parameter	Value
Rated voltage, kV	6
Rated current, A	400
Radius of the core section r_c, m	0.105
Magnetic circuit width A, m	0.471
Height of the magnetic core window h, m	0.84
Superconducting screens height h_{scr}, m	0.82
Winding height h_{coil}, m	0.81
Winding number of turns w	367
Gap between the main screen and winding δ_{scr}, mm	1-5

The distribution of the magnetic field in the window of the magnetic core of the current limiter at the nominal mode, which is calculated in the FEMM package, is shown in Fig. 3.

The geometric model of the limiter magnetic circuit is built in FEMM for inductance calculations with the assumption that the cross-section of the current limiter is rectangular and the distribution of the magnetic flux does not change in radial direction [14].

Calculation of the inductive resistance of the equivalent model of the current limiter in nominal mode is performed on the basis of the calculation of the magnetic field and is shown in Table 3.

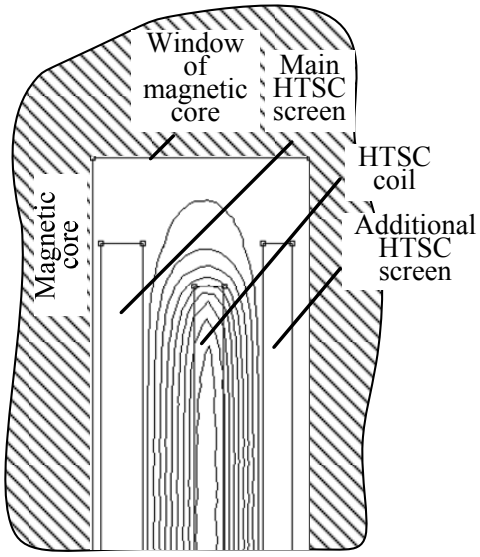

Fig. 3. Magnetic field distribution in the current limiter core window

Table 3

Inductive resistance X_L at $\mu_r = 1$

δ_{scr}/h_{coil}, %	X_L, Ω	k_{CL}
0.1	0.0917	$6.11 \cdot 10^{-03}$
0.2	0.129	$8.61 \cdot 10^{-03}$
0.3	0.165	$1.10 \cdot 10^{-02}$
0.4	0.199	$1.32 \cdot 10^{-02}$
0.5	0.239	$1.59 \cdot 10^{-02}$

The inductance of the winding due to the magnetic fluxes of scattering, taking into account shielding, is negligible. The full resistance of this current limiter at the rated operating mode of the power supply is small enough, which does not lead to a significant reduction in the voltage on the load $U_{CL} < 3$ % of U, and the nature of the voltage drop is inductive.

In the nominal mode of operation, an additional superconducting screen provides the passage of magnetic flux outside of the winding. Magnetic scattering fields the outside of the winding are shielded by an additional superconducting screen. The magnetic flux does not penetrate the extreme magnetic circuit bars, therefore, the losses in the magnetic circuit are not present at the nominal mode. The transient process at the operation of a screened superconducting current limiter can take place in several stages.

There are two options for operating the current limiter with an additional screen. In the case of loss of superconductivity by an additional superconducting screen at the critical magnetic field strength H_{cr}, when the current in the winding reaches the value $I_{cr1} = 3I_n$, the inductance of the winding is $L = 0.3$ mH. The magnetic flux extends from the outside of the surface of the main superconducting screen and penetrates the extreme bars of the magnetic circuit. The calculation of the distribution of the magnetic field of the winding with $\mu_r = 1$ is presented in Fig. 4.

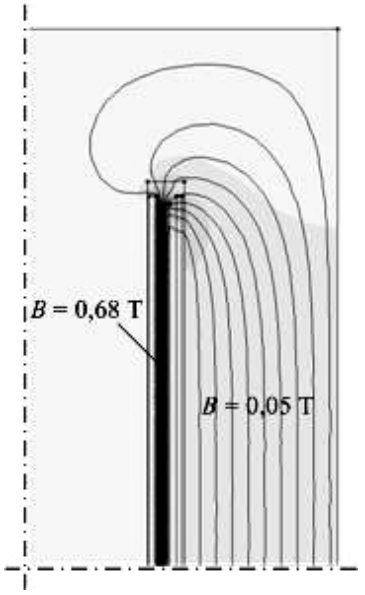

Fig. 4. Distribution of the magnetic field at the loss of superconductivity by additional screen

In the case of loss of superconductivity by additional screen, the magnetic flux extends along the area belonging to the window of the section of the magnetic core and forms the flux linkage, but this is not sufficient to provide a limiting short-circuit current. With the subsequent loss of the superconductivity of the main screen after the loss of superconductivity by the additional one, the inertial component and scattering fields will take place. The distribution of magnetic flux density B along the area from the outer wall of the main superconducting screen to the inner wall of the additional screen, which has lost the superconducting properties, is given in the graph in Fig. 5.

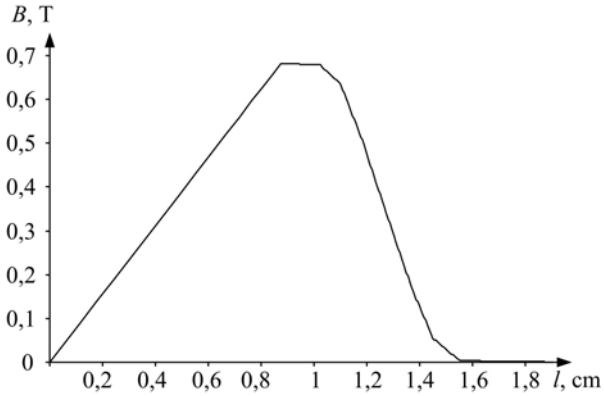

Fig. 5. Distribution of the magnetic flux density between the screens

In this case, the magnetic flux density has the maximal value in the middle section of the superconducting winding.

For example, in case of loss of superconductivity by the main screen, provided $I_{cr2} = 3I_n$, the critical parameters of the main screen should be lower than for the additional screen $H_{cr1}(I_{cr1}) < H_{cr2}(I_{cr2})$. The magnetic flux of scattering is sprayed in the window of the magnetic core, but only penetrates the middle bar of the magnetic circuit core, except the extreme (axial

symmetry). The calculation of the distribution of the magnetic field is given in Fig. 6, the inductance of the winding in this case is L = 0.24 mH.

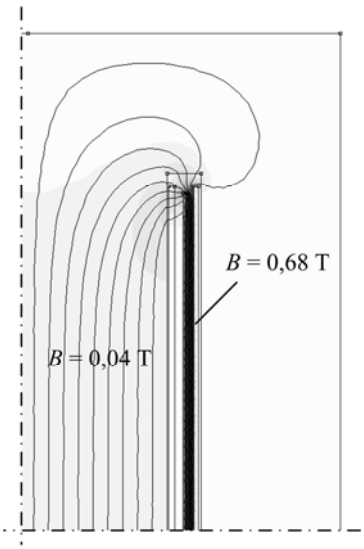

Fig. 6. Distribution of the magnetic field at the loss of superconductivity by main screen

The distribution of magnetic flux density in the area between the screens will be similar, with the difference that the magnetic scattering flux goes away the winding from the outside at the extreme bar.

When the current in the coil reaches the critical value corresponding to the main and additional screens $I_{cr1} = I_{cr2} = 3I_n$, simultaneous loss of their superconductivity will occur. The magnetic flux instantly penetrates the middle bar of the magnetic circuit, the inductance increases, which provides a current limitation and increases the time constant of increase of current, which in general will facilitate the switch operation. The transient will take place in two stages. In this case, the mathematical model of the transient is determined by the equations [15]:

$$\begin{cases} i_{cr1}(t) = \dfrac{U_{nm}}{Z_{CL1}}\sin(\omega t + \psi_u - \varphi_{CL1}) + \\ + \left[I_{nm}\sin(\psi_u - \varphi_L) - \dfrac{U_{nm}}{Z_{CL1}}\sin(\psi_u - \varphi_{CL1}) \right] e^{-\frac{R_{CL1}}{L_{CL1}}t}; \\ i_{cr2}(t) = \dfrac{U_{nm}}{Z_{CL2}}\sin[\omega(t + t_{cr1}) + \psi_u - \varphi_{CL2}] + \\ + \left[k_{i1} I_{nm} - \dfrac{U_{nm}}{Z_{CL2}}\sin(\omega t_{cr1} + \psi_u - \varphi_{CL2}) \right] e^{-\frac{R_{CL2}}{L_{CL2}}t}; \end{cases}$$

where $R_{CL1} = R_{CL2} = P_0 / I_n^2$ is the winding resistive resistance; P_0 is the winding power losses; $L_{CL1} = \mu_0 n^2 w \dfrac{b_w}{a_w}\pi r_c$, $L_{CL2} = \dfrac{w B_c \pi r_c^2}{k_{i1} I_{nm}}$ are the inductances of the current limiter of the first and the second stages; w is the winding number of turns; a_w is the film wire width; b_w is the film wire thickness; r_c is the radius of the magnetic circuit core section; B_c is the magnetic flux density of the core; t_{cr1} is the time of the end of the first stage of the transient; $Z_{CL1} = \sqrt{R_{CL1}^2 + (\omega L_{CL1})^2}$, $Z_{CL2} = \sqrt{R_{CL2}^2 + (\omega L_{CL2})^2}$ are the impedances of the current limiter of the first and the second stage; $\varphi_{CL1} = \text{arctg}\dfrac{\omega L_{CL1}}{R_{CL1}}$, $\varphi_{CL2} = \text{arctg}\dfrac{\omega L_{CL2}}{R_{CL2}}$ are the phase angles of the current limiter of the first and the second stages; k_{i1} = 2.5-3 is the current excess ratio.

Conclusions. The use of an additional superconducting screen in an inductive current limiter provides shielding of magnetic scattering fields thereby the heat flux and power losses in nominal mode reduce, although the use of an additional superconducting screen slightly increases the core mass of the magnetic circuit.

Analysis of the distribution of the magnetic field shows that the variant of operation of the current limiter at the moment of short circuit is more suitable at the primary loss of superconductivity of the main screen, which makes it advisable for it to use material with lower critical parameters, for example, bismuth ceramics, and for the additional screen to use yttrium ceramics.

REFERENCES

1. Leung E.M. Superconducting fault current limiters. *IEEE Power Engineering Review*, 2000, vol.20, no.8, pp. 15-18. **doi: 10.1109/39.857449.**

2. Paul W., Chen M., Lakner M., Rhyner J., Braun D., Lanz W. Fault current limiter based on high temperature superconductors – different concepts, test results, simulations, applications. *Physica C: Superconductivity*, 2001, vol.354, no.1-4, pp. 27-33. **doi: 10.1016/s0921-4534(01)00018-1.**

3. Bock J., Breuer F., Walter H., Elschner S., Kleimaier M., Kreutz R., Noe M. CURL 10: development and field-test of a 10 kV/10 MVA resistive current limiter based on bulk MCP-BSCCO 2212. *IEEE Transactions on Applied Superconductivity*, 2005, vol.15, no.2, pp. 1955-1960. **doi: 10.1109/tasc.2005.849344.**

4. Elschner S., Breuer F., Noe M., Rettelbach T., Walter H., Bock J. Manufacturing and testing of MCP 2212 bifilar coils for a 10 MVA fault current limiter. *IEEE Transactions on Applied Superconductivity*, 2003, vol.13, no.2, pp. 1980-1983. **doi: 10.1109/tasc.2003.812954.**

5. Joo M. Reduction of fault current peak in an inductive high-Tc superconducting fault current limiter. *Cryogenics*, 2005, vol.45, no.5, pp. 343-347. **doi: 10.1016/j.cryogenics.2004.11.007.**

6. Paul W., Chen M., Lakner M., Rhyner J., Widenhorn L., Guérig A. Test of 1.2 MVA high-T_c superconducting fault current limiter. *Superconductor Science and Technology*, 1997, vol.10, no.12, pp. 914-918. **doi: 10.1007/978-4-431-66879-4_292.**

7. Goncharov E.V. *Strumoobmezhuyuchyy reaktor z nadprovidnym kombinovanym ekranom* [Superconducting current-limiting reactor combined screen]. Patent UA, no. 112671, 2016. (Ukr).

8. Goncharov E.V. Improving shielding of superconducting inductively resistive short-circuit current limiter. *Materialy nauk.-tekhn. konf «Problemy suchasnoi enerhetyky i avtomatyky v systemi pryrodokorystuvannia».* [Abstracts of Sci.-Techn. Conf. «Problems of modern energy and automation system of nature»]. Kyiv, 14-18 November 2016, pp. 107-108. (Ukr).

9. Dan'ko V.G., Goncharov E.V. Analysis of high-temperature superconducting short-circuit current limiter. *Eastern-European Journal of Enterprise Technologies*, 2007, vol.6/5(30), pp. 45-48. (Ukr).
10. Goncharov E.V. Equivalent magnetic permeability of superconducting winding. *Electrical engineering & electromechanics*, 2010, no.1, pp. 11-13. (Ukr). **doi: 10.20998/2074-272X.2010.1.03.**
11. Dan'ko V.G., Goncharov E.V. Calculating the parameters of an inductive short-circuit current limiter with a superconducting shield. *Russian Electrical Engineering*, 2013, vol.84, no.9, pp. 478-481. **doi: 10.3103/s1068371213090046.**
12. Meeker D. *Finite Element Method Magnetics. FEMM 4.2 32 bit 11 Oct 2010 Self-Installing Executable.* Available at: www.femm.info/wiki/OldVersions (accessed 10 March 2014).
13. Dan'ko V.G., Goncharov E.V., Polyakov I.V. Analysis of energy efficiency of a superconducting short circuit current limiter. *Eastern-European Journal of Enterprise Technologies*, 2016, vol.6, no.5(84), pp. 4-12. **doi: 10.15587/1729-4061.2016.84169.**
14. Dan'ko V.G., Goncharov E.V. Synthesis aspects of cryogenic high-temperature superconducting shielding inductive short-circuit current limiter. *Bulletin of NTU «KhPI»*, 2016, no.32(1204), pp. 3-7.
15. Dan'ko V.G., Goncharov E.V. Features of operation of a superconducting current limiter at the sudden short circuit. *Electrical engineering & electromechanics*, 2014, no.6, pp. 30-33. (Ukr). **doi: 10.20998/2074-272X.2014.6.04.**

Received 02.06.2017

V.G. Dan'ko[1]*, Doctor of Technical Science, Professor,*
E.V. Goncharov[1]*, Candidate of Technical Science,*
I.V. Poliakov[1]*, Candidate of Technical Science, Associate Professor,*
[1] National Technical University «Kharkiv Polytechnic Institute», 2, Kyrpychova Str., Kharkiv, 61002, Ukraine,
phone +380 57 7076427,
e-mail: e.goncharov.v@gmail.com

How to cite this article:
Dan'ko V.G., Goncharov E.V., Poliakov I.V. Analysis of the operation peculiarities of the superconducting inductive current limiter with additional superconducting screen. *Electrical engineering & electromechanics*, 2017, no.4, pp. 16-20. **doi: 10.20998/2074-272X.2017.4.03.**

UDC 621.313.32 **doi: 10.20998/2074-272X.2017.4.04**

V.S. Malyar, V.S. Maday, I.R. Kens

RESONANT PROCESSES IN STARTING MODES OF SYNCHRONOUS MOTORS WITH CAPACITORS IN THE EXCITATION WINDINGS CIRCUIT

Purpose. Development of a mathematical model that enables to detect resonance modes during asynchronous startup of salient-pole synchronous motors, in which capacitors are switched on to increase the electromagnetic moment in the circuit of the excitation winding. Methodology. The asynchronous mode is described by a system of differential equations of the electric equilibrium of motor circuits written in orthogonal coordinate axes. The basis of the developed algorithm is the mathematical model of the high-level adequacy motor and the projection method for solving the boundary value problem for the equations of the electric equilibrium of the circuits written in orthogonal coordinate axes, taking into account the presence of capacitors in the excitation winding. The coefficients of differential equations are the differential inductances of the motor circuits, which are determined on the basis of the calculation of its magnetic circuit. As a result of the asymmetry of the rotor windings in the asynchronous mode, the current coupling and currents change according to the periodic law. The problem of its definition is solved as a boundary one. Results. A mathematical model for studying the asynchronous characteristics of synchronous motors with capacitors in an excitation winding is developed, by means of which it is possible to investigate the influence of the size of the capacity on the motor's starting properties and the resonance processes which may arise in this case. Scientific novelty. The developed method of mathematical modeling is based on a fundamentally new mathematical basis for the calculation of stationary dynamic modes of nonlinear electromagnetic circuits, which enables to obtain periodic coordinate dependencies, without resorting to the calculation of the transients. The basis of the developed algorithm is based on the approximation of state variables by cubic splines, the projection method of decomposition for the boundary value problems of the calculation of the established periodic modes and the differential method of calculating static characteristics. Practical value. Using the developed algorithm of calculation it is possible to determine the required capacitances of the capacitors in the excitation winding to start the synchronous motor and to investigate the possibility of occurrence of the resonance at startup with the selected capacitance value of the capacitors by calculating the static characteristics as a sequence of asynchronous modes. References 8, figures 2.
Key words: **salient-pole synchronous motor, capacitors, excitation winding, resonance, static characteristics.**

Рассматривается проблема возникновения резонанса во время асинхронного пуска явнополюсных синхронных двигателей, в которых для повышения электромагнитного момента в цепь обмотки возбуждения включены конденсаторы. Для расчета пусковых статических характеристик и исследования влияния величины емкости конденсаторов на протекание пуска двигателя, в частности появления резонанса, используется математическая модель синхронного двигателя явнополюсной конструкции высокого уровня адекватности, в которой учитывается насыщение магнитопровода. Асинхронный режим описывается системой дифференциальных уравнений электрического равновесия, составленной в ортогональных координатных осях с учетом наличия конденсаторов в обмотке возбуждения. Электромагнитные параметры контуров определяются путем расчета разветвленной схемы замещения магнитной цепи двигателя. В основу разработанного алгоритма положен основанный на аппроксимации кубическими сплайнами проекционный метод решения краевых задач расчета установившихся периодических режимов и дифференциальный метод расчета статических характеристик. Библ. 8, рис. 2.
Ключевые слова: **явнополюсний синхронный двигатель, конденсаторы, обмотка возбуждения, резонанс, статические характеристики.**

Introduction. Despite the higher cost and complexity comparing with induction motors in manufacturing, synchronous motors are used in electric drives of high power, especially where low rotation speeds are required. The problem of starting synchronous motors, which operate in powerful electric drives, is one of the main. Its essence is to provide the necessary starting torque, which is conditioned by the operating conditions of the drive. They are made primarily with salient poles, which have an excitation winding. To access the synchronous mode, the rotor of the motor must be accelerated to close to the synchronous speed of rotation, after which to apply to the winding excitation DC, the rotor will become an electromagnet and will enter into synchronism.

Among the known methods of starting, most often used asynchronous start, as simple and reliable, which is carried out through direct switching to a network with a nominal voltage. For asynchronous start-up, copper or brass rods are inserted into each pole of a salient-pole synchronous motor (SSM), which are connected from the ends with short-circuiting rings. As a result, we obtain a starting winding, which is analogous to the short-circuit winding of the rotor of the induction motor, and allows to accelerate the motor to a sub-synchronous speed. This winding simultaneously acts as a damper and eliminates random oscillations. Since there are no rods in the interpolar gap, it is asymmetric, as a result of which the distribution of magnetic flux density in the air gap differs from the sinusoidal one, and the electromagnetic torque in the stable asynchronous mode has constant and variable components. In addition, the saturation of the magnetic circuit affects the processes in the SSM.

During the induction start the excitation winding is usually short-circuit on resistive resistance value of

5-10 Ω, and it almost does not participate in the creation of electromagnetic torque. Nevertheless, in case of starting of SSM under load the electromagnetic torque which is created by starting winding of the rotor in asynchronous mode, is insufficient for the successful startup, so they use various means to improve it. One of the ways to solve the problem is to use the excitation winding. However, it has a large inductance, and therefore alternating current that takes place in it in the starting mode is inductive and can not create significant additional torque. To compensate inductive reactance of the excitation winding is possible by sequentially switching capacitors [6, 7], but SSM start with capacitors in the excitation winding requires thorough research as an unfortunate choice of their capacitance values can lower starting electromagnetic torque [2, 5]. Also, having capacitors in excitation winding can cause effects of voltages resonance, which is dangerous for winding and for the motor as a whole due to resonance caused unacceptably high currents and electromagnetic torque. So the problem of the study of the processes that arise in synchronous electric drives in the case of the connection of capacitors in the winding of excitation is of great practical importance.

The method of increasing the starting electromagnetic torque by means of connection in the excitation winding of the SSM capacitors known in the literature for a long time, but the problem of mathematical modeling of processes, which accompany their asynchronous start, remains unresolved so far. This is mainly due to the fact that the study of processes occurring under such a start-up method was carried out on simplified mathematical models based on the classical equivalent circuits of the motor [6, 7], which a priori requires experimental verification. However, experiments on high-power SSM are too expensive, and some of them can not be implemented for technical reasons. Clarification of the calculations on the basis of the use of chain multi-circuit equivalent circuits [1] is not universal, since it is tied to a specific electric drive, and therefore does not solve the problem of the adequacy of the calculation results. Therefore, the methods of analysis, which are based on both the classical and advanced equivalent circuits of the IM, do not provide the reliability of the parameters in the dynamic modes, and the errors in the parameters can lead to incorrect results.

As is known, the condition of resonance is determined by the parameters of the electric circuit, in particular, the excitation winding, which does not work isolated, but in the system of complex electromagnetic connections with other circuits of the motor, which carry out reciprocal displacement. Therefore, the problem of selecting the capacitance of the start capacitors for connection to the excitation winding requires the calculation of these parameters with high reliability, which can be realized only with the use of advanced mathematical models of the SSM, which ensure the high reliability of the results of the mathematical experiment, regardless of the type of motor, its dimensions and parameters.

The goal of the work is the development of a mathematical model that makes it possible to detect and investigate resonance modes during the start-up of SSM with capacitors in the excitation winding circuit.

Algorithm of the problem solution. Let us consider the SSM which stator winding is powered by a three-phase network, a starting winding and an excitation winding are placed on the rotor, which at the time of an asynchronous start is shortened to capacitors. The processes are considered in the coordinate axes *d*, *q*, and the actual winding of the rotor is equivalented by two circuits according using the generally accepted technique. As a result, the electric circuit of the SSM has three contours (*d*, *f*, *D*) along the longitudinal axis and two (*q*, *Q*) along the transverse one, between which there are interinductive connections due to the saturation of the magnetic core.

The electromagnetic processes in the SSM in the case of shortening of the single-phase excitation winding on capacitors of capacitance *C* are described by a nonlinear system of differential equations (DE) of the electromagnetic equilibrium of the circuits, which describes the asynchronous mode in the axes *d, q*

$$\begin{aligned}
&\frac{d\psi_q}{dt} = -\omega_0(1-s)\psi_d - ri_q + u_q;\\
&\frac{d\psi_D}{dt} = -r_D i_D;\\
&\frac{d\psi_Q}{dt} = -r_Q i_Q;\\
&\frac{d\psi_f}{dt} = -r_f i_f + u_k;\\
&\frac{du_k}{dt} = \frac{i_f}{C},
\end{aligned} \tag{1}$$

there by the indexes *D* and *Q* values concerning equivalent circuits of the starting winding are indicated; ψ_d, ψ_q, ψ_D, ψ_Q, ψ_f, i_d, i_q i_D, i_Q, i_f are the flux linkages and currents of the equivalent circuits; $s = (\omega_0 - \omega) / \omega_0$; ω_0, ω are the voltage of the feeding voltage of the stator winding and the angular frequency (s^{-1}) of the rotor rotation; $u_d = U_m \sin\theta$, $u_q = U_m \cos\theta$, θ is the angle of rotor runoff, U_m is the amplitude value of the stator phase voltage, u_k is the voltage on the capacitor in the excitation winding circuit.

As a result of the periodic change of the angle θ in the asynchronous mode of the SSM with the sliding of the rotor $s = s_0$ flux linkages, currents, voltage on the capacitors of the excitation winding vary according to the periodic law with the period

$$T_a = 2\pi/(s\omega_0).$$

Thus, the problem of calculating the stationary mode with constant sliding is to determine these periodic dependencies. As is well known [3, 8], it can be solved with a minimum computational volume by solving a boundary value problem with periodic boundary conditions.

In order to reduce the description of the calculation algorithm for the periodic dependencies of the coordinates of the regime on the period T_a, we write the system of DE (1) by one vector equation

$$\frac{d\vec{y}}{dx} = \vec{z}\left(\vec{x}, \vec{y}, \vec{u}\right), \tag{2}$$

where the corresponding vectors have the following content:

$$\vec{y} = \begin{vmatrix} \psi_d \\ \psi_q \\ \psi_D \\ \psi_Q \\ \psi_f \\ u_k \end{vmatrix}; \quad \vec{x} = \begin{vmatrix} i_d \\ i_q \\ i_D \\ i_Q \\ i_f \\ u_k \end{vmatrix}; \quad \vec{u} = \begin{vmatrix} u_d \\ u_q \\ 0 \\ 0 \\ 0 \\ 0 \end{vmatrix};$$

$$\vec{z} = \begin{vmatrix} u_d + \omega_0(1-s)\psi_q - ri_d \\ u_q - \omega_0(1-s)\psi_d - ri_q \\ -r_D i_D \\ -r_Q i_Q \\ u_k - r_f i_f \\ i_f / C \end{vmatrix}.$$

Having made the approximation of the coordinates of equation (2), which describes the stable asynchronous mode of SSM, on the mesh of n+1 nodes of the period T_a by the splines of the third order in accordance with [3] with the step $h = T_a / n = 2\pi/(s\omega_0 n)$, we obtain an algebraic analogue of DE (2) of the m=6th order in the form of a nonlinear algebraic equation of the nm-th order

$$H\vec{Y} - D\vec{Z} = 0, \tag{3}$$

where $\vec{Y} = (y_1, ..., y_n)^*$; $\vec{Z} = (z_1, ..., z_n)^*$; H, D are the transition matrices from continuous change of coordinates to their discrete (nodal) values whose elements are determined by the approximation of periodic coordinates of the coordinates by cubic splines [3].

The algebraic equation (3) is a discrete analogue of the nonlinear system of DE (2). Its solution is the value of the vector

$$\vec{X} = (x_1, ..., x_n)^*,$$

$$\left(\vec{x} = \left(i_{dj}, i_{qj}, i_{Dj}, i_{Qj}, i_{fj}, u_{kj}\right)^*\right), \quad j = 1, ..., n.$$

The system (3) includes coordinate values that correspond to fixed values of the time coordinate t in the nodes of the period, the relationships between which at each time point are nonlinear. To solve a nonlinear algebraic system (3), the method of extension by parameter in conjunction with the iterative Newton method is applied. The driving force (perturbation) in equation (3) is the vector $\vec{U} = (u_1, ..., u_n)^*$ of discrete values of the applied voltages, where

$$\vec{u}_j = \left(\sqrt{2}U \sin\theta_j, \sqrt{2}U \cos\theta_j, 0, 0, 0, 0\right)^*,$$

increasing which from zero to a given value, we obtain the values of vectors $\vec{Y}$ and $\vec{X}$ which correspond to the specified value of sliding $s = s_0$.

Investigation of the effect of the value of capacitors' capacitance C on the asynchronous mode is carried out by the differential method. For this, system (3) is differentiated by C. As a result, we obtain the DE of the argument C of the form

$$W\frac{\partial\vec{X}}{\partial C} = D\vec{U}, \tag{4}$$

where W is the Jacobi matrix of the system (3).

To obtain the multidimensional static characteristic as the dependence of the nodal values of the coordinates of the mode of operation of the SSM on C, the system of DE (4) must be integrated by the numerical method [3, 8]. At each step of the integration the derivative vector $\partial\vec{X}/\partial C$ is determined by solving the equation (4), which makes it possible to reduce it by the numerical method to the Cauchy form. Elements of the blocks of the Jacobi matrix are the differential inductive resistances of the motor's circuits, which are determined by calculating the magnetic circuit of the SSM in accordance with the accepted model [8]. The basis of their calculation is the determination of the magnetic field curve in the air gap of the motor by the methods of the theory of circuits, which enables to determine the flux linkages of the circuits that enter to the vector of discrepancies and depend on the set of currents of all motor's circuits.

Examples of the results obtained by calculations based on the above-described algorithm of periodic processes in the stable asynchronous mode and static characteristics provided that the excitation winding is shortened on the capacitors for the motor СДН3-2-19-49-24 (P = 1600 kW, U_l = 600 V, I = 180 A; I_z = 230 A; 2p=24) are presented in Fig 1,*a*,*b* and Fig. 2,*a*-*f*.

From presented in Fig. 1 dependencies of electromagnetic torque and effective stator current value on the capacitor's capacitance in the excitation winding of the SSM at sliding s = 1 it can be seen that when C = = 50 μF the resonant mode occurs, resulting in the torque becomes negative, the current value becomes unacceptably large and the motor start becomes impossible. However, the SSM has satisfactory starting properties at capacitance values of capacitors C = 45 μF. The multiplicity of the driving electromagnetic torque in relation to the nominal value for such a capacity is M^* = 3.48. Fig. 2 shows the periodic dependences of electromagnetic torque, the voltage on the capacitor and the excitation current at two values of capacitors' capacitance: C = 45 μF and C = 50 μF, which show that in the case of resonance (C = 50 μF) capacitor voltage and current excitation repeatedly exceed nominal values. In addition, the excitation winding current in the absence of resonance has a sharp third harmonic, which is absent in the resonance mode.

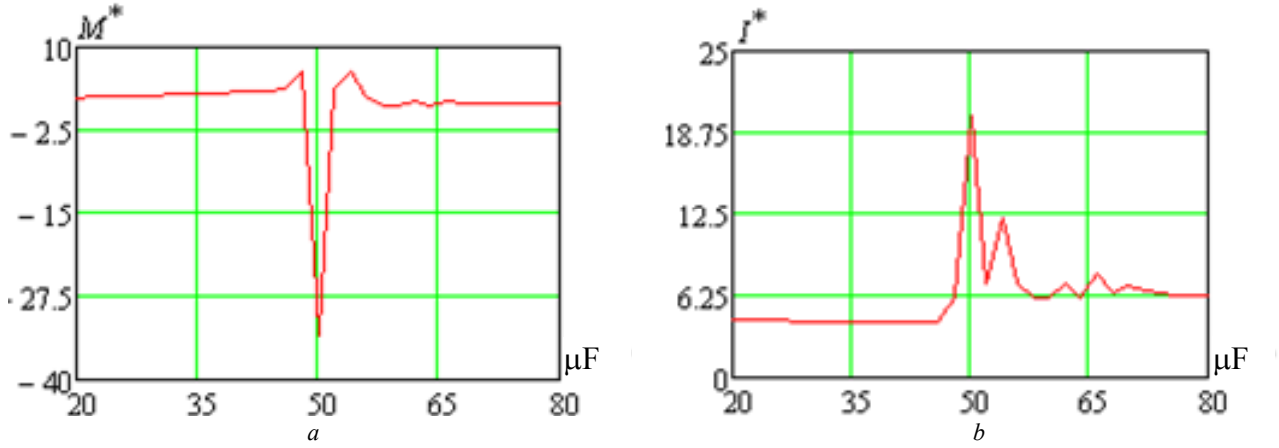

Fig. 1. Dependencies of the driving (s =1) electromagnetic torque (*a*) тand effective stator current value (*b*) on the capacitor's capacitance value in the motor's excitation winding: *a*) C = 50 μF, *b*) C = 45 μF

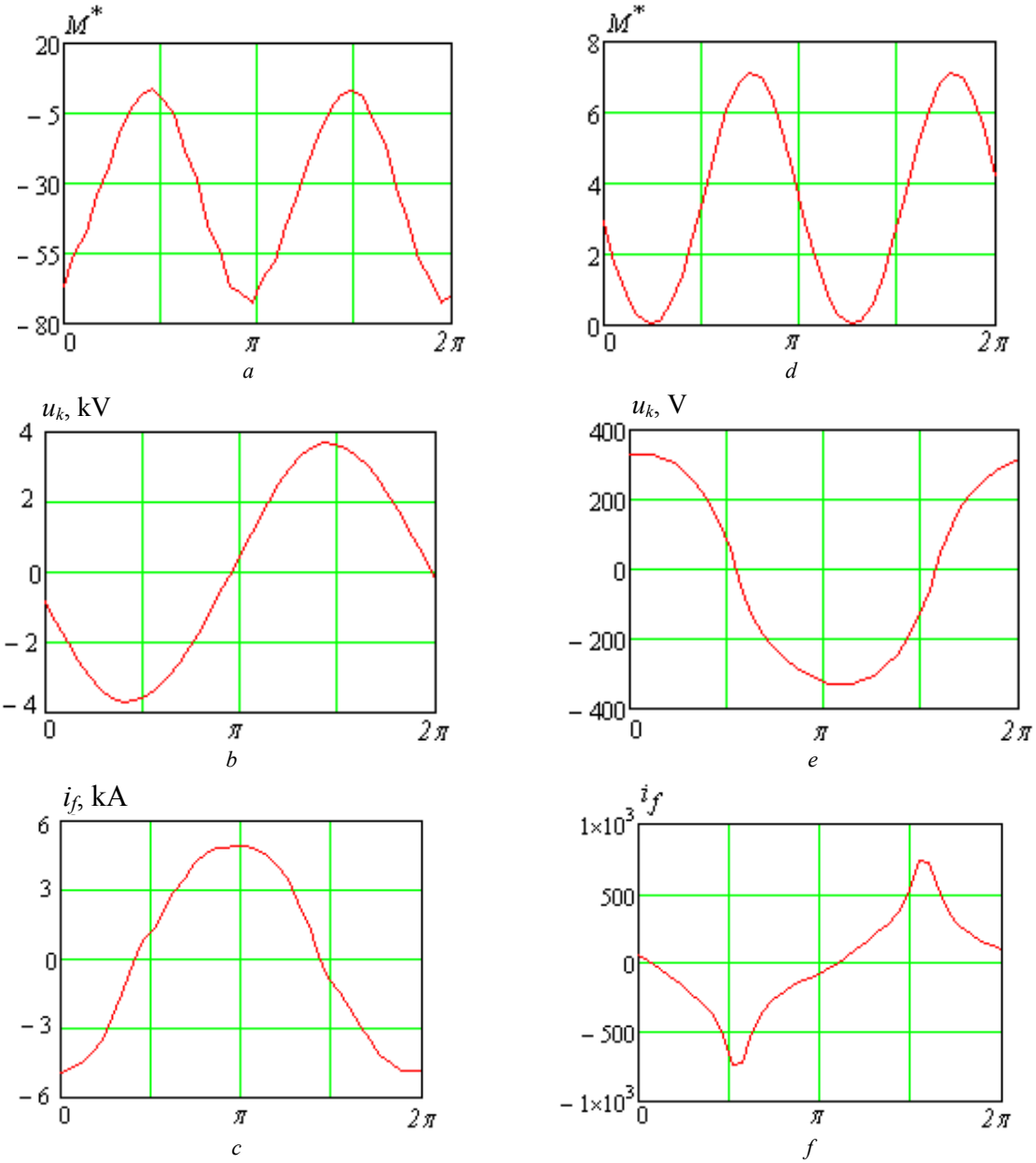

Fig. 2. Periodic dependencies of electromagnetic torque, voltage on the capacitor and excitation current at sliding s = 1 and two values of the capacitor's capacitance in the excitation winding: C = 50 μF (*a-c*) and C = 45 μF (*d-f*)

Conclusions.

1. By connecting capacitors in the excitation winding it is possible to significantly increase the driving electromagnetic torque of the SSM. However, the choice of needed to improve the starting properties of the SSM value of capacitors' capacitances the behavior of the motor in starting modes should be verified, because here may be a resonance in the excitation winding which leads to excessive growth of all circuits currents and the negative value of starting torque, which by the absolute value much exceeds the nominal value and the motor start is impossible.

2. Investigations of the operation of the SSM with capacitors in the excitation winding in asynchronous mode with high adequacy are possible only based on a complete DE system that describes the dynamic mode of operation. This makes it possible to carry out a multivariate analysis of the operation of the electric drive in the starting modes by methods of mathematical modeling.

3. The proposed algorithm and developed on its basis computer code for calculation of steady modes and static asynchronous characteristics of the SSM in the starting mode, allowing you to investigate dynamic processes of the motor start with different capacitors' capacitance values and identify a possibility of resonance phenomena with the aim of preventing them. On the basis of the calculation algorithm a mathematical model of the motor of a high level of adequacy, which considers nonlinearity of electromagnetic connections between circuits of the SSM, distributed along the stator bore the character of magnetic flux in the air gap, is assigned.

REFERENCES

1. Boroday V.A. *Racional'ni parametry i puskovi vlastyvosti synhronnyh dvyguniv z vazhkymy umovamy pusku*. Avtoref. diss. kand. tekh. nauk [Rational parameters and starting properties of synchronous motors with heavy start conditions. Abstracts of cand. tech. sci. diss.]. Lviv, 2009. 19 p. (Ukr).

2. Malyar V.S., Maday V.S., Dobushovska I.A. The dependence of a synchronous motor starting torque on the type and value of the resistance in its exitation winding. *Electromechanical and energy saving systems*, 2012, no.3(19), pp. 99-101. (Ukr).

3. Malyar V.S., Malyar A.V. Mathematical modeling of periodic modes of operation of electrical devices. *Electronic Modeling*, 2005, vol.27, no.3, pp. 39-53. (Rus).

4. Malyar V.S., Malyar A.V., Dobushovs'ka I.A. Simulation of asynchronous modes of synchronous motors with capacitors in the excitation circuit. *Electrical engineering & electromechanics*, 2012, no.5, pp. 31-33. (Ukr). **doi: 10.20998/2074-272X.2012.5.06.**

5. Malyar V.S., Malyar A.V., Dobushovska I.A. Static characteristics of synchronous motor with capacitors in excitation circuit. *Tekhnichna elektrodynamika*, 2012, no.1, pp. 57-62. (Ukr).

6. Pivnjak G.G., Kirichenko V.I., Borodaj V.A. About new direction in improvement large synchronous electric motors. *Technical electrodynamics. Thematic issue «Problems of modern electrical engineering»*. 2002, chapter 2, pp. 62-65. (Rus).

7. Pyvnjak G.G., Kyrychenko V.Y., Borodaj V.A., Petrov A.G. Selection and arrangement of external capacitors of synchronous motors with excitation winding of special design. *Materialy mezhd. nauchn.-tekhn. konf. «Problemy avtomatizirovannogo elektroprivoda. Teoriia i praktika»* [Proceedings of the Int. Sci.-Techn. Conf. «Problems of automated electric drive. Theory and practice»]. Kharkov, 2002, pp. 171-173. (Rus).

8. Filc R.V., Ljabuk N.N. *Matematicheskoe modelirovanie iavnopoliusnykh sinkhronnykh mashin* [Mathematical simulation of explicitly polarized synchronous machines]. Lvov, Svit Publ., 1991. 176 p. (Rus).

Received 25.05.2017

V.S. Malyar[1]*, Doctor of Technical Science, Professor,*
V.S. Maday[1]*, Candidate of Technical Science, Associate Professor,*
I.R. Kens[2]*, Candidate of Technical Science, Associate Professor,*
[1] Lviv Polytechnic National University,
12, S. Bandera Str., Lviv, 79013, Ukraine,
phone +380 32 2582119,
e-mail: mvs@polynet.lviv.ua, volodymyr.s.madai@lpnu.ua
[2] Ukrainian National Forestry University,
103, Gen. Tchuprynky Str., Lviv, 79057, Ukraine,
e-mail: ikens@mail.ru

How to cite this article:
Malyar V.S., Maday V.S., Kens I.R. Resonant processes in starting modes of synchronous motors with capacitors in the excitation windings circuit. *Electrical engineering & electromechanics*, 2017, no.4, pp. 21-25. **doi: 10.20998/2074-272X.2017.4.04.**

UDC 62-83:629.584 **doi: 10.20998/2074-272X.2017.4.05**

Ya.B. Volyanskaya, S.M. Volyanskiy, O.A. Onischenko

BRUSHLESS VALVE ELECTRIC DRIVE WITH MINIMUM EQUIPMENT EXCESS FOR AUTONOMOUS FLOATING VEHICLE

Purpose. Development of a brushless valve electric drive with a minimum apparatus excess for an autonomous floating vehicle. Methodology. The construction of models of an automated electric drive with a contactless DC motor and the subsequent technical implementation of such automated electric drive under various control methods are possible using coordinate transformations of differential equations describing the electric motor under the assumed assumptions. Results. The analysis of the current state of an automated electric drive with a brushless DC motor in a special technique is carried out, possible directions for the improvement of automated electric drives are determined. A simple technical solution of an automated electric drive with a brushless DC motor was proposed and its mathematical model for an electric drive of an automatic floating vehicle with improved technical and economic parameters was developed. Model of an automated electric drive with a brushless DC motor are carried out. Originality. A simple technical solution for the construction of an automated electric drive with a brushless DC motor is proposed, which excludes the use of intermediate computation of coordinates and an expensive encoder. Practical value. Model of the proposed scheme of an automated electric drive with a minimum hardware redundancy, which confirmed the operability of the proposed solution, were carried out. Analysis of the dynamic and static characteristics of the proposed scheme of an automated asynchronous electric drive with a brushless DC motor with a simplified rotor position sensor has made it possible to determine the maximum speed control range with an allowable level of its pulsations. References 20, tables 2, figures 7.

Key words: **automated electric drive, autonomous floating vehicle, DC brushless motor, Hall sensor, coordinate transformations, encoder.**

Предложено простое схемотехническое решение построения автоматизированного электропривода (АЭП) с бесконтактным двигателем постоянного тока (БДПТ), отличающееся исключением промежуточных программно-аппаратных преобразований координат, широтно-импульсного модулятора, двух регуляторов тока и высокоразрядного энкодера. Проведено компьютерное моделирование предложенной модификации АЭП с БДПТ и показана его работоспособность в заданных диапазонах регулирования скорости. На основании результатов моделирования АЭП с БДПТ обоснована возможность его применения в автономных плавательных аппаратах. Библ. 20, табл. 2, рис. 7.

Ключевые слова: **автоматизированный электропривод, автономный плавательный аппарат, бесконтактный двигатель постоянного тока, датчик Холла, координатные преобразования, энкодер.**

Introduction. Currently, in most electromechanical systems of small-sized autonomous floating vehicle (AFV) for various purposes, brush DC electric motors (DCM) are used. Such motors have a significant starting torque, excellent adjusting and dynamic characteristics [1-3], as well as well-developed control systems. Because brush DCM have irreparable defects (frequent maintenance, high mechanical wear, acoustic noise, sparking), more and more utilization in foreign samples of the AFV have contactless DC motors (BLDCM), in other words – *Brushless DC* (*BLDC*) *motors* [4-6]. Such electric motors, due to the use of high-coercivity magnets in the excitation system, have the best energy characteristics in comparison with classical DC electric motors and induction electric motors [9, 10]. The adjusting, dynamic and static characteristics of modern automated electric drives (AED) with vector control methods of BLDCM are close to properties of AED based on high-frequency pulse-width modulation (PWM) with a brush DCM of independent excitation.

AED with BLDCM foreign production (Japan, USA, Western Europe) are widely used in domestic aviation, medicine, various industries. It should be noted that the majority of mass-produced foreign AED based on BLDCM are oriented to complex applications. These are, for example, high-precision tracking devices, numerical control machines, electromechanical systems where a very high speed control range, precise positioning or tracking modes are required. That is why such AEDs have very high selling prices. Thus, the AED of the *Mitsubishi Electric* Company MR-C10A-UE, 100W, 3000 rpm with the speed control range D = 1000 in the middle of 2016 was released in Ukraine at a price of almost USD 600 (approximately USD 400 – a system unit, USD 200 – BLDCM with a built-in high-speed encoder). Such solutions of the leading manufacturers of electrical equipment (*Mitsubishi*, *Danfoss*, *ABB* and others) have very high functional and technological properties, developed self-diagnostics and protection systems, management capabilities over the local network and have many other additional service functions. Despite the relatively high cost of the BLDCM, such parameters as reliability, a high value of the design coefficient C_m, speed and low-speed reception allow us to consider very promising application of AED with BLDCM in special marine technology [7, 8] of domestic production, for example, in experimental samples of the AFV type «Hydrograph», Nikolaev (Table 1). If you analyze the basic requirements for AED for devices of a similar type, you can see that to provide the basic functions of the AFV, it is enough to have a range of speed control D = 3 ... 15 with the accuracy of maintaining it at the lower control ranges of up to 10 %. At the same time, there is no need for most internal protections, interfaces, a high-resolution encoder is not needed.

In Ukraine, automated electric drives with BLDCM are only beginning to be manufactured (LLC «Electrical Engineering – New Technologies», Odessa), and their circuitry base has not been fully worked out yet. Since specialized AFVs, as dual-purpose devices, are in high demand, and since there are no mass production of such devices in Ukraine, the creation of an AFV with simple and functional electromechanical systems based on the BLDCM based on the domestic industrial base is an important and urgent scientific and technical task.

Table 1

Some characteristics of the experimental AFV «Hydrograph» (Nikolaev)

No.	Indicator	Value
1	Mass of the device	65 kg
2	Propulsion motors power, design	2×250 W, baro-unloaded
3	Working speed range of the device	0.25…2 m/s
4	Hydropropulsion complex	Direct transmission
5	Diameter of screws in the nozzle	250 mm
6	Performance with a step change in the set speed	3 s
7	The accuracy of maintaining the speed of horizontal rectilinear displacement on the lower characteristic of the range	0.05 m/s
8	Maximum speed overshoot	20 %

The goal of the paper is development of a contactless valve electric drive with a minimum hardware excess for an autonomous floating device.

Main material. It is generally known that the BLDCM is a synchronous AC motor whose stator windings are powered by a frequency converter that switches the phase currents as a function of the angular position of the rotor with an envelope frequency equal to the number of poles of the rotor multiplied by the angular rotational speed of the rotor. For operation of the AED based on the BLDCM in a wide range of speed control a high-quality (1000 or more pulses per revolution) rotor position sensors (RPS, encoders) are needed and therefore expensive ones are used [11, 12].

Simpler AED with BLDCM use scalar control methods and, often, experimental BLDCM samples are produced on the basis of serial induction motors, replacing the short-circuited rotor with a rotor with permanent high-coercivity magnets, using the simplest rotor position sensors – based on Hall effects, photoelectric or induction effects [13].

Traditionally, the development and research of the majority of modern AED are carried out with the help of coordinate transformations (KT). It is known that KT of variables are valid if the basic assumptions for the generalized electric machine are fulfilled: the sinusoidal distribution of the MMF of the stator winding with sinusoidal feeding of the symmetrically distributed stator and rotor windings. Therefore, to apply KT for investigations of AED with BLDCM and scalar control, there are no formal conditions: relatively simple BLDCMs are created with lumped windings and, since the stator windings are powered from a rectangular-shaped voltage source, their MMF is close to rectangular.

In order to increase the competitiveness of the built-in electromechanical control systems of the AFV created on the domestic element base, the authors carried out investigations [14-16], which, as a result, allowed to abandon the vector control method of the BLDCM [17, 18]. Naturally, the use of RPS with a low number of pulses per revolution [13] leads to a significant reduction in the range of speed control and an increase in the pulsations of the electromagnetic torque. Taking into account the inertial nature of the load of the propulsion complex [19, 20] of the AFV and its «fan» nature, and also the not very high requirements for the range and accuracy of maintaining the speed, according to modern hardware capabilities, it can be assumed that there are reserves for simplifying the circuit design basis for constructing the AED with BLDCM for AFV.

Since in BLDCM, applied in experimental AFV samples, the windings are symmetrically located on the stator, then under the rectangular form of the supply voltage, it is possible to determine the main voltage harmonics and MMF. Since the assumptions adopted in the model of a generalized electric machine are satisfied for the first harmonics, then subsequently further coordinate transformations are also valid, and the main properties and characteristics of the BLDCM with scalar control can be identified on the basis of two-phase models.

The indicated approach is often used, for example, in the analysis of the operation of induction electric motors (IM) powered by frequency converters (FC). Note that if the symmetry conditions for an electrical machine are made constructively and its power is supplied from a non-sinusoidal source, then the application of coordinate transformations of variables will be adequate to real physical processes only for quasi-steady dynamic modes. In such modes, the speed and the electromagnetic torque oscillate about the mean values, while the amplitude, frequency, and shape of the oscillations of the variables will be different for the two- and three-phase descriptions of the AED.

Thus, the construction of models of AED with BLDCM and the subsequent technical realization of such AED under different control methods are possible using coordinate transformations of differential equations describing the electric motor under the assumed assumptions. It is clear that the technical implementation of the AED should be justified by comparing the operation modes of the BLDCM with various control methods to the characteristic reactive static load, which for the AFVPA is a fan type.

In the rotating coordinate system *d-q*, the coordinate transformations for the equivalent voltages of the symmetrical winding of the BLDCM stator are related to the phase voltages by the two systems of equations – (1) and (2). When changing from a three-phase to a two-phase coordinate system {3/2}, the following is valid:

$$\left.\begin{aligned}
u_d(\tau) &= \frac{2}{3}[U_a(\tau)\cdot\sin(\omega_c\cdot\tau)+U_b(\tau)\times \\
&\times\sin\left(\omega_c\cdot\tau-\frac{2\pi}{3}\right)+U_c(\tau)\cdot\sin\left(\omega_c\cdot\tau+\frac{2\pi}{3}\right)]; \\
u_q(\tau) &= \frac{2}{3}[U_a(\tau)\cdot\cos(\omega_c\cdot\tau)+U_b(\tau)\times \\
&\times\cos\left(\omega_c\cdot\tau-\frac{2\pi}{3}\right)+U_c(\tau)\cdot\cos\left(\omega_c\cdot\tau+\frac{2\pi}{3}\right)]; \\
u_0(\tau) &= \frac{1}{3}[U_a(\tau)+U_b(\tau)+U_c(\tau)],
\end{aligned}\right\} \quad (1)$$

and when changing from a two-phase to a three-phase coordinate system {2/3}:

$$\left.\begin{aligned}
U_a(\tau) &= u_d(\tau)\cdot\sin(\omega_c\cdot\tau)+u_q(\tau)\times \\
&\times\cos(\omega_c\cdot\tau)+u_0(\tau); \\
U_b(\tau) &= u_d(\tau)\cdot\sin\left(\omega_c\cdot\tau-\frac{2\pi}{3}\right)+ \\
&+u_q(\tau)\cdot\cos\left(\omega_c\cdot\tau-\frac{2\pi}{3}\right)+u_0(\tau); \\
U_c(\tau) &= u_d(\tau)\cdot\sin\left(\omega_c\cdot\tau+\frac{2\pi}{3}\right)+ \\
&+u_q(\tau)\cdot\cos\left(\omega_c\cdot\tau+\frac{2\pi}{3}\right)+u_0(\tau),
\end{aligned}\right\} \quad (2)$$

where $U_a(\tau)$, $U_b(\tau)$ and $U_c(\tau)$ are the phase voltages of the three-phase system; $u_d(\tau)$ and $u_q(\tau)$ are the projections of the phase voltages on the axes of the rotating with frequency ω_c coordinate system d-q; $u_0(\tau)$ is the vector of the zero sequence equal to zero at zero initial conditions and the stator winding symmetry; $\Theta=\omega_c\cdot\tau$ is the angular position of the vector in the coordinate system d-q. We emphasize that for other variables of the BLDCM (currents, MMF), the coordinate transformations {3/2} and {2/3} are valid.

In the case of vector single-zone control of the BLDCM, in the most general case, the projections of the phase voltages $u_d(\tau)$ and $u_q(\tau)$ are formed by the signals of the high-order RPS in the function of given from the external source along the corresponding coordinate axes voltages. This formation is carried out, for example, by means of a sinusoidal-cosine rotating transformer (SCRT) having a small proper delay time τ_n, with the geometric angle of the RPS setting is oriented along the d axis. Then:

$$\left.\begin{aligned}
u'_d(\tau) &= u_d(\tau)\cdot\cos(\omega_c\cdot\tau_n)-u_q(\tau)\cdot\sin(\omega_c\cdot\tau_n); \\
u'_q(\tau) &= u_q(\tau)\cdot\cos(\omega_c\cdot\tau_n)+u_d(\tau)\cdot\sin(\omega_c\cdot\tau_n).
\end{aligned}\right\} \quad (3)$$

We write the equations of the BLDCM in the coordinate system d-q, tied to the rotational angular frequency of the rotor.

Equations of electrical equilibrium in the operator form:

$$\left.\begin{aligned}
u_d(s) &= R_s\cdot i_d(s)+L_d\cdot s\cdot i_d(s)-\omega_c(s)\times \\
&\times L_q\cdot i_q(s); \\
u_q(s) &= R_s\cdot i_q(s)+L_q\cdot s\cdot i_q(s)+\omega_c(s)\times \\
&\times L_d\cdot i_d(s)+\omega_c(s)\cdot\psi_e(s),
\end{aligned}\right\} \quad (4)$$

where R_s is the stator phase resistance; $i_d(s)$, $i_q(s)$ и L_d, L_q are the currents and inductances by coordinate axes d-q, respectively; $\psi_e(s)$ = ψ_e = const is the flux linkage determined by the coercive force of the rotor magnets.

We preliminary analyze the properties of a vector single-band AED with a BLDCM for a single-mass constant reactive load and a RPS functioning on the basis of a sinusoidal-cosine rotating transformer (SCRT), i.e. «ideal» position sensor. In this case, $L_d = L_q$, the equations of motion of the AED and the electromagnetic torque will be as follows:

$$M(s)-M_c(s)=J\cdot s\cdot\omega(s)\,; \quad (5)$$

$$M(s)=\frac{m\cdot p_n}{2}\cdot i_d(s)\cdot\psi_e\,, \quad (6)$$

where p_n and m are the number of pole pairs and number of phases of BLDCM; $\omega(s)$ = $\omega_c(s)\cdot p_n$ is the angular frequency of the rotation of the BLDCM rotor; J is the moment of inertia of the BLDCM rotor.

A simplified functional scheme of AED with BLDCM functioning on the basis of PWM and using high-rate RPS when powered from an industrial network is shown in Fig. 1. Note that it is on the basis of such a scheme that most foreign-made AEDs are created.

In Fig. 1 setting signals are indicated by «*», the current stabilization circuit in coordinate d and the control circuit for the clamp circuit (VT, R_T) are not shown, the angular position of the rotor is defined as $\Theta(s)=s\cdot\omega(s)$.

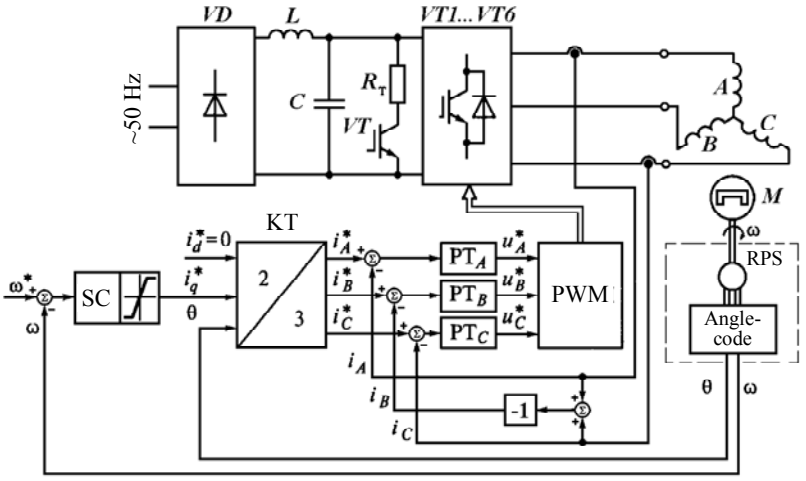

Fig. 1. Simplified functional scheme of a single-zone vector AED for AFV based on BLDCM and high-rate RPS

The authors offer a simpler technical solution, which, although it limits the functional and technological capabilities of the electric drive, but allows the implementation of its technical characteristics in accordance with Table 1. Simplification is associated with the exclusion of high-rate RPS and the installation of a simpler RPS [13], as well as the exclusion of PWM and the KT unit from the control system.

Let's consider an example of construction of a contactless valve electric drive with a minimum hardware Excess for an autonomous floating device with total weight of 20 kg. For further analysis, let us consider the operation of the system constructed on the basis of the scheme shown in Fig. 1 using the experimental sample of BLDCM with high-coercivity samarium-cobalt magnets produced by LLC «Electrical Engineering – New Technologies» (Odessa). The main technical parameters of the BLDCM are given in Table 2.

Table 2

Main parameters of the BLDCM

Number of poles	8
Number of phases	3
Rated feed voltage, V	24
Rated rotated speed, rad/s	418.9
Rated torque, N·m	0.041
Maximal torque, N·m	0.17
Rated power, W	17
Phase resistance at 60 °C, Ω	1.2
Maximal permitted current, A	6.4
Phase inductance, mH	1.0
Rotor moment of inertia, kg·m^2	$1 \cdot 10^{-4}$

In Fig. 2,*a* a diagram of the power part of the inverter is presented, and in Fig. 2,*b* – a functional PWM circuit with distributor of control pulses of inverter keys is shown. The operation of the speed controller SC and current controllers CC corresponds to known schemes. The coordinate converter KC is described by system (1), BLDCM and RPS – by equations (2)-(6).

The results of simulation of the starting process with M_r=0.04 N·m and the subsequent load shedding at time τ = 0.35 s to the value M_r=0.015 N·n for the AED corresponding to the scheme shown in Fig. 1 at generator frequency *G* of PWM 8 kHz and $\tau_n=0.25 \cdot 10^{-3}$ s are shown in Fig. 3. The system was simulated in the *Matlab / Simulink* environment.

With the help of coordinate transformations, it is possible to simulate AED with BLDCM in natural axes (for a three-phase model) and, if necessary, take into account the features introduced by higher harmonics of MMF and voltages. In the course of the investigations, it was found that when the PWM frequency is increased by more than 20 kHz, the time τ_n reduced by an order of magnitude and reducing the hysteresis loop of the *DA*1-*DA*3 elements, a high speed control range (if necessary, 500 and more) can be obtained with practically zero torque pulsations. The application of a rather complex software and hardware base of AED with BLDCM according to the scheme shown in Fig. 1 (high-rate RPS and microprocessor with programmable PWM, two galvanically separated current sensors, three current controllers) dramatically increases the cost of such AED with excess for AFV range of speed regulation of the motor shaft of the propulsion complex [19, 20] of AFV.

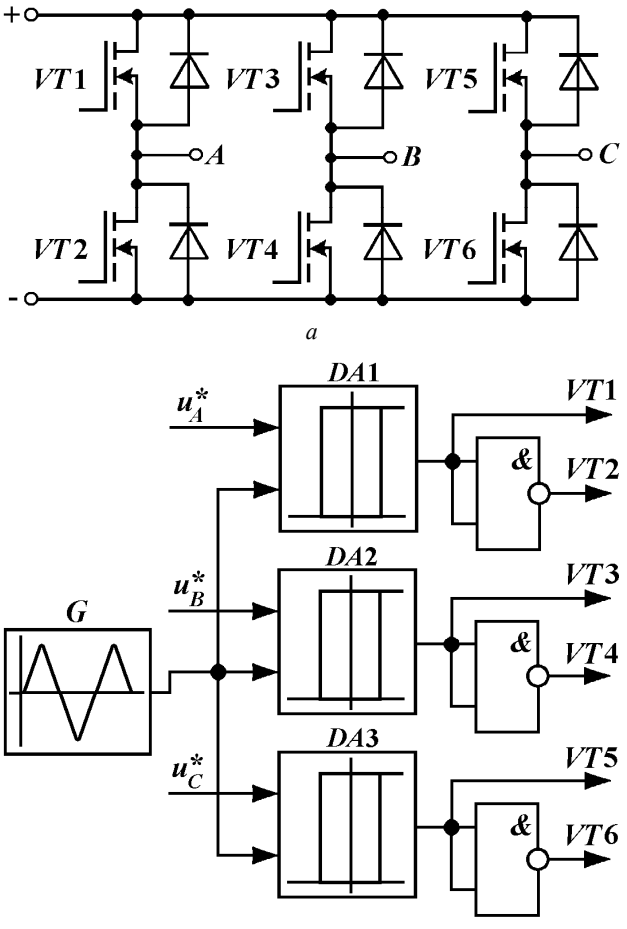

Fig. 2. The circuit of the transistor inverter (*a*) and PWM (generator *G*, comparators *DA*) with a distributor of pulses on the elements «2AND-NO» (b)

A simpler technical solution of AED with a BLDCM is proposed, which excludes the use of intermediate computation of coordinates and an expensive encoder (Fig. 4).

This AED uses as RPS three geometrically offset Hall sensors [13] and a specialized inexpensive control microcontroller *MC33035*. The main function of the microcontroller is to generate the pulse distribution (PD) signals to the *VT*1, ... , *VT*6 keys of the inverter by the RPS commands. Another feature of the proposed solution is the feature of realizing negative current feedback. This feedback is realized with the help of only one current sensor installed in the power supply circuit, which made it possible to apply the current controller common for the three phases, although slightly reducing the accuracy of its stabilization. The speed feedback signal is formed from the impulse signals of an extremely simple RPS (6 pulses per revolution of the shaft, [13]) using an active analog filter AF with dominant time constant of 0.015 s, which significantly affects the dynamics of the AED.

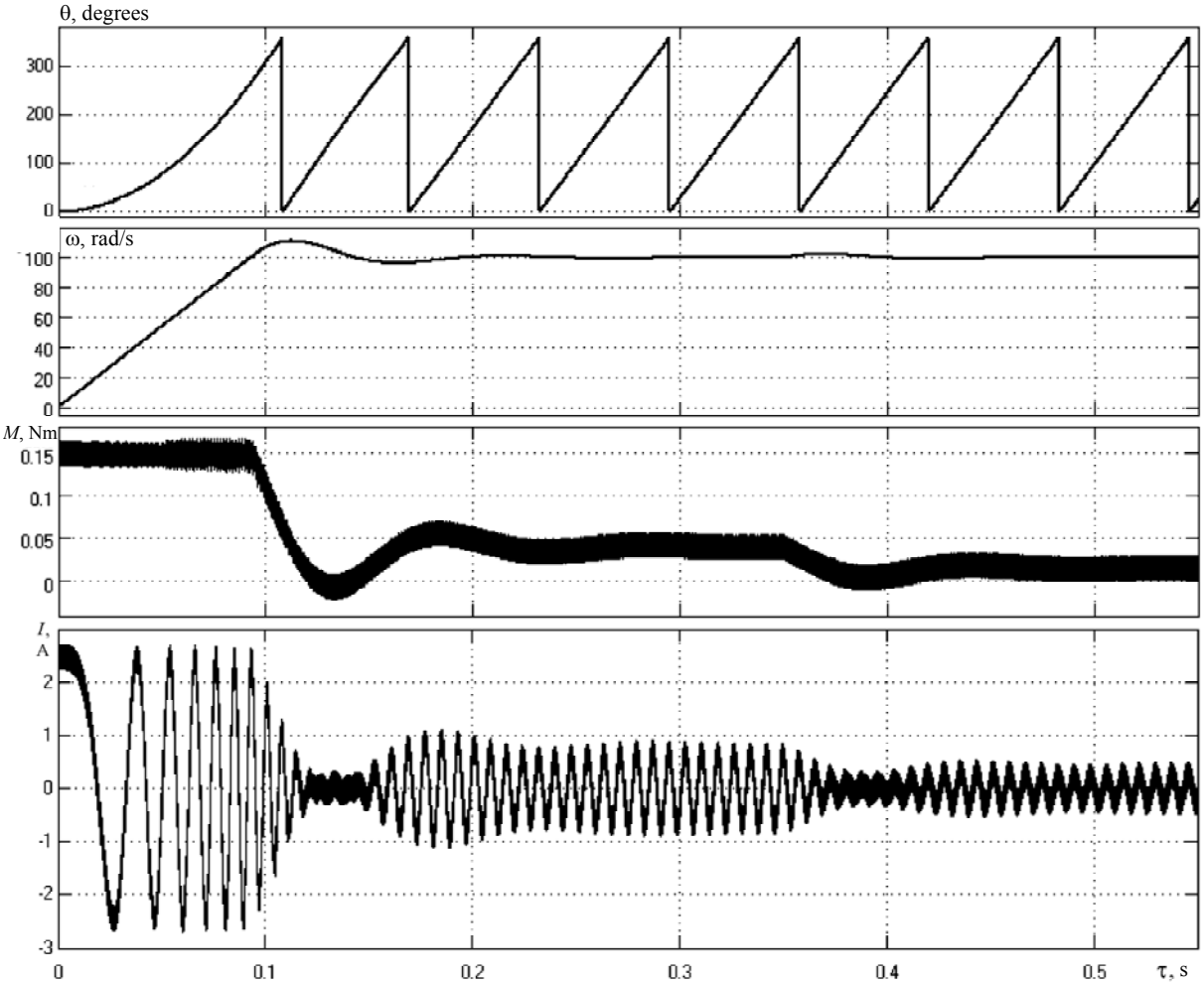

Fig. 3. Start of AED with BLDCM (according the scheme presented in Fig. 1) at rated M_r with a subsequent load shedding to 0.015 N·m

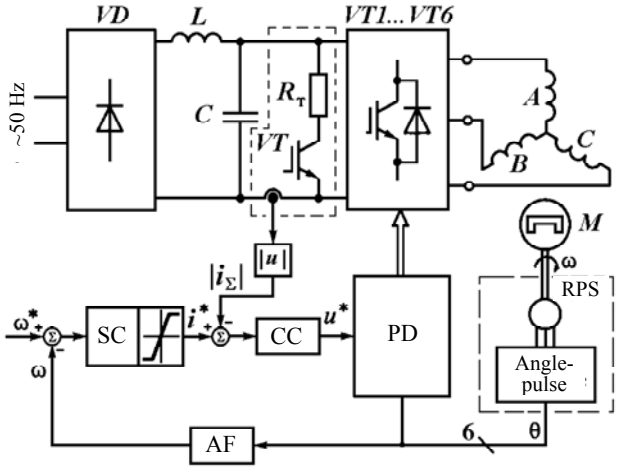

Fig. 4. Simplified functional diagram of single-zone AED for AFV based on BLDCM with Hall RPS

Let us compare the solutions represented by the schemes in Fig. 1 and Fig. 4.

1. Preliminary analysis of design solutions, based on a comparison of the hardware of the AED, constructed according to the schemes depicted in Fig. 1 and Fig. 4, points to certain advantages of AED with BLDCM, constructed according to the scheme shown in Fig. 4:

a) the expected reduction in the cost of the structure in small-scale production by 18 ... 25 %;

b) decrease in the weight and dimensions of the control board by 5 ... 7 %;

c) improving the reliability of the structure by using a smaller number of components, by 7 ... 14 %.

It is obvious that with such a technical solution, the torque pulsations on the motor shaft will increase, but the cost of the technical realization of the electric drive will be significantly less.

2. Graphs of the formation at the output of the PD of logical signals for controlling the keys of the inverter *VT*1, ..., *VT*6 (according to Fig. 2,*a*) in the function of the RPS signals V_{H1}, V_{H2} and V_{H3} in the mode of 50 % duty cycle at the steady rotor speed are shown in Fig. 5. The graphs of the change in the electric and mechanical angular position of the BLDCM eight-pole rotor are also shown here.

Fig. 6 presents the results of simulating the start-up processes of AED with BLDCM, according to the scheme shown in Fig. 4: start in the «linear» mode at speed of 20 rad/s (graphs 1) and start in the current limiting mode (graphs 2). It is determined that the maximum value of the speed control range in this case can reach $D \approx 30$, which is quite enough for performing any technological tasks of the AFV. In Fig. 7 the graphs of the currents change in the phases of the BLDCM at start-up for speed of 100 rad/s are additionally presented confirming the efficiency of the current control circuit with one common current sensor.

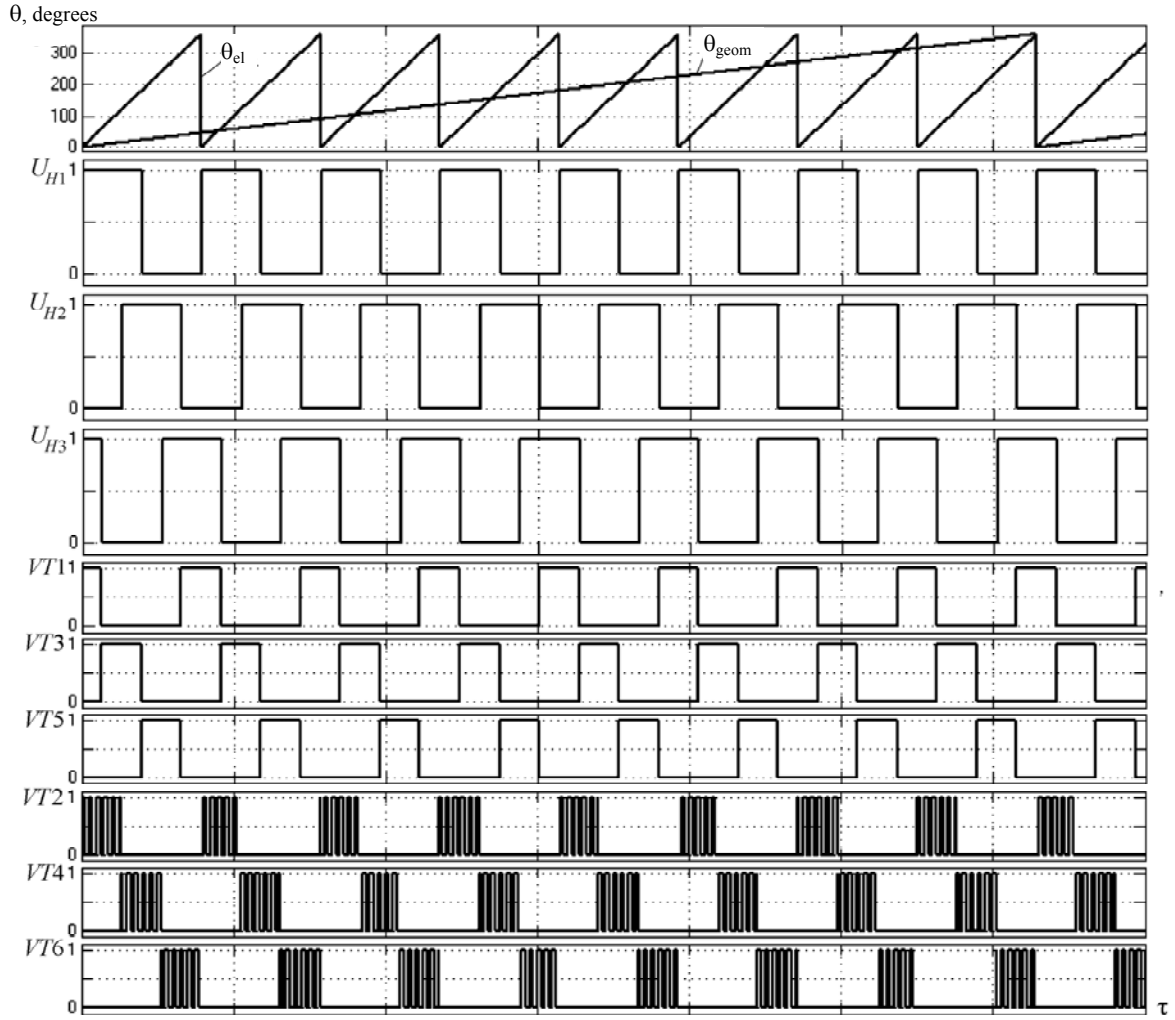

Fig. 5. Formation of key control pulses of the inverter *VT*1, …, *VT*6 at the output of the PD as a function of the RPS signals (V_{H1}, V_{H2}, V_{H3}) and change in the angular position Θ of the BLDCM eight-pole rotor

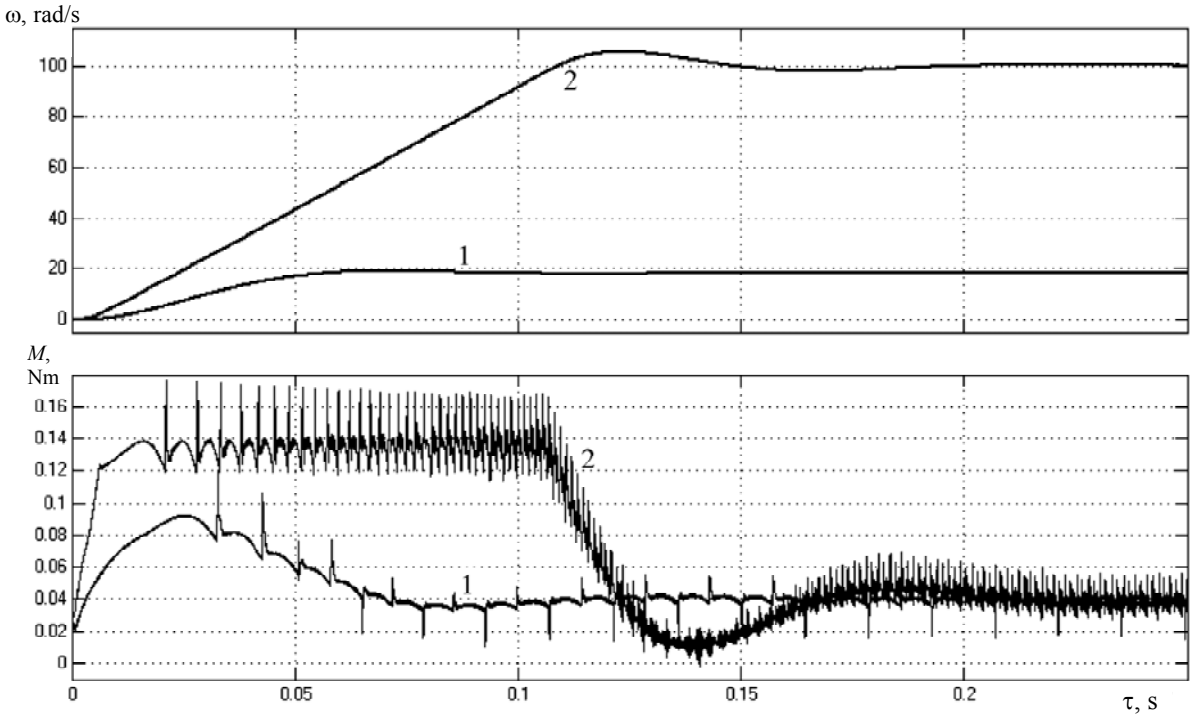

Fig. 6. Start of AED with BLDCM at M_r=0.04 N·m (according the circuit presented in Fig. 5): 1 – for small rotation speed (till current limiting); 2 – for high rotation speed (at current limiting)

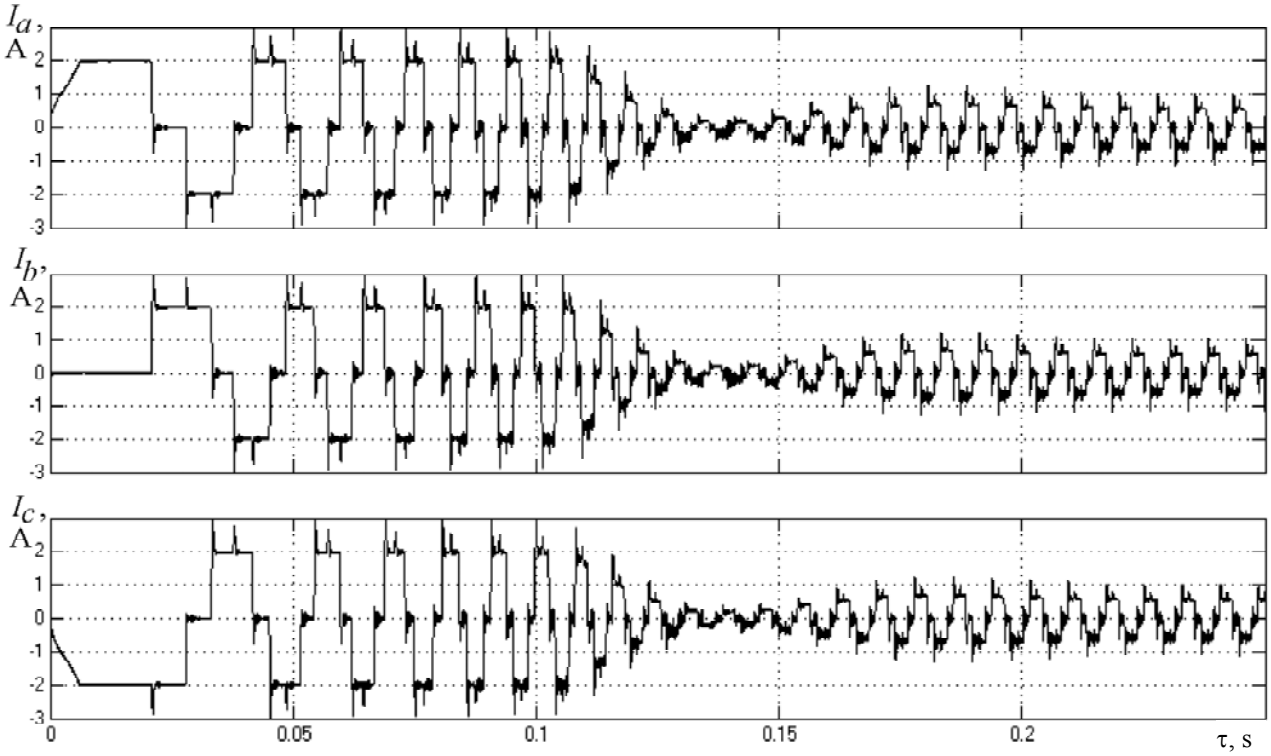

Fig. 7. BLDCM phase currents at start in the current limiting mode

The graphs shown in Fig. 6 and Fig. 7 were obtained by installing the RPS with an «advance» angle Θ_{aa} of 45 electrical degrees, which was determined after a number of model investigations of the proposed AED with minimal hardware excess. The rate of increase in speed was limited by the active filter (AF) of the second order and the torque pulsations allowed for the BDPT.

Thus, if we compare the start-up graphs (Fig. 3 and Fig. 7) to the frequency of 100 rad/s of two AEDs functioning on the basis of the solutions shown in Fig. 1 and Fig. 4, then one can be convinced only of the insignificant differences in the processes of speed variation.

Conclusions.

1. Based on the analysis of the specified technical characteristics of the electric drive of an autonomous floating vehicle with a brushless DC motor («fan» load character, speed control range 1-10 with allowable overshoot of 20 %), the possibility of implementing an electric drive with minimum hardware excess due to justified rejection of PWM modulation and vector control with a high-resolution encoder is shown.

2. Model investigations of the proposed circuit of the electric drive in the *Matlab / Simulink* software environment have been carried out, which confirmed the operability of the proposed technical solutions and the possibility of realizing the required static and dynamic characteristics of the electric drive with maximum speed control range of 1-30 at acceptable level of its pulsations up to 10 % under inertia conditions of the load comparable with the moment of inertia of the applied motor.

3. The expected reduction in the cost of the structure of the electric drive with BLDCM performed according to the proposed circuit with minimal hardware excess, in the small-scale production will be 18 ... 25 %, while reducing the weight and size of the control card will be 5 ... 7 %.

REFERENCES

1. Mokhtar A.S.N., Raez M.B.I., Marufuzzaman M., Ali M.A.M. Hardware implementation of a high speed inverse park transformation using CORDIC and PLL for FOC brushless servo drive. *Electronics and Electrical Engineering*, 2013, vol.19, no.3, pp. 23-26. **doi: 10.5755/j01.eee.19.3.1267.**

2. Srinivasan K., Vijayan S., Paramasivam S., Sundaramoorthi K. Power Quality Analysis of Vienna Rectifier for BLDC Motor Drive Application. *International Journal of Power Electronics and Drive System*, 2016, vol.7, no.1, pp. 7-16.

3. Archa V.S., Rajan C. Sojy. A comparison on the performance of BLDC motor drive with DBR, Luo and BL-Luo. *Imperial Journal of Interdisciplinary Research*, 2016, vol.2, no.9, pp. 1038-1042.

4. Topaloglu I., Korkmaz F., Mamur H., Gurbuz R. Closed-loop speed control of PM-BLDC motor fed by six Step inverter and effects of inertia changes for desktop CNC machine. *Electronics and Electrical Engineering*, 2013, vol.19, no.1, pp. 7-10. **doi: 10.5755/j01.eee.19.1.3244.**

5. Noyal Doss M.A., Vijayakumar S., Mohideen A.J., Kannan K.S., Sairam N.D.B., Karthik K. Reduction in cogging torque and flux per pole in BLDC motor by adapting U-clamped magnetic poles. *International Journal of Power Electronics and Drive Systems (IJPEDS)*, 2017, vol.8, no.1, pp. 297-304. **doi: 10.11591/ijpeds.v8.i1.pp297-304**.

6. S. Masroor, Peng C., Anwar Ali Z., Aamir M. Leader following consensus of BLDC motor speed with sampling intervals. *International Journal of Modeling and Optimization*, 2016, vol.6, no.2, pp. 119-123. **doi: 10.7763/IJMO.2016.V6.515**.

7. Jaber A.S. A novel tuning method of PID controller for a BLDC motor based on segmentation of firefly algorithm. *Indian Journal of Science and Technology*, 2017, vol.10, no.6, pp. 1-5. **doi: 10.17485/ijst/2017/v10i6/111209.**

8. Kim I.-G., Hong H.-S., Go S.-C., Oh Y.-J., Joo K.-J., Lee J. A study on the stable sensorless control of BLDC motor inside auxiliary air compressor. *Journal of Electrical Engineering and Technology*, 2017, vol.12, no.1, pp. 466-471. **doi: 10.5370/JEET.2017.12.1.466.**

9. Mullick J.A. Fuzzy controller for speed control of BLDC motor using MATLAB. *International Research Journal of Engineering and Technology*, 2017, vol.4, no.2, pp. 1270-1274.

10. Bhadani A., Koladiya D., Devani J., Tahiliani A. Modeling and controlling of BLDC motor. *International Journal of Advance Engineering and Research Development*, 2016, vol.3, no.3, pp. 139-144.

11. Singh S.Kr., Katal N., Modani S.G. Optimization of PID controller for brushless DC motor by using Bio-inspired algorithms. *Research Journal of Applied Sciences, Engineering and Technology*, 2014, vol.7, no.7, pp. 1302-1308. **doi: 10.19026/rjaset.7.395**.

12. Kamil O., Kaan C., Abdullah B., Adnan D. Real-time speed control of BLDC motor vased on fractional sliding mode controller. *International Journal of Applied Mathematics, Electronics and Computers*, 2016, vol.4, pp. 314-318.

13. Karpovich O.Ya., Onishchenko O.A. Features of the implementation of the feedback sensor for speed and position in the valve-inductor electric drive. *Bulletin of NTU «KhPI»*, 2003, no.11, pp. 65-70. (Rus).

14. Karpovich O.Ya., Porajko A.S., Onishchenko O.A. Experimental-debugging control scheme of the valve-inductor electric motor. *Scientific papers of Donetsk National Technical University*, 2003, no.67, pp. 152-155. (Rus).

15. Karpovich O.Ya., Onishchenko O.A. Development of models with simplified current loops for a valve-inductor microelectro drive. *Bulletin of NTU «KhPI»*, 2004, no.43, pp. 91-94. (Rus).

16. Volyanskaya Ya. B., Volyanskiy S.M. Features of construction of automatic control systems by motion of objects of marine robotics. *Electrotechnic and computer systems*, 2016, no.23(99), pp. 39-44. (Ukr).

17. Mutanov G.K., Shadrin N.V., Arinova A.N. Comparative analysis of methods of developing automatic control systems. *Vestnik of D. Serikbaev East Kazakhstan state technical university*, 2010, no.2, pp. 110-117. (Rus).

18. Karpovich O. YA., Onishchenko O. A., Radimov I. N. Two-quadrant valve-inductor electric drive. *Transactions of Kremenchuk State Polytechnic University*, 2003, no.5(22), pp. 56-60. (Rus).

19. Budashko V.V., Yushkov E.A., Onishchenko O.A. Improvement of the control system of the propulsion device of the combined propulsion complex. *Bulletin of NTU «KhPI»*, 2014, no.38(1081), pp. 45-51. (Ukr).

20. Budashko V.V., Onischenko O.A., Yushkov E.A. Physical modeling of multi-propulsion complex. *Collection of scientific works of the Military Academy (Odessa City)*, 2014, no.2, pp. 88-92. (Rus).

Received 01.06.2017

Ya.B. Volyanskaya[1], *Candidate of Technical Science, Associate Professor,*
S.M. Volyanskiy[1], *Candidate of Technical Science, Associate Professor,*
O.A. Onischenko[2], *Doctor of Technical Science, Professor,*
[1] Admiral Makarov National University of Shipbuilding,
9, Heroiv Ukrainy Ave., Mykolayiv, 54000, Ukraine,
phone +380 67 7981870, e-mail: yanavolyanskaya@gmail.com
[2] Odessa National Maritime Academy,
8, Didrikhson Str., Odessa, 65029,
phone +380 48 7775774, e-mail: oleganaton@gmail.com

How to cite this article:
Volyanskaya Ya.B., Volyanskiy S.M., Onischenko O.A. Brushless valve electric drive with minimum equipment excess for autonomous floating vehicle. *Electrical engineering & electromechanics*, 2017, no.4, pp. 26-33. **doi: 10.20998/2074-272X.2017.4.05.**

UDC 622.647.2 **doi: 10.20998/2074-272X.2017.4.06**

V.I. Lobov, K.V. Lobova

THE THYRISTOR CONVERTER INFLUENCE ON THE PULSATIONS OF THE ELECTROMAGNETIC TORQUE OF THE INDUCTION MOTOR AT PARAMETRICAL CONTROL

Purpose. ***The purpose of the work is to identify the parameters influence of the electric motor, the power circuits elements of the converters, built on resistor-thyristor modules, the static torque and the moment of inertia of the mechanism on the vibrational components of the induction motor's electromagnetic moment.*** ***Methodology.*** ***The methodological basis for the solution of the task is an integrated approach. The application of the generalized control circuit for an induction electric motor and its mathematical description made it possible to analyze various power circuits of parametric control of an induction electric motor. To create a common control algorithm, effectively use the computer for calculations. To perform qualitative and quantitative analysis of the amplitudes and frequencies of the vibrational components of the electromagnetic torque of the electric motor.*** ***Results.*** ***The conducted researches allowed to reveal the peculiarities of the effect of the parameters of the elements of various types of power circuits of the parametric control converters on the vibrational components of the electromagnetic torque of an induction electric motor. Calculations and physical modeling have been performed, it has been possible to establish the conditions for the occurrence of electromagnetic pulsations and to determine the ways of their elimination. It was found that the magnitude of pulsations of the electromagnetic moment of an induction electric motor in quasi-permanent modes depends on the selected power circuit of the converter's stator and rotor commutators, the composition of the elements included in them, and the connection circuits. Comparison of calculated and experimental waveform when starting induction electric motors indicates that the pulsation of the electromagnetic torque is affected by: the size of the opening angle of the valves, their control methods, the rotor speed, the parameters of the electric motor and the mechanism are static and inertial moments. At the same time, it was revealed that the use of resistor-thyristor modules in the power circuits of the stator and rotary commutators reduces the magnitude of the pulsation of the electromagnetic torque of the induction electric motor. Increase the value of its maximum and average torques. Limit the magnitude of the shock and alternating torques when it starts and the transition from one speed to another.*** ***Scientific novelty.*** ***It is proposed to use a generalized circuit of parametric control of an induction electric motor for studying the change in the electromagnetic torque. The circuit consists of resistor – thyristor modules in stator and rotary commutators. The presented technique allowed simultaneously to investigate transients during the control of an induction electric motor by various power circuits of converters. The results of calculations allow choosing the necessary power circuit, taking into account the vibrational components of the electromagnetic torque of the induction motor.*** References 11, tables 1, figures 4.
Key words: **induction electric motor, generalized circuit, thyristor converter, pulsations.**

Представлены расчеты и физическое моделирование колебательных составляющих электромагнитного момента при изменении параметров асинхронного электродвигателя, элементов силовых схем преобразователей, построенных на резисторно-тиристорных модулях. Установлено, что величина пульсаций электромагнитного момента в квазипостоянных режимах зависит от выбранной силовой схемы статорной и роторной коммутаторов преобразователя, состава элементов, входящих в них, и схемы их соединения, изменения величины углов открытия вентилями, способы их управления, частота вращения ротора, параметры механизма – моменты статический и инерции. Предложено использовать для исследования обобщенную схему параметрического управления асинхронного электродвигателя. Библ. 11, табл. 1, рис. 4.
Ключевые слова: **асинхронный электродвигатель, обобщенная схема, тиристорный преобразователь, пульсации.**

Problem definition. Power circuits for converters for controlling induction motors (IMs) are constructed using various elements - resistors, inductors, diodes, thyristors, etc. Converters using these elements are included in the stator, rotary or simultaneously in the stator and rotor circuits of the IM and are referenced to parametric control converters [1, 2]. Depending on the power circuit of the converter, respectively, the static and dynamic characteristics of the IM are changed. Circuits of converters in different ways determine the starting, brake, reversing, power characteristics of IM. When loading the IM controlled by such converters, there are dynamic forces in the elements of the kinematic chain, which can be detected in transient and steady modes of operation due to fluctuations of the electromagnetic torque (ET) of the IM.

It is known that the ET contains the mean and oscillatory components, but how the latter one varies, with what frequency, depending on the chosen power circuit of the converter and the location of the connection of its elements in the circuit, has not been investigated. The ET pulsations caused by the influence of higher harmonics of voltage on the IM lead to deterioration of the vibration and acoustic characteristics of the IM and mechanism, that is, the noise and vibration are increased. This phenomenon is accompanied by resonance phenomena and the deterioration of the strength of mechanical equipment of the electric drive and the mechanism. With an increase in the moment of inertia, the number of pulsations of IM increases. Particularly large values of maximum throwing torques are achieved with reverse of IM. However, to date, for some types of converters there are no investigations and is not defined as the value of electromagnetic oscillations of the ET

depending on the IM and electric circuit parameters, chosen converter circuits, the value of opening angles of thyristors, a way to control the valves, rotor speed, and more. Therefore, these phenomena require a thorough investigation.

For an integrated approach and systematic analysis, finding or obtaining rational variants of power circuits of converters with parametric control of IM, it is most convenient to use a generalized (common) power circuit and its mathematical description, which allows to create a general control algorithm and to use effectively computers conducting investigations (Fig. 1,*a*).

The sequential connection of a power thyristor with an active resistor, parallel to which the second additional resistor is connected, forms a module that is not only a separate functional module but can also be a constructively manufactured block called a resistor-thyristor module (RTM). As can be seen from Fig. 1,*a*, a generalized power circuit of the converter of the IM control consists of stator (SC) and rotor (RC) commutators.

Let us consider possibilities of the proposed generalized converter circuit with RTM in stator circuits indicated for RTM1 – RTM6 as: R_{si} and r_{si} and for rotor circuits RTM7 – RTM12 as: R_{ri} і r_{ri}, at the condition that:

$$R_{si} = R_s;\ R_{ri} = R_r;\ r_{si} = r_s;\ r_{ri} = r_r,$$

where i = 1, 2, ... for boundary (0, ∞) and intermediate values of R_s, r_s, R_r and r_r and three devices Z_0, Z_s, Z_i, of the communication module kind of Z.

In accordance with the accepted constraints in the tables (Fig. 1,*b*,*c*), the possible variants of the power circuits for the SC and the RC are respectively indicated, which are indicated by: S_{ij} and Z_{kij}. The ij indexes in the tables indicate the serial number of the corresponding row and column, and the index k takes values 0, s, i, that is, indicates the type of communication module Z and forms a DC link. In module Z separately three different devices are used: Z_0, Z_s, Z_i forming corresponding groups of RC.

In the first group Z_0 devices are included that shorten a DC circuit, in the second group Z_s - allow you to discretely change the value of the parameters of elements Z, and the third group Z_i - carry out impulse control of these parameters. However, in the communication module of the Z-type the value of the resistance of the active resistor included between the points P and N is changed according to a certain law.

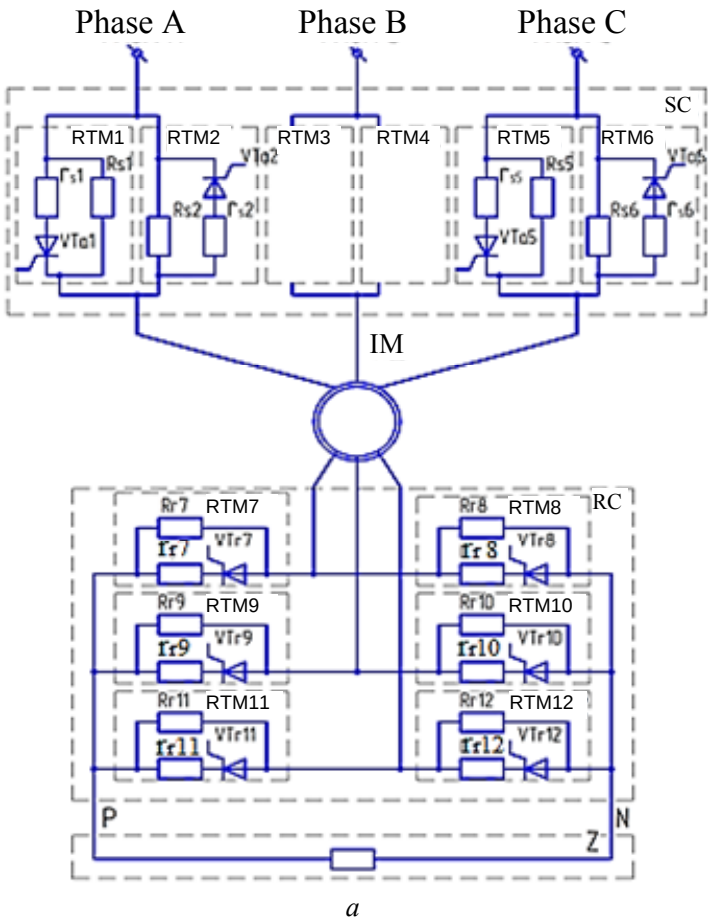

a

r_{si}	R_{si}		
	0	const	∞
0	S_{11}	S_{12}	S_{13}
const	S_{21}	S_{22}	S_{23}
∞	S_{31}	S_{32}	S_{33}

b

Z_k		R_{ri}		
		0	const	∞
Z_0	const	Z_0R_{11}	Z_0R_{12}	Z_0R_{13}
	∞	Z_0R_{21}	Z_0R_{22}	Z_0R_{23}
	0	Z_0R_{31}	Z_0R_{32}	Z_0R_{33}
Z_s	const	Z_sR_{11}	Z_sR_{12}	Z_sR_{13}
	∞	Z_sR_{21}	Z_sR_{22}	Z_sR_{23}
	0	Z_sR_{31}	Z_sR_{32}	Z_sR_{33}
Z_i	const	Z_iR_{11}	Z_iR_{12}	Z_iR_{13}
	∞	Z_iR_{21}	Z_iR_{22}	Z_iR_{23}
	0	Z_iR_{31}	Z_iR_{32}	Z_iR_{33}

c

Fig. 1. Generalized power circuit of parametric control of IM with SC and RC as a part of the converter (*a*) and variants of power circuits: SC (*b*) and RC (*c*)

Despite the introduction of constraints, the variant of the proposed generalized circuit of the converter encompasses many known circuits of parametric control of IM, as illustrated by the following examples. A separate parametric control circuit using thyristors in the stator of type S_{13} is known as a nonreversible thyristor voltage regulator (TVR). In circuit S_{13} $R_{si}=\infty$ and $r_r=0$ are adopted, that is, in each phase of the IM stator two thyristors are connected, which are connected to each other in a counter-parallel circuit. If in SC R_{si}=const and $r_r=0$ are taken, then in each phase of the IM only R_{si} resistor will remain. Another circuit of S_{12} type is provided for the case where R_{si}=const and $r_{si}=0$. Stator windings of the IM in the S_{12} type circuit are connected to the supply network via RTM. In the circuit of type S_{12}, RTM contains one resistor R_{si}, in parallel with which the thyristor VT_i is connected. Moreover, in each phase of the stator of the IM two RTM are connected, interconnected counter-parallel.

We pay attention to the fact that the converters, which have in their composition valve elements with incomplete control (thyristors or simistors), included in the circuit of alternating current, operate in the mode of natural switching. This type of converters implements the phase control in the stator or rotor circuits of the IM.

Fig. 1,*c* presents twenty-seven different options for power control circuits for IM rotor circuits. Options for power control circuits for IM rotor Z_0R_{11}, Z_0R_{21}, Z_0R_{11}, Z_0R_{21}, Z_0R_{31}, Z_sR_{11}, Z_sR_{21}, Z_sR_{31}, Z_iR_{11}, Z_iR_{21}, Z_iR_{31} at R_{ri} = 0 provide only closing rotor windings to the overall connection point, making thus normal rotor as short-circuited. According to the circuit of generalized parametric control of IM at R_{ri} = const and r_{ri} = const in each phase of the rotor of the IM parallel to resistance R_{ri} a circuit of serial interconnected resistors r_{ri} and thyristors VT_i is connected, and at $R_{ri} = \infty$ and r_{ri} = const - only a serial connected circuit of these elements remains. All this leads to different power circuits. Thus, at R_{ri} = const varieties types of schemes are produced: Z_kR_{12}, Z_kR_{22} and Z_kR_{32}, and at $R_{ri} = Z_kR_{13}$, Z_kR_{23}, Z_kR_{33}, and also a number of other circuits presented in Fig. 1,*c*. Circuit of type Z_kR_{13} at $r_{ri} = 0$ is known as Larionov bridge circuit, in the DC circuit of which communication module type Z_k is connected. Two other circuits type Z_kR_{22} (R_{ri} = const and r_{ri} = const and $Z_k = \infty$) and Z_kR_{23} (at $R_{ri} = \infty$ and r_{ri} = const and $Z_k = \infty$) have no open DC circuit, therefore they can be used independently.

Applying the communication module of *Z* type, the corresponding Z_0 circuit of Z_kR_{22} type is converted into Z_0R_{32} type circuit, and Z_kR_{23} type circuit, respectively, into Z_0R_{33} type circuit. In addition, from circuit of type Z_0R_{32} with $R_{ri} = \infty$ and r_{ri} = const there is already a new circuit of type Z_0r_{13}, and when R_{ri}=const i $r_{ri}=\infty$, the circuit of type Z_0r_{22}, containing only additional resistors in the rotor circuit is quite commonly used in industrial conditions. When R_{ri}=const i $r_{ri}=0$, we get circuit of type Z_0R_{32} and at R_{ri}=const, $r_{ri}=0$ - type Z_0r_{33}. Similarly, from circuit Z_0R_{33} at $r_{ri}=0$, another circuit of Z_0r_{33} type, in which the rotor windings are connected to the «star» circuit and are connected sequentially to the thyristors and resistors, which are closed to each other to a zero point, is formed. The power structure of the RC will change considerably for Z_0R_{32} type circuit if devices of type Z_s or Z_i are present in the DC circuit.

From the circuit of type $Z_{s(i)}R_{32}$ a rotor commutator is obtained, in which the thyristors are connected to the circuit of the triangle. In this case of the arrangement of Z_s or Z_i, there is only one thyristor, connected in the DC circuit. If we assume that in the generalized scheme of type $Z_{s(i)}R_{32}$ resistors: $R_{r1} = R_{r2} = R_{r3} = R_{r4} = R_{r5} = R_{r6} = \infty$, $r_{r2} = r_{r3} = r_{r5} = r_{r6} = \infty$ =const, $r_{r1} = r_{r4}$ =0, then it turns out, that the triangular commutator is connected to the zero point of the connection of the IM rotor, and power circuit of type Z_1R_{32} is obtained, in the rotor circuit there are no resistance resistors. If taken in the circuit of type $Z_{s(i)}R_{32}$ that $R_{r1} = R_{r4} = R_{r5} = R_{r6} = \infty$ = const, and $r_{r1}=r_{r4}=0$, $r_{r2} = r_{r3} = r_{r5} = r_{r6} = \infty$ = const, then the commutator will be connected by the Z_2R_{32} circuit.

Thus, the use of a generalized converter circuit for parametric IM control will allow to use for the investigation of different power circuits of converters, which are obtained from the generalized one and solve the actual problem of determining the value of pulsations, overvoltages, amplitudes and frequencies of oscillating components of ET by simple engineering methods.

Analysis of previous investigations and publications. A large number of publications are devoted to the study of the control of IM in different operation modes. These questions are one of the key issues that are discussed today by experts. The authors do not provide sufficient information for the construction of automated systems of parametric control of IM, taking into account the change of electromagnetic torques, which essentially change on transients during start-ups, braking, reversal and operation. The main problem of IM, which researchers solve, is to reconcile the torque with the load torque, as during start-up, for example, torque for a fraction of second often reaches 150-200 %, which can lead to failure of the kinematic chain of the drive [3]. At the same time, high starting current at start can be 6-8 times more than nominal, causing problems with the stability of the supply and fluctuations of ET, the values of which in the presented information are not defined and are not presented. To eliminate some of these disadvantages, the industry manufactures controllers EnergySaver (soft starters with power saving function and power factor correction) which are intermediate between soft starters and frequency converters. EnergySaver uses the traditional for soft starters circuit of counter-parallel connected thyristors [4], that is, TVR, which upon closure of the start-up process are locked by contactors. The moment created by the IM, depends on the values of the applied voltage and sliding. The smaller the moment of loading is applied to the rotor, the more the rotor «catches up» with the stator field (sliding decreases), the further the IM becomes less economical. If appropriately reduce the supply voltage on the stator windings of IM, the sliding will return to the nominal value. The mechanical characteristics of the IM with reduced voltage on the stator windings have corresponding reduced ET. This will reduce the current flowing through the windings of the IM, and the consumed power is proportional to the product of the voltage and current, the loss decreases, the efficiency of the electric motor will increase [5].

However, there is no qualitative and quantitative analysis of changes in the amplitudes and frequency of oscillatory ET components in this work.

The analysis of the dynamic processes of energy transformation in IM is a complex task in connection with the essential nonlinearity of the equations describing IM, due to the product of variables. Therefore, the study of dynamic characteristics of IM should be conducted with the use of computers [6]. A common solution of the system of differential equations in the software environment MathCAD allows you to calculate graphs of transient processes of speed ω and ET M at numerical values of parameters of the equivalent circuit of the IM. As the analysis of the dynamic mechanical characteristics of the IM shown [6], the maximum shock torques at direct starting exceed the nominal moment M_n of static mechanical characteristic of more than 4.5 times and can achieve unacceptably high strength values from point of view of mechanical strength. Shock torques during start-up, and especially at the reverse of the IM, lead to the failure of the kinematics of production mechanisms and the IM itself. At the same time, the oscillations of the torques of IM at the control of the converters are not defined.

Among the topical tasks in the field of IM control is the development of relatively simple and effective converters to expand the range of regulation of the rotation speed of the IM down from the nominal value. The possibility of transferring the electric drive to reduced rotational speeds allows us to realize the economic modes of operation when reducing the technological loads and extends its regulatory properties. The need for such regulation inevitably appears in the current production. Traditional systems of regulated IM with short-circuit motor «thyristor voltage regulator - induction motor» (TVR-IM) are oriented for soft start-up and for creation of braking modes [7]. The circuit involves voltage regulation by forming predetermined angles of thyristor control. The basis of such a converter is phase or pulsed control. This allows the use of relatively inexpensive single-acting thyristors, which have rather high energy performance [8]. When controlling such converters, it is necessary to increase the rotor rotation evenness by reducing the amplitude and/or controlling the frequency of the pulsations of the ET, distorted by the operation of the power elements of the converter [9].

Investigation of pulsations of ET in frequency converters with PWM inverter with constant and variable frequency is considered in work [10]. The results of research in this paper indicate the existence of this problem in the control of IM, but the calculation method can not be transferred to the calculation of torque oscillations for parametric control converters. The basis of converters with phase or impulse control is another power circuit, consisting of RTM [11]. Together with the obvious advantages of using simple converters constructed on the basis of RTM, as the analysis of scientific and technical literature shown, the question of determining the levels of pulsations of ET of IM was not thoroughly considered by specialists.

Methods of analytical calculations made for frequency converters, asynchronous-valve cascades or valve motors can be partially used to calculate ET pulses when controlling such types of converters. The main differences here are caused, as by a feature of regulating the value of current through controlled valves, as well as by possible circuits of connection of resistors, thyristors, stator and rotor windings of IM. In addition, it is known that at the IM in the process of regulation the values such as the angle of opening thyristors, the stator voltage, the EMF of the rotor, the stator and rotor currents, ET, its sliding and others change, and they are interconnected by the corresponding functional dependences [10]. The variation of the ET oscillations ΔM depends on the selected power circuits connected to the stator and the rotor, the values of the angles of opening the thyristors, the method for controlling the valves, the rotor speed, the parameters of the electric motor and the electric drive [5, 6, 9].

When designing modern electric drives, it often becomes necessary to determine the dynamic forces in the elements of the kinematic chain, which can be detected in transient and steady modes of operation due to oscillations of the ET. In transient operating modes of the electric drive, the deviation of the shape of the voltage curve on the clamps of the IM from the sinusoidal one causes high-frequency oscillations of the ET and uneven rotor rotational frequency.

Determination of oscillating components of ET is of great practical importance, since they significantly affect not only the mechanical strength of the electric drive units and the state of the technological mechanism. If the frequencies of the natural oscillations of the mechanical part of the electric drive will be close to the frequencies of the oscillatory components of the ET, then there may be a danger of significant overvoltages in the elements of the electric drive.

The goal of the work is determination of the influence of the parameters of the electric motor, elements of power circuits of the converters constructed on the RTM, the static torque and the moment of inertia of the mechanism on the oscillatory components of the ET of the IM.

Investigation techniques. Comprehensive analysis of the diversity of power circuits for converters and the study of the main modes of IM is associated with a large amount of analytical calculations and the need for experimental research. Therefore, the methodological basis for solving the tasks is a comprehensive approach that allows the most convenient use of the generalized control circuit of the IM [11], its mathematical description, the general control algorithm and to conduct the study of the oscillatory components of the ET by mathematical modeling.

Material presentation and results. To assess the values of oscillations ET a generalized control circuit of the IM is used. The circuit has a converter consisting of stator and rotor commutators. Each commutator is implemented with RTM (Fig. 1,*a*). Using computers calculations of different operating modes of the IM are performed. It has been established that pulsations in some cases reach significant values. Thus, for the IM of type MTF 411-8, controlled by the power circuits of types $S_{13}Z_0r_{11}$, $S_{13}Z_0r_{22}$, $S_{13}Z_0r_{32}$, $S_{13}Z_2R_{32}$, $S_{22}Z_kR_{32}$, $S_{11}Z_LR_{33}$, the

maximum M_{max}, the minimum M_{min} and the mean M_m values of the ET are calculated. Using the calculated ET values, the oscillations ΔM are determined at different opening angles α_s, α_r of the thyristors of the stator and rotor commutators and rotor rotation speeds ω_r, respectively, equal to: minus 600, 400, 200, plus 200, 400 and 600 rpm. The results of calculations are summarized by the graphs presented in Fig. 2.

The values of resistors' resistances of the RTM, included in the investigated power circuits, adopted in accordance with Table 1.

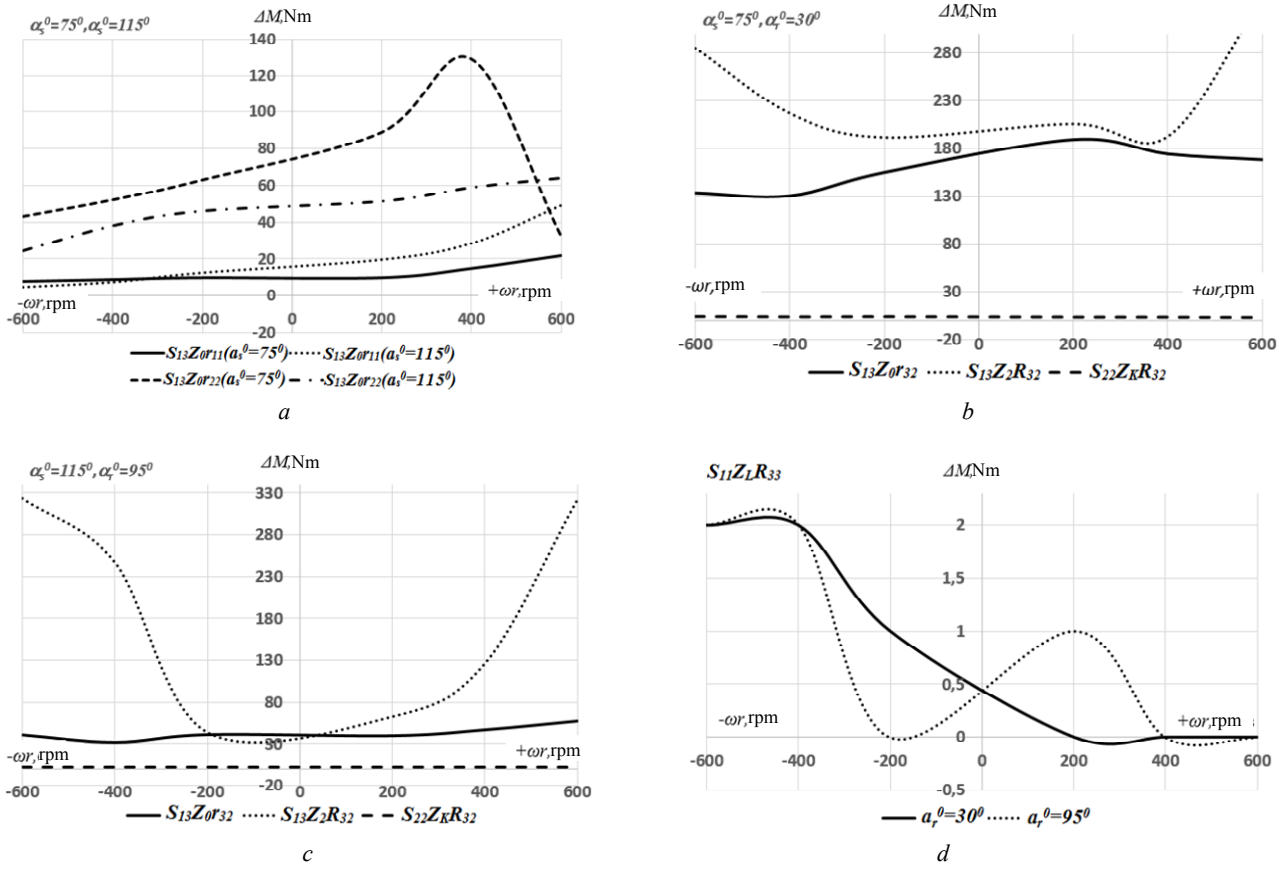

Fig. 2. Oscillations of the electromagnetic torque of the IM at the rotor rotation speeds, opening angles α_s, α_r of thyristors of SC and RC for different power circuits

Table 1

Values of the resistors' resistances of the RTM or circuits

Type of power circuit	Value of the resistors' resistances, Ω			
	R_{si}	R_{ri}	r_{si}	r_{ri}
$S_{13}Z_0r_{22}$	–	1.95	–	–
$S_{13}Z_0r_{32}$	–	2.8	–	–
$S_{13}Z_2R_{32}$	–	2.8	–	–
$S_{22}Z_KR_{32}$	0.32	4.4	0.1	0.48
$S_{11}Z_LR_{33}$	–	4.4	–	0.9

In the circuits, the connection of RTM in series with the windings of IM causes the appearance of additional oscillations of components of ET, the frequency and amplitude of which are determined by the specificity of the operation of thyristors in the converter. When commutating by the valves resistors in the circuits of IM there is a quasi-steady mode, which is a sequence of transients. In this mode the structure of the power circuits of the IM changes. Intervals of the existence of structures for stator and rotor circuits are determined by the moment of supply of control impulses and the conditions of natural commutation of valves.

As a result of the change in the structure of the power circuits, the equivalent value of the resistance of the resistors of the RTM varies, the change of which leads to oscillations of stator and currents of IM. The latter, in turn, change the magnetic flux and ET of the electric motor. As calculations show (Fig. 2), the smallest fluctuations of the ET of the IM are provided by power circuits with separate control in the rotor circuit (type $S_{11}Z_LR_{33}$) and with compatible control in the stator and rotor circuits (type $S_{22}Z_KR_{32}$). The first circuit practically eliminates the oscillations of ET. This circuit increases M_m and maintains it approximately at the nominal level throughout the all range of measurement of the frequency of rotation of the IM. The reduction of the pulsation of ET is achieved here due to the increase of the coefficient of attenuation of the current of the rotor circuit. It is increased by increasing the equivalent resistance of the resistors of RTM. The second circuit is inferior to the first one in the amplitude of the pulsations ΔM of the electric motor.

Increasing the opening angle α_r for the first circuit leads to increase in the maximum torque in the low velocity zone and decreases it at high velocity of the IM. This is due to the changing voltage harmonic composition of the IM. The connection of RTM in only two phases of

the rotor (circuit of type $S_{13}Z_2R_{32}$) leads to significant oscillations of the ET of IM. A large value ΔM causes vibration, strong noise and strikes, so their value should be reduced to a minimum. The value of these oscillations is higher compared to other power circuits. For example, for this circuit at speed n_r = 600 rpm and at angles α_s = 75° and α_r = 30° ΔM reaches a value equal to 377 Nm, which is 1.5 times higher than the nominal torque of the IM. At rotation frequency of the rotor, equal to 400 rpm and at angles α_s = 115° and α_r = 95° ΔM reaches the value equal to its rated torque. In this case, the oscillation of the torque ΔM may reach a triple value of the critical torque of the IM. At the asymmetric connection of the elements of the converter in the rotor circuit, the ET of IM as in the case of single-phase connection, contains the average and vibrational components.

The amplitude of the oscillating component of the ET depends on the degree of asymmetry in the circuit of the rotor, and its frequency is always equal to twice the sliding frequency. As for the average torques of the IM, they are at phase control of the valves in the stator circuit (the circuit of type $S_{13}Z_0r_{32}$) increase with increasing rotor rotation speed and, conversely, decrease with the presence of additional resistors in the rotor circuit (circuit type $S_{13}Z_0r_{22}$) or RTM (circuits of types $S_{13}Z_0r_{32}$, $S_{13}Z_2r_{32}$, $S_{13}Z_\kappa r_{32}$, $S_{13}Z_Lr_{32}$). The average torque of the IM is changed slightly in the rotor rotational frequency control in the circuit with separate control in the rotor circuit ($S_{11}Z_Lr_{33}$) and in the circuit with joint control in the stator and rotor circuits ($S_{22}Z_Kr_{32}$). For the first mentioned circuit, the value of the mean torque is greatest in the entire range of changes in the velocity of IM.

Thus, the use of RTM in the circuit of IM allows significantly reduce the value of pulsations of the ET, increase the value of the maximum and average torques and limit values of shock and alternating torques at the start as well as, as investigations have shown that the transition from one speed to another. The increase of the equivalent value of resistors' resistance of the RTM in the stator circuit slightly improves the power factor of the circuit, thereby shock alternating torques are reduced not only by lowering the voltage on the stator, but also by reducing their values and increase the damping aperiodic currents.

The moment of inertia of the electric drive has a significant impact on the duration and nature of the flow of transients. In Fig. 3 obtained on the computer and experimental installation oscillograms of the electric drive start in the presence on the IM shaft of different by their value additional flyweights. Analyzing these graphs, we can conclude that with increasing the moment of inertia of the electric drive the amount of considerable by their values shots of the transient IM at the beginning of the start process first increases and oscillations of the rotor rotation speed and ET near synchronous speed decrease. This is because some attenuation coefficients of free components of the ET at low speeds are very small.

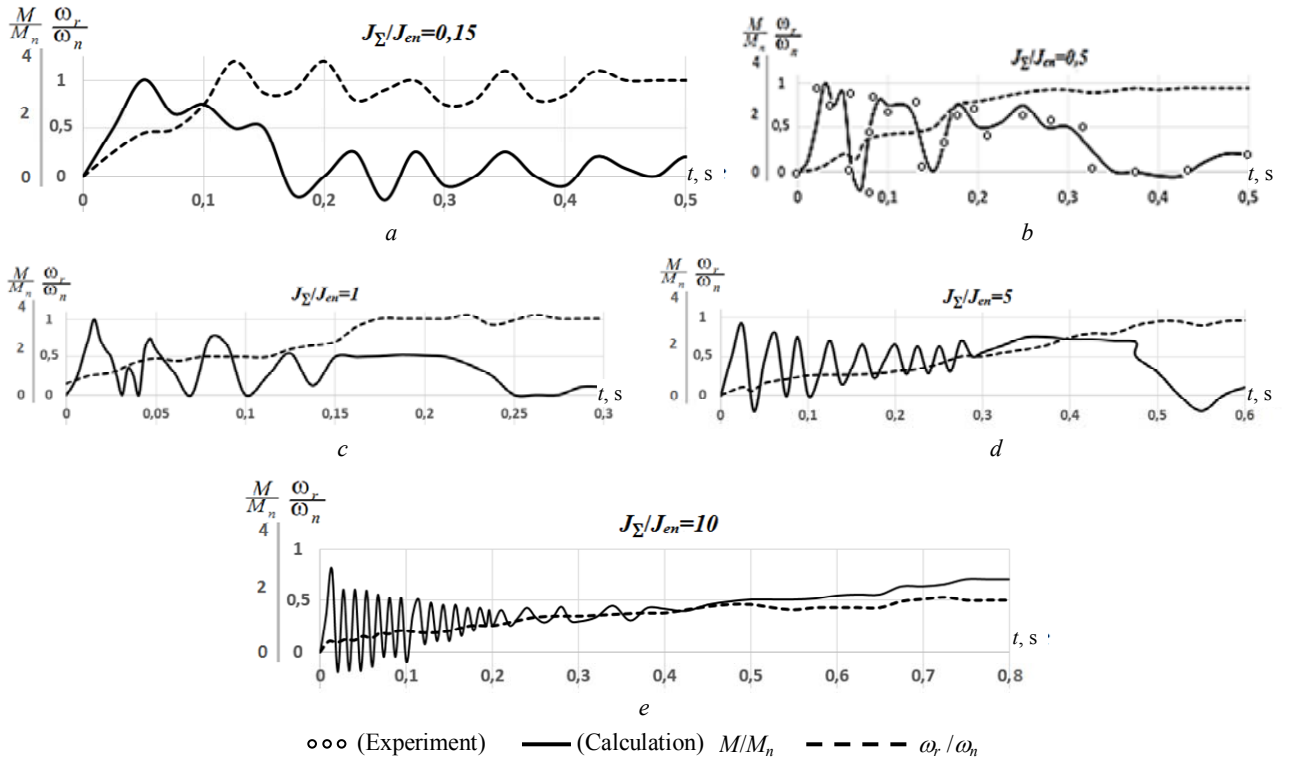

Fig. 3. Oscillograms of the electric drive start at different values of flyweights

If the increase the moment of inertia of the electric drive, then the IM will operate longer at reduced speeds, where the coefficients of attenuation of the stator and rotor circuits are small, which determines slower ET attenuation with increase in the total moment inertia J_Σ of the electric drive and the mechanism. With increasing J_Σ, the frequency increases and the peak amplitude of the transient ET increases. From the beginning of the process

with decreasing J_{Σ} the number of these peaks reduces. However, in this case, the speed and ET oscillations increase in the zone of low sliding of the IM.

Comparison of a large number of calculated and experimental oscillograms for the IM of different power with normal and elevated sliding indicates that the results obtained when changing the total moment of inertia are adequate. The effect of the total moment of inertia on the transient process for other power control circuits of the IM is almost the same as for the $S_{13}Z_0r_{32}$ type circuit.

Increase in the static torque on the shaft of the IM also results in a more long-term course of the acceleration process (Fig. 4).

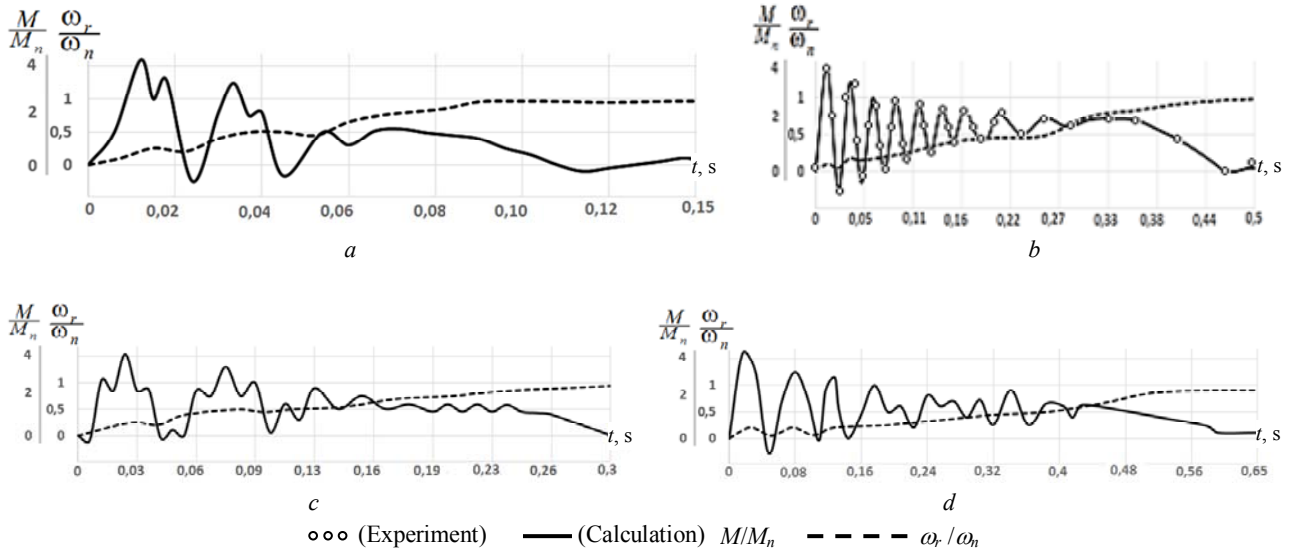

Fig. 4. Experimental and calculated oscillograms of the IM start at the change of the static torque for the circuit $S_{13}Z_0r_{11}$: *a* – $M_s = 0$, *b* – $M_s = M_n$; and for the circuit $S_{13}Z_0r_{32}$: *c* – $M_s = 0$, *d* – $M_s = M_n$

The frequency of pulsations of the ET at the beginning of the acceleration process increases. With the increase in the speed of the rotor, the frequency of pulsations significantly decreases, and in the region of the synchronous speed the torque oscillations completely disappear. The picture of the transient when changing the static torque looks like the picture of the transient when changing the moment of inertia. Oscillograms of the start of the IM with the change of the static torque on the shaft of the rotor shown in Fig. 4 for the two power circuit types $S_{13}Z_0r_{11}$ and $S_{13}Z_0r_{32}$ clearly confirm the above. For the first circuit, the opening angle α_S of the thyristors is assumed to be 90°, and for the second circuit the angles α_S and α_r respectively were 30° and 60°. The results of modeling on the computer show that the picture of the transient for other power circuits when changing the load on the shaft of IM is similar to the transient created by the circuits of types $S_{13}Z_0r_{11}$ and $S_{13}Z_0r_{32}$. Their difference is manifested only in different oscillations of ET.

Conclusions and perspectives of further research. Thus, the conducted investigations allowed to reveal the peculiarities of the influence of the parameters of elements of different types of power circuits of converters constructed on RTM, on the amplitude and frequency of oscillatory components of the ET of the IM.

The performed mathematical and physical modeling allowed to establish the conditions for the occurrence of electromagnetic pulsations, to determine the ways to eliminate them and to confirm the effectiveness of the chosen research method. It is established that the value of the pulsations of the electromagnetic torque of the IM in the quasi-steady modes depends on the selected power circuit of the converter, the stator and rotor commutators, the composition of the elements included therein, and the circuits of their connection in the modules.

Comparison of calculated and experimental oscillograms of the IM start of different power with normal and increased sliding indicates that the impact on the pulsation of the ET is provided by the values of the angles of opening the valves, their control methods, the rotational speed of the rotor, the parameters of the electric motor and the mechanism - the static torque and the moment of inertia.

At the same time, it was discovered that the use of RTM in the power circuits of the stator and rotor commutators of the converter reduce the value of the pulsation of ET in IM and increase the value of its maximum and the average torques and limit the value of shock and alternating torques, both during its start and at the transition from one speed to another.

In future investigations, it is planned to focus on testing the developed methodology in industrial conditions.

REFERENCES

1. Marenich K.N., Burlaka A.N. Substantiation of the principle of parametric control of an asynchronous motor of a load stand in the generator mode. *Scientific papers of Donetsk National Technical University. Series: Mining and electromechanical*, 2001, no.27, pp. 278-282. (Rus).

2. Odnolko D.S. Mathematical simulation of sensorless vector control induction motor under parametric perturbations. *System analysis and applied information science*, 2015, no.2, pp. 31-35. (Rus).

3. Principle of operation of soft starters: equipment for electric drive control. Available at: https://www.softstarter.ru/plavnij-pusk/upp/princip_dejstviya/ (accessed 15 October 2015).

4. Controllers-optimizers EnergySaver: equipment for electric drive control. – Available at: https://www.softstarter.ru/catalog/plavnij-pusk/energysaver/. (accessed 22 May 2016).
5. Makarov A.M., Sergeyev A.S., Krylov Ye.G., Serdobintsev Yu.P. *Sistemy upravleniia avtomatizirovannym elektroprivodom peremennogo toka: ucheb. posobie* [Control systems automated AC drive. Tutorial]. Volgograd, VolgGTU Publ., 2016. 192 p. (Rus).
6. Dementyev Yu.N., Chernyshev A.Yu., Chernyshev I.A. *Elektricheskii privod: ucheb. posobie* [Electric drive. Tutorial]. Tomsk, TPU Publ., 2010. 232 p. (Rus).
7. Anisimov V.A., Gornov A.O., Moskalenko V.V. Thyristor starting devices in AC drives. *Drive and control*, 2002, no.1, pp. 32-34. (Rus).
8. Cherepanov V.P., Khrulev A.K. *Tiristory i ikh zarubezhnye analogi: spravochnik* [Thyristors and their foreign counterparts. Directory]. Moscow, IP RadioSoft Publ., 2002. 512 p. (Rus).
9. Krasovskiy A.B. *Osnovy elektroprivoda: ucheb. posobie* [Bases of the electric drive. Tutorial]. Moscow, Publishing House MSTU N.E. Bauman, 2015. 405 p. (Rus).
10. Chernyshev A.Yu., Dementyev Yu.N., Chernyshev I.A. *Elektroprivod peremennogo toka: ucheb. posobie* [AC electric drive. Tutorial]. Tomsk, Publishing house of Tomsk Polytechnic University, 2011. 213 p. (Rus).
11. Lobov V.Y. Method for research of parametric control schemes by asynchronous motor. *Metallurgical and Mining Industry*, 2015, no.6, pp. 102-108.

Received 10.02.2017

V.I. Lobov[1], *Candidate of Technical Science, Associate Professor,*
K.V. Lobova[1],
[1] Kryvyi Rih National University,
11, V. Matusevycha Str., Kryvyi Rih, 50027, Ukraine,
phone +380 564 4090635,
e-mail: lobovvjcheslav@gmail.com

How to cite this article:
Lobov V.I., Lobova K.V. The thyristor converter influence on the pulsations of the electromagnetic torque of the induction motor at parametrical control. *Electrical engineering & electromechanics*, 2017, no.4, pp. 34-41. **doi: 10.20998/2074-272X.2017.4.06.**

UDC 621.3.022: 621.319.53 **doi: 10.20998/2074-272X.2017.4.07**

M.I. Baranov, S.V. Rudakov

APPROXIMATE CALCULATION OF ACTIVE RESISTANCE AND TEMPERATURE OF THE PULSE ELECTRIC ARC CHANNEL IN A HIGH-CURRENT DISCHARGE CIRCUIT OF A POWERFUL HIGH-VOLTAGE CAPACITOR ENERGY STORAGE

Purpose. *To obtain calculation correlations for active resistance R_{ce} and maximal temperature T_{me} of plasma channel of pulse electric arc in the air double-electrode system (DES) with metal (graphite) electrodes, and also practical approbation of the obtained correlations for R_{ce} and T_{me} in the conditions of high-voltage laboratory on the powerful capacity energy storage (CES) of electric setting, intended for reproducing on the electric loading of protracted C- component of current of artificial lightning with the USA rationed on normative documents by amplitude-temporal parameters (ATP).* ***Methodology.*** *Electrophysics bases of high-voltage impulse technique, scientific and technical bases of development and creation of high-voltage high-current impulse electrical equipment, including powerful CES, and also measuring methods in discharge circuits of powerful high-voltage CES of pulse currents of millisecond temporal range.* ***Results.*** *On the basis of engineering approach the new results of approximate calculation of values of R_{ce} and T_{me} are resulted in the plasma channel of pulse electric arc discharge in air DES of atmospheric pressure with metallic (graphite) electrodes. Practical approbation of results of calculation of values of R_{ce} and T_{me} is executed as it applies to air DES, to connected in a discharge circuit of powerful high-voltage CES with protracted C- of component current of artificial lightning, characterized rationed ATP. It is shown that calculation of numeral value R_{ce} approximately in 100 times exceeds the proper value of active resistance for the plasma channel of impulsive spark of electric discharge in air DES other things being equal, and a calculation of numeral value T_{me} well corresponds with the known thermodynamics information for classic electric arc in air DES of atmospheric pressure with graphite electrodes.* ***Originality.*** *New engineering approach is developed for the approximate calculation of values of R_{ce} and T_{me} in electron-ion plasma of channel of pulse electric arc, arising in air DES of high-current discharge circuit of powerful high-voltage CES of proof-of-concept of electric setting of the technological setting. A formula is first obtained for the approximate calculation of equivalent active resistance of R_{ce} of channel of pulse electric arc in air DES, remaining unchanging in the process of high-current discharge on RL- load of indicated CES.* ***Practical value.*** *Drawing on the got calculation results for the values of R_{ce} and T_{me} in high-voltage impulse technique provides the rational choice of own electric parameters and construction elements of basic devices of powerful high-voltage CES of technological of electric setting, and also account of influence of electrical engineering descriptions of air DES on electromagnetic processes, taking place in the high-current discharge circuit of indicated CES with protracted C- of component current of artificial lightning.* References 16, figures 6.

Key words: **powerful high-voltage capacitor energy storage, air double-electrode system, pulse electric arc, active resistance of pulse electric arc channel, maximal temperature of pulse electric arc channel.**

Приведены результаты расчетной оценки эквивалентного активного сопротивления R_{ce} канала импульсного дугового электрического разряда в воздушной двухэлектродной системе (ДЭС) сильноточной разрядной цепи мощного высоковольтного емкостного накопителя энергии (ЕНЭ), используемого при моделировании в лабораторных условиях длительной С- компоненты тока искусственной молнии. Рекомендовано расчетное соотношение для оценки максимальной электронной температуры T_{me} в низкотемпературной плазме канала импульсной электрической дуги в исследуемой воздушной ДЭС. Выполнена практическая апробация полученных соотношений для R_{ce} и T_{me} применительно к воздушной ДЭС сильноточной разрядной цепи действующего мощного высоковольтного ЕНЭ генератора ГИТ-С, предназначенного для проведения испытаний технических объектов на электротермическую стойкость к воздействию длительной С- компоненты тока искусственной молнии с амплитудно-временными параметрами, соответствующими нормативным документам США SAE ARP 5412: 2013 и SAE ARP 5416: 2013. Библ. 16, рис. 6.

Ключевые слова: **мощный высоковольтный емкостный накопитель энергии, воздушная двухэлектродная система, импульсная электрическая дуга, активное сопротивление канала импульсной электрической дуги, максимальная температура канала импульсной электрической дуги.**

Introduction. It is known that in gas-discharge gaps (for example, in air gaps of high-voltage air switches and other electrode systems of electrical loads) circuits of powerful capacitor energy storage devices (CES) designed to reproduce in the laboratory conditions of high-current electrophysical phenomena (for example, artificial lightning with pulse *A*- and long-term *C*- current components), both pulsed spark electric discharges and pulse arc electric charges can occur poisons [1-3]. For pulse spark electric discharges flowing in the air gaps of the discharge circuits of high-power high-voltage CES, the characteristic parameters are their duration $\tau_{pd} \le 1$ ms and the amplitude of their current $I_{md} \le 1000$ kA [1]. With regard to pulsed arc discharges in the discharge circuits of high-power high-voltage CES, for them the indicated electric parameters τ_{pd} and I_{md} are characterized by the following numerical values [2, 3]: 1000 ms$\ge\tau_{pd}\ge$100 ms and 1000 A$\ge I_{md}\ge$100 A. In the latter the numerical values of the parameters τ_{pd} and I_{md} practically correspond to the known characteristics of the classical electric arc

discharge arising in the air double-electrode system (DES) between its cathode and anode at a constant or alternating current in the electric circuit [4]. According to the data given in [4, 5], the arc electric discharge in the air DES is maintained by thermionic emission from the surface of a metallic or graphite cathode electrode. Due to the acceleration of electrons in the interelectrode gap and the shock ionization of the air molecules between the cathode and the anode of the DES, a column (channel) of a brightly-luminous strongly ionized gas appears, called electron-ion plasma in electrophysics. For a classic example of an electric arc discharge in the open air between graphite (carbon) electrodes of a DES, the thermodynamic temperature of the arc channel with radius of up to 4 mm at constant current of 200 A on the anode surface in its central zone can reach a value of up to 4200 K, and on the surface of the cathode - up to 3500 K [4, 5].

In [6, 7], the results of an approximate calculation of the active resistance R_c of the channel of pulse spark electric discharge between the metal electrodes of a high-voltage high-current air switch at atmospheric pressure were presented. Simple and convenient formulas for estimating the maximum temperature T_{me} of the electron-ion plasma of pulse electric arc in an air DES are not currently known to us. Of undoubted scientific and practical interest are the electrophysical problems associated with the design determination of the active resistance R_{ce} and the maximum temperature T_{me} of the pulse arc electric discharge channel between the metallic (graphite) electrodes of the air DES in the high-current discharge circuit of the high-power high-voltage power testing unit of the electrical testing apparatus.

The goal of the paper is approximate calculation of the active resistance R_{ce} and the maximum temperature T_{me} of the plasma channel of the pulsed arc electric discharge in the air DES that is part of the high-current discharge circuit of the powerful high-voltage CES, as well as the practical approbation of the calculation data in the conditions of the high-voltage laboratory on a real powerful CES of the electrical installation.

1. Problem definition. Let us consider an air DES located in a high-current discharge circuit of high-power high-voltage pulse current generator (PCG), whose CES is built on a single-module circuit based on parallel-connected high-voltage pulse capacitors. It is designed to reproduce in the air gap of length ha of a long-term *C*-component of artificial lightning current with normalized amplitude-time parameters (ATPs) according to the technical requirements of the current US regulatory documents SAE ARP 5412: 2013 and SAE ARP 5416: 2013 [8, 9]. Recall that the normalized ATPs for the aperiodic long-time *C*- component of the lightning current have the following numerical values [8, 9]: current amplitude I_{mdc}=±(200-800) A; the transferred electric charge q_{dc}=±(200±40) C; duration of current flow τ_{pdc}=(0,25−1) s. It can be seen that the ATPs of this component of the artificial lightning current correspond to the main characteristics of the current of the electric arc discharge between the cathode and the anode of the air DES [4, 5]. We assume that the metallic or graphite electrodes of the DES are considered in atmospheric air under normal conditions (air pressure is $1.013\cdot10^5$ Pa and its temperature is θ_0=0 °C [4]). Taking into account the indicated numerical values of τ_{pdc}, we use the plasma isothermicity condition in the channel of the considered electric arc, according to which its maximum electron temperature T_{me} will be practically equal to the maximum temperature T_{mi} of the carriers of its ion current ($T_{me}\approx T_{mi}$) [4]. We assume that in the DES, the length l_{ce} of the cylindrical channel of the equilibrium plasma of the pulsed electric arc is in the first approximation equal to the minimum length of the interelectrode gap in the investigated DES. We assume that in a high-current channel of an electric arc discharge in an air DES, the current density δ_{dc}, the thermodynamic electron T_{me}, and the ion temperature T_{mi} of its equilibrium plasma are, in a first approximation, characterized by a practically uniform distribution along its radius. It is required, within the engineering approach, to obtain a new design ratio for the active resistance R_{ce} and to recommend a simple formula for the estimated estimation of the maximum temperature T_{me} of the plasma of the pulse arc electric discharge channel in the air DES, and also to carry out practical approbation of the approximate calculations of the R_{ce} and T_{me} values applied to the real high-current discharge circuit of an operating powerful PCG (PCG-*C*) simulating a long-tem *C*- component of artificial lightning current on a low-resistance *RL*- load.

2. Basic calculation relationships. Using the plasmodynamic method of calculating the value of R_{ce} [6], for the variable in time t active resistance of the plasma channel of a pulse arc of electric discharge in the air DES under study, we write the following expression:

$$R_{ce}(t) = l_{ce}[\pi r_{ce}^2(t)\gamma_{ce}]^{-1}, \qquad (1)$$

where $r_{ce}(t)$ is the changing in time t radius of the plasma channel of the arc electric discharge between the metal (graphite) electrodes of the DES; γ_{ce} is the average conductivity of low-temperature plasma in a cylindrical channel of pulse arc between DES electrodes.

It is known that the value $r_{ce}(t)$ during the course of the pulse discharge current $i_{dc}(t)$ of the powerful CES of the PCG-*C* generator through the DES under investigation changes on the increasing part of the aperiodic current pulse from its minimum zero value (time t=0) to its maximum value r_{cem} corresponding to the instant t_{mdc}, when the current strength $i_{dc}(t)$ reaches its maximum value I_{mdc}. On the falling part of the indicated current pulse, the quantity $r_{ce}(t)$ varies from the maximum value r_{cem} (time instant t_{mdc}) to the minimum zero value corresponding to the moment when the pulse discharge current $i_{dc}(t)$ ceases to flow through the air DES (time $t=\tau_{pdc}$). Obviously, at the instants of time t=0 and $t=\tau_{pdc}$, the active resistance of the plasma channel of the pulsed arc electric discharge in the air DES takes, according to

(1), infinitely large numerical values. In this connection, it is impossible to use directly the relation (1) for practical calculations of the value $r_{ce}(t)$. Therefore, we are faced with a new electrotechnical problem associated with the replacement of the variable in time t with the value of the active resistance $r_{ce}(t)$ of the pulse electric arc by some equivalent value of its active resistance R_{ce}, which remains constant throughout the process of the impulse discharge current $i_{dc}(t)$ form through the considered DES. One of the possible ways of approximate solution of such a problem can be the averaging in (1) in time t of the quantity $r_{ce}(t)$. Moreover, this is an unconventional averaging, when a time function of the form $f(r_{ce})=r_{ce}^2(t)$ is averaged on the right-hand side of expression (1). We have said about the limits of the change of this function above. Then, for the equivalent active resistance R_{ce} of the pulsed arc electric discharge channel in the air DES, we obtain the relation:

$$R_{ce} = l_{ce} /(\pi\gamma_{ce} r_{cem}^{-1} \int_0^{r_{cem}} r_{ce}^2 dr_{ce}) = 3l_{ce}(\pi r_{cem}^2 \gamma_{ce})^{-1}. \quad (2)$$

It follows from (2) that in order to find the numerical value of the equivalent active resistance R_{ce} of the arc discharge channel of length l_{ce}, it is necessary to know its two parameters such as the maximum radius r_{cem} and the average conductivity γ_{ce} of the electron-ion plasma forming the column of the considered electric arc. The radius r_{cem} (m) of the channel of pulse arc discharge in air DES depends on the strength of the discharge current $i_{dc}(t)$ of the high-power high-voltage generator PCG-C, flowing in it and for normal atmospheric conditions in the SI system is given in the form [3, 10]:

$$r_{cem} = 1.1\cdot 10^{-4}(I_{mdc})^{1/2}. \quad (3)$$

where I_{mdc} is the amplitude (A) of the aperiodic long-term *C*- current components of artificial lightning in the plasma channel of the pulse electric arc of DES.

Substituting (3) into (2), for the equivalent active resistance R_{ce} (Ω) of the plasma channel of the pulse electric arc in the DES of the high-current discharge circuit of the powerful high-voltage CES of the generator PCG-C, we obtain the following relation:

$$R_{ce} = 78.92\cdot 10^6 l_{ce}(I_{mdc}\gamma_{ce})^{-1}. \quad (4)$$

It follows from (4) that as the current I_{mdc} increases in the discharge circuit of the powerful CES, the maximum voltage drop $U_{mdc}=R_{ce}I_{mdc}$ on the pulse electric arc in the air DES will decrease. This is due to the fact that the degree of ionization of the gas in its discharge gap will also increase with the increase of the current I_{mdc} due to an increase in the thermionic emission from the cathode of the DES. The increase in the ionization of gas in the air discharge gap of the DES will result in increase in the average specific electric conductivity γ_{ce} of the electron-ion plasma of the channel of the arc under investigation. As a result of these electrophysical processes in the gas-discharge gap of the air DES, according to (1), the equivalent active resistance R_{ce} of its pulsed electric arc will be greatly reduced. As a result, this will lead to a decrease in the voltage U_{mdc} on the pulsed electric arc in the air DES with an increase in the current amplitude I_{mdc}. The established feature corresponds to the character of the behavior of the arc discharge in the DES described in [4]. This circumstance indirectly indicates the reliability of the obtained calculated relation (4) for the equivalent active resistance of the plasma channel of a pulsed arc electric discharge in an air DES.

As for the quantitative values for the quantity γ_{ce} entering into (4), according to the calculated experimental data, they are numerically approximately 5000 $(\Omega\cdot m)^{-1}$ in the first approximation, taking into account (2). We will point out that for the highly ionized electron-ion plasma of the channel of pulse arc electric discharge in the air DES, the upper limit of the numerical values of γ_{ce} can reach a level of the order of $20\cdot 10^3$ $(\Omega\cdot m)^{-1}$ [1, 6].

In the calculated estimate of the largest electron temperature T_{me} in the electron-ion equilibrium plasma of a pulse arc discharge for an air DES, taking into account the assumptions made (3) and the thermophysical approach given in [12], the following approximate expression can be recommended:

$$T_{me} \approx 95.35\cdot \sqrt[4]{U_{ac}/\sigma_c}, \quad (5)$$

where $\sigma_c=5.67\cdot 10^{-8}$ $W\cdot(m^2\cdot K^4)^{-1}$ is the Stefan-Boltzmann constant [4]; $U_{ac}\leq 11$ V is the near-electrode voltage drop in the air DES with metal (graphite) electrodes (for the graphite anode $U_{ac}\approx U_a\approx 11$ V, and for the graphite cathode $U_c\approx 10$ V [5]).

3. Powerful high-voltage CES of the generator PCG-*C* and its application for testing technical objects for lightning resistance. Fig. 1, 2 show the principal circuit diagram and the general view of the powerful CES of the generator PCG-*C* used in experimental studies of electrothermal lightning strength of test objects (TO) of various elements (for example, metal or composite plating) of various technical objects (for example, aircraft). The own electrical parameters of the discharge circuit of the generator PCG-*C* were equal [2]: the resistance is $R_C\approx 4.74$ Ω; inductance $L_C\approx 11.43$ mH; capacitance is $C_C\approx 45.36$ mF.

A powerful single-module CES of the PCG-*C* generator was assembled on the basis of 324 parallel-connected high-voltage pulse capacitors of the ИМ -5-140 type (rated voltage ±5 kV, nominal capacity 140 μF) [2, 13]. The nominal value of the stored electrical energy in the CES of the PCG-*C* generator was $W_{C0}\approx 567$ kJ [2]. In accordance with Fig. 1 in the circuit of the generator of high-voltage ignition pulses (GHIP), a two-electrode air switch F_1 with massive basic steel electrodes for voltage up to ±50 kV was installed and in the discharge circuit of the generator PCG-*C* a high-voltage two-electrode air switch F_2 of the ВДВК-10 type with rectangular graphite electrodes for voltage of up to ±10 kV [14] (Fig. 3).

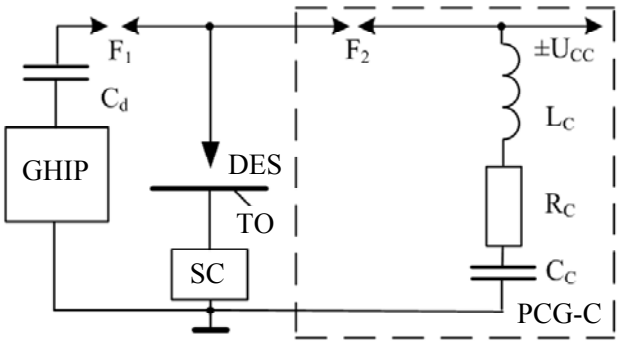

Fig. 1. The principal electrical circuit diagram of the high-current discharge circuit of the powerful high-voltage CES of the generator PCG-*C*, used to study the effect of the arc channel on the TO of the metal cladding of a technical object (GHIP - generator of high voltage ignition pulses of voltage amplitude up to ±100 kV; F_1, F_2 - two-electrode high-voltage air spark switches; C_d - separation capacitance of 180 pF and for impulse voltage of up to ±120 kV in the GHIP circuit, which controls the operation of the switches F_1 and F_2; DES - double-electrode system with air gap; TO - a test specimen of the metal skin of the object; SC - shunt of coaxial type ШК-300 for measuring the current of pulse electric arc in the air gap of DES and TO; $\pm U_{CC}$ - charging voltage of high-voltage capacitors of the generator PCG-*C*; $L_C \approx 11.43$ mH, $R_C \approx 4.74$ Ω, $C_C \approx 45.36$ mF - own electrical parameters of the generator, including inductance, active resistance and capacitance of its high-current discharge circuit)

Fig. 2. General view of the powerful CES of the high-voltage generator PCG-*C* (in the foreground are the forming active-inductive elements of its high-current discharge circuit, and in the background - the parallel-connected high-voltage pulse capacitors ИМ-5-140) [2, 3]

In practical approbation of the calculated ratios (4) and (5) with reference to the high-current discharge circuit of the PCG-*C* generator, an air DES was used, schematically shown in Fig. 4. To initiate an electrical breakdown of the air gap h_a in this DES and in accordance with the requirements of [8, 9], a thin copper electrically exploding wire (EEW) was used, having radius of $r_e \approx 0.1$ mm and length $l_e \approx 37$ mm. The air working gaps h_a and h_e in this DES were 14 and 1 mm, respectively. In Fig. 5, in enlarged form, the external view of the air DES used in the high-voltage discharge circuit of the powerful CES of the high-voltage generator PCG-*C* is shown.

Fig. 3. External view of high-voltage two-electrode air switch type ВДВК-10 with graphite electrodes of rectangular shape for voltage up to ±10 kV used in the discharge circuit of the generator PCG-*C* [2]

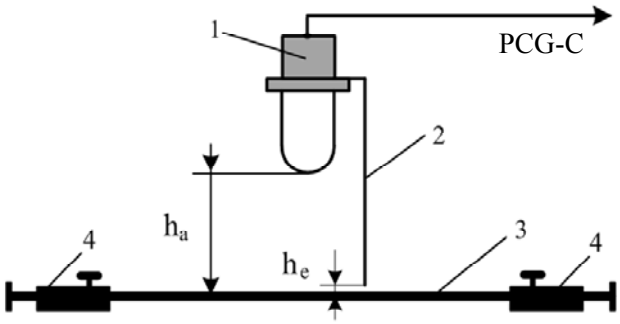

Fig. 4. General view of the air DES in the high-current discharge circuit of the generator PCG-*C* (1 - the upper massive cylindrical steel electrode; 2 - the round thin copper EEW; 3 - the lower massive flat electrode which is the metal shell of the technical object; 4 - the massive rectangular aluminum electrodes intended for rigid double-sided fastening in their grooves of a flat TO; h_a - the length of the air gap in the DES; h_e - the length of the air gap between the lower edge of the copper EEW and the outer flat surface of the TO)

The charging voltage of the high-voltage capacitors of the high-power CES of the generator PCG-*C* for choosing the appropriate experiments was chosen with negative polarity equal to $U_{CC} \le 4.2$ kV. The choice of the polarity of the charging voltage U_{CC} was determined by the necessity to simulate the most severe conditions in the electrothermic sense in the investigated DES and, accordingly, in the circular zone of the fastening of a high-current cylindrical plasma channel of a pulsed electric arc with a long-term *C*- component of the artificial lightning current on the outer flat surface of the metal structure of the technical object. To prevent

Fig. 5. Enlarged appearance of the air DES with a thin copper EEW on the desktop of the high-voltage generator PCG-*C* with powerful CES when tested in its high-current discharge circuit of the TO sheet metal plating of the technical object for electrothermal resistance to direct action on it for a long-term *C*- components of artificial lightning current with normalized ATPs (h_a≈14 mm; h_e≈1 mm; r_e≈0.1 mm; l_e≈37 mm) [10]

mechanical damage in a high-power capacitor bank of the PCG-*C* generator and to provide the required safety precautions for the high-voltage CES personnel undergoing maintenance by it during emergency operation (for example, with an electrical breakdown of the insulation of at least one of the 324 mentioned capacitors when they are charged or discharged) on all high-voltage terminals of the used capacitors of the CES of the generator PCG-*C*, protective resistances were constructed, made of high-voltage permanent graphite-ceramic resistors type ТВО-60 at constant voltage up to ±25 kV [2, 15].

In the high-voltage CES of the generator PCG-*C* on the high-voltage terminals of each of 324 pcs of its capacitors type ИМ-5-140 to one protective resistor ТВО-60-100 Ω [2, 15] were fixed.

Synchronous operation of the spark switches F_1 and F_2 in the circuit in Fig. 1 was carried out by feeding a microsecond voltage pulse with amplitude up to ±100 kV [2, 14] through a high-voltage separation capacitor C_d to a spherical steel electrode 30 mm in diameter of the switch F_1 from the GHIP.

In the case of an electric breakdown from the GHIP of the air working gap of the spark switch F_1 and its subsequent operation, the resulting pulse overvoltage on the DES with the TO leads to an almost simultaneous operation with it and a spark switch F_2. After the spark switches F_1, F_2, the electric breakdown of the air gap of length h_e≈1 mm and the electrical explosion of a thin copper wire in the zone of the DES are triggered by the discharge of the pre-charged high-voltage capacitors of the CES generator PCG-*C* through the air DES and the metal shell of the technical object, long-term *C*- current components of artificial lightning with the required [8, 9] ATPs. Measurement of ATP for the long-term *C*- components of the current of artificial lightning in the channel of the electric arc in the aerial DES and the metal shell of the object were carried out using a measuring coaxial shunt of the ШК-300 type [2, 14] certified by the state metrological service, having a conversion factor of K_C≈5642 A/V, and a digital storage oscilloscope Tektronix TDS 1012.

4. Results of experimental approbation of calculations of active resistance and temperature of the channel of pulse electric arc in the air DES. According to Fig. 1 and the above scientific and technical materials in the considered high-current discharge circuit of the powerful high-voltage generator of the PCG-*C* generator there are two air power plants connected in a common electrical circuit: the first one is directly in the zone of the TO placement of the sheet metal covering of the technical object with the air gap h_a≈14 mm; the second one - in the zone of the spark switch F_2 with an interelectrode gap of air of length h_{ak}≈4 mm. It is the total air gap of these two DES with length l_{ce}=(h_a + h_{ak}) and will determine the minimum total length of the pulsed electric arc channel in the high-current circuit of the powerful high-voltage CES of the generator PCG-*C* and, accordingly, its minimum total active resistance R_{ce}. In Fig. 6 shows the oscillogram of a long-term *C*- component of the current of artificial lightning flowing through the above air DES and the metal shell of the object.

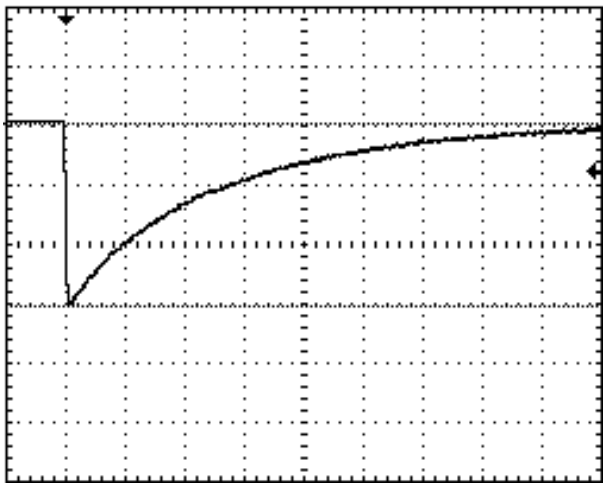

Fig. 6. The oscillogram of the long-term *C*- component of the current of artificial lightning with normalized ATPs in the high-current circuit of the PCG-*C* generator at the discharge of its powerful CES on the air DES with an electrically exploding thin copper wire (r_e=0.1 mm; l_e=37 mm) and sheet TO from aluminum AMr2M alloy of 2 mm thickness (U_{cc}≈−4.2 kV; W_C≈400 kJ; I_{mdc}≈−0.869 kA; t_{mdc}≈9 ms; τ_{pdc}≈1000 mc; q_{dc}≈192 C; vertical scale: 282 A/cell; horizontal scale - 100 ms/cell)

From the data in Fig. 6 that the ATP used in the experiments of the long-term *C*- current component of the artificial lightning correspond to the requirements [8, 9] and to the characteristics of the pulse arc electric discharge in this air DES. Assuming that γ_{ce}≈$5\cdot10^3$ $(\Omega\cdot m)^{-1}$ [11], l_{ce}≈$18\cdot10^{-3}$ m and I_{mdc}≈869 A, from (4) we find that

in the considered experimental case the total equivalent active resistance of the plasma channel of pulse electric arc in the investigated air DES will be not less than R_{ce} ≈0.327 Ω. The resulting calculated value of R_{ce} will be up to 7% of the intrinsic active resistance of the R_C of the discharge circuit of the powerful high-voltage generator of the PCG-*C* generator. Taking into account the data obtained in [6], it can be concluded that for identical values of l_{ce} and average plasma specific conductivity, equal to γ_{ce}≈$5\cdot10^3(\Omega\cdot м)^{-1}$, in atmospheric air pressure of the high-current circuit of the powerful high-voltage CES, the equivalent active resistance of the pulse arc electric discharge channel at I_{mdc}≈0.869 kA (t_{mdc}≈9 ms; τ_{pdc}≈1 s) will be approximately 100 times greater than the equivalent active resistance of the channel of pulse spark electric discharge at I_{md}≈202 kA (t_{md}≈36 μs; τ_{pd}≈0.5 ms). This result is explained for R_{ce} in that for the specified ATPs the millisecond (with the amplitude I_{mdc}) and the microsecond (with amplitude I_{md}) currents in the air DES, the maximum radius in (3) r_{cem}≈3.24 mm of the pulsed arc electric discharge channel turns out to be other things equal Conditions is practically an order of magnitude smaller than the maximum radius r_{cm}≈32.7 mm of the pulsed spark electric discharge channel, which satisfies the Braginsky formula for high currents of microsecond duration [1, 7, 16].

At U_{ac}≈U_a≈11 V from the formula (5), we obtain that in the high-current experiment under consideration with the use of a powerful high-voltage CES of the PCG-*C* generator, the maximum electron temperature T_{me} of an equilibrium electron-ion plasma in a cylindrical channel of pulse arc discharge in an air DES for the switch type ВДВК-10 (l_{ce}≈4 mm) is approximately 11250 K. It can be seen that the calculated numerical value of the electron temperature T_{me} of the plasma in the brightly shining column (channel) of the pulsed electric arc near the graphite anode of the above air DES is in good agreement with the known thermodynamic data typical for the near-axis region of the classical arc discharge flowing in an air DES with graphite electrodes at atmospheric pressure and 200 A current [4, 5]. In this case, according to [5], in the near-axis zone of the «coal» («graphite») arc (l_{ce}≈46 mm), which freely «burns» in the air DES, the temperature of its equilibrium plasma is about 10^4 K, and near the cathode – $1.2\cdot10^4$ K.

Conclusions.

1. A new relation (4) is obtained for approximate calculation of the equivalent active resistance R_{ce} of the plasma channel of pulse electric arc in air DES of the high-current discharge circuit of a powerful high-voltage CES of a test electrophysical installation generating the long-term *C*- component of artificial lightning current.

2. For the calculated estimate of the maximum electron temperature T_{me} in equilibrium electron-ion low-temperature plasma of pulse arc electric discharge in the air DES with metallic (graphite) electrodes used in the described experiments of the powerful high-voltage CES of the generator PCG-*C*, it is recommended that electrical engineers use the approximate formula (5).

3. High-voltage experiments carried out at the Scientific-&-Research Planning-&-Design Institute «Molniya» of the NTU «KhPI» on a powerful high-voltage CES of the PCG-*C* generator, which reproduces on the low-resistance load the long-term *C*-component of the current of artificial lightning with normalized ATPs in accordance with the current requirements of the US regulatory documents SAE ARP 5412: 2013 and SAE ARP 5416: 2013, confirmed the validity of the proposed calculation relationships (4) and (5) for determining the electrical and thermal physical values of R_{ce} and T_{me} in the plasma channel of the pulsed arc discharge in air DES.

REFERENCES

1. Dashuk P.N., Zayents S.L., Komel'kov V.S., Kuchinskiy G.S., Nikolaevskaya N.N., Shkuropat P.I., Shneerson G.A. *Tehnika bol'shih impul'snyh tokov i magnitnyh polej* [Technique large pulsed currents and magnetic fields]. Moscow, Atomizdat Publ., 1970. 472 p. (Rus).

2. Baranov M.I., Koliushko G.M., Kravchenko V.I., Nedzel'skii O.S., Dnyshchenko V.N. A Current Generator of the Artificial Lightning for Full-Scale Tests of Engineering Objects. *Instruments and Experimental Technique*, 2008, no.3, pp. 401-405. **doi: 10.1134/s0020441208030123**.

3. Baranov M.I. *Izbrannye voprosy elektrofiziki. Tom 2, Kn. 2: Teoriia elektrofizicheskikh effektov i zadach* [Selected topics of Electrophysics. Vol.2, Book 2. A theory of electrophysical effects and tasks]. Kharkiv, Tochka Publ., 2010. 407 p. (Rus).

4. Kuz'michev V.E. *Zakony i formuly fiziki* [Laws and formulas of physics]. Kiev, Naukova Dumka Publ., 1989. 864 p. (Rus).

5. Raiser Yu.P. *Fizika gazovogo razryada* [Physics of gas discharge]. Moscow, Nauka Publ., 1987. 592 p. (Rus).

6. Baranov M.I. A close calculation of active resistance of plasma channel of a spark digit is in the high-voltage heavy-current air switchboard of atmospheric pressure. *Bulletin of NTU «KhPI». Series: «Technique and electrophysics of high voltage»*, 2017, no.15(1237), pp. 5-11. (Rus).

7. Baranov M.I., Rudakov S.V. An approximate calculation of energy dissipation and electric erosion of electrodes in the high-voltage high-current air switch of atmospheric pressure. *Electrical engineering & electromechanics*, 2017, no.3, pp. 32-39. **doi: 10.20998/2074-272X.2017.3.05.**

8. SAE ARP 5412: 2013. Aircraft Lightning Environment and Ralated Test Waveforms. SAE Aerospace. USA, 2013. − pp. 1-56.

9. SAE ARP 5416: 2013. Aircraft Lightning Test Methods. SAE Aerospace. USA, 2013. − pp. 1-145.

10. Abramov N.R., Kuzhekin I.P., Larionov V.P. Characteristics of penetration of the walls of metal objects when exposed to lightning. *Electricity*, 1986, no.11, pp. 22-27. (Rus).

11. Baranov M.I. *Izbrannye voprosy elektrofiziki. Tom 3: Teorija i praktika elektrofizicheskih zadach* [Selected topics of Electrophysics. Vol. 3: Theory and practice of electrophysics tasks]. Kharkiv, Tochka Publ., 2014. 400 p. (Rus).

12. Baranov M.I. An approximate calculation of the maximum temperature of the plasma in high-current high-voltage spark discharge channel switch air atmospheric pressure. *Tekhnichna Elektrodynamika*, 2010, no.5, pp. 18-21. (Rus).

13. Berzan V.P., Gelikman B.Yu., Guraevsky M.N., Ermuratsky V.V., Kuchinsky G.S., Mezenin O.L., Nazarov N.I.,

Peregudova E.N., Rud' V.I., Sadovnikov A.I., Smirnov B.K., Stepina K.I. *Elektricheskie kondensatory i kondensatornye ustanovki. Spravochnik* [The electrical capacitors and condenser options. Directory]. Moscow, Energoatomizdat Publ., 1987, 656 p. (Rus).

14. Baranov M.I., Koliushko G.M., Kravchenko V.I., Nedzel'skii O.S., Nosenko M.A. High-voltage high-current air-filled spark gaps of an artificial-lightning-current generator. *Instruments and Experimental Techniques*, 2008, vol.51, no.6, pp. 833-837. **doi: 10.1134/s0020441208060109.**

15. Baranov M.I., Rudakov S.V. Development of new charts of capacitance-resistance defense of high-voltage capacitors of powerful capacity stores of energy from emergency currents. *Electrical engineering & electromechanics*, 2015, no.6, pp. 47-52. (Rus). **doi: 10.20998/2074-272X.2015.6.08**.

16. Lozanskiy E.D., Firsov O.B. *Teorija iskry* [Theory of spark]. Moscow, Atomizdat Publ., 1975. 272 p. (Rus).

Received 20.04.2017

M.I. Baranov[1], *Doctor of Technical Science, Chief Researcher,*
S.V. Rudakov[2], *Candidate of Technical Science, Associate Professor,*
[1] Scientific-&-Research Planning-&-Design Institute «Molniya», National Technical University «Kharkiv Polytechnic Institute»,
47, Shevchenko Str., Kharkiv, 61013, Ukraine,
phone +38 057 7076841,
e-mail: baranovmi@kpi.kharkov.ua
[2] National University of Civil Protection of Ukraine,
94, Chernyshevska Str., Kharkiv, 61023, Ukraine,
phone +38 057 7073438,
e-mail: serg_73@i.ua

How to cite this article:
Baranov M.I., Rudakov S.V. Approximate calculation of active resistance and temperature of the pulse electric arc channel in a high-current discharge circuit of a powerful high-voltage capacitor energy storage. *Electrical engineering & electromechanics*, 2017, no.4, pp. 42-48. **doi: 10.20998/2074-272X.2017.4.07.**

UDC 621.373 **doi: 10.20998/2074-272X.2017.4.08**

M.I. Boyko, A.V. Makogon

GENERATOR ON ARCADYEV-MARX SCHEME WITH PEAKING OF THE PULSE FRONT IN ITS CASCADES FOR FOOD DISINFECTING

Purpose. *To obtain experimentally that the duration of the high-voltage pulse front is less than 1.5 nanoseconds on the load of a pulse voltage generator of less than 50 ohms in the form of more than two working chambers with a water-containing product. That increases the efficiency of disinfection of treated products.* ***Methodology.*** *To obtain high-voltage pulses in working chambers - the generator load - the pulse generation method was used according to the Arkadyev-Marx scheme. The pulses on the load were measured with a low-ohm resistive voltage divider, transmitted over a broadband coaxial cable, and recorded using a C7-19 oscilloscope with a 5 GHz bandwidth. The working chambers were filled with water and consisted of an annular body made of PTFE 4 and metal electrodes forming the bottom and the chamber cover having flat linings of food stainless steel for contact with the food product inside the chamber.* ***Results.*** *The high-voltage pulses on the generator load of about 50 Ohm or less have a trapezoidal shape with a rounded apex and a base duration of no more than 80 ns. The experimentally obtained pulse amplitudes on the generator load are up to 18 kV. As the load resistance decreases, the amplitude of the pulses decreases, and the duration of the front and pulse duration in general are shortened because of the accelerated discharge of cascade capacitive storages.* ***Originality.*** *For the first time we have obtained experimentally on the load of the generator in the form of three parallel working chambers with water, the active resistance of each of which is less than 50 Ohm, the pulse front duration $t_f \approx 1$ ns. In addition, we have obtained experimentally a stable 9-10 channel triggering mode of the trigatron type spark gap in a five-cascade pulse voltage generator with a step-by-step peaking (exacerbation) of the pulse front in its cascades (GPVCP).* ***Practical value.*** *We have obtained experimentally the nanosecond pulse front duration on the GPVCP load and that opens the prospect of industrial application of such generators for microbiologically disinfecting treatment (inactivation of microorganisms in food) water-containing food products.* References 6, figures 8.

Key words: **generator of pulsed voltages, peaking of the pulse front in cascades of generator, working chamber, spark gap or switch, inactivation of microorganisms in food products.**

Цель. *Экспериментально получить на нагрузке генератора импульсных напряжений величиной менее 50 Ом в виде более двух рабочих камер с водосодержащим продуктом длительность фронта импульсов высокого напряжения менее 1,5 наносекунд, что повышает эффективность обеззараживания обрабатываемых продуктов.* ***Методика.*** *Для получения высоковольтных импульсов на рабочих камерах - нагрузке генератора применена методика генерирования импульсов по схеме Аркадьева – Маркса. Импульсы на нагрузке измерялись при помощи низкоомного резистивного делителя напряжения, передавались по широкополосному коаксиальному кабелю и регистрировались при помощи осциллографа С7-19 с полосой пропускания 5 ГГц. Рабочие камеры заполнялись водой и состояли из кольцеобразного корпуса, выполненного из фторопласта, и металлических электродов, образующих дно и крышку камеры, имеющих плоские накладки из пищевой нержавеющей стали для контакта с пищевым продуктом внутри камеры.* ***Результаты.*** *Высоковольтные импульсы на нагрузке генератора примерно 50 Ом и менее имеют трапециевидную форму со скругленной вершиной и длительность по основанию не более 80 нс. Экспериментально полученные амплитуды импульсов на нагрузке генератора – до 18 кВ. При уменьшении сопротивления нагрузки амплитуда импульсов уменьшается, а длительность фронта и импульсов в целом укорачивается из-за ускоренного разряда емкостных накопителей каскадов.* ***Научная новизна.*** *Впервые на нагрузке генератора в виде трех параллельно включенных рабочих камер с водой, активное сопротивление каждой из которых менее 50 Ом, экспериментально получена длительность фронта импульсов $t_f \approx 1$ нс. Кроме того, отлажен стабильный 9-10 канальный режим срабатывания выходного разрядника тригатронного типа в пятикаскадном генераторе импульсных напряжений с покаскадным обострением фронта импульсов (ГИНПО).* ***Практическая значимость.*** *Полученная экспериментально наносекундная длительность фронта импульсов на нагрузке ГИНПО открывает перспективу промышленного применения таких генераторов для микробиологически обеззараживающей обработки (инактивации микроорганизмов) водосодержащих пищевых продуктов.* Библ. 6, рис. 8.

Ключевые слова: **генератор импульсных напряжений, покаскадное обострение фронта импульсов, рабочая камера, разрядник, инактивация микроорганизмов в пищевых продуктах.**

Introduction. Generators on Arcadyev-Marx are widely used in high-voltage pulse technology [1]. Due to the ability to obtain nanosecond fronts at a voltage of 100 kV and more on the load of such generators [2], repetition rates of 200 pulses per second or more, they are promising for decontaminating treatment of liquid water-containing products.

The processing of products by pulsed electric fields (PEF) with nanosecond fronts makes it possible to conserve the initial quality of food products with the use of traditional thermal methods while reducing the specific energy consumption for inactivating microorganisms in them [3, 4]. In the PEF method, or a complex of high-voltage impulse actions (CHIA), short electric pulses are used, which can be obtained with the help of Arcadyev-Marx generators. Decontamination treatment is carried out in working chambers with a processed product, which is a load for generators of high-voltage pulses. The typical duration of pulses of strong pulsed electric field strength in working chambers can vary from 50 ns to 1 μs, the amplitude ranges from 5 kV/cm to 200 kV/cm without breakdowns. Several working chambers with a water-containing product connected to the generator output are a low-impedance load for the generator, which can not exceed 50 Ω and can lead to undesired elongation of the

voltage pulse front. In [5], a method for treating liquids and flowing products in several working chambers is proposed, which makes it possible to avoid undesirable extension of the front due to the use of impulse frontizers. The Arcadyev-Marx pulse voltage generators in the regime of the step-by-step aggravation of the pulse front (GPVCP) make it possible in practice to solve the problem of undesirable elongation of the front. In this paper, an experimental check of the operation of the GPVCP on a load of not more than 50 Ω in the form of three working chambers with water, connected in parallel, without extension of the front of the pulses on the load, was carried out.

The goal of the work is to experimentally obtain on a generator load of less than 50 Ω in the form of more than two working chambers with a water-containing product, the duration of the high-voltage pulse front less than 1.5 nanoseconds, which increases the efficiency of disinfection of the processed products.

Experimental installation. The installation circuit is shown in Fig. 1.

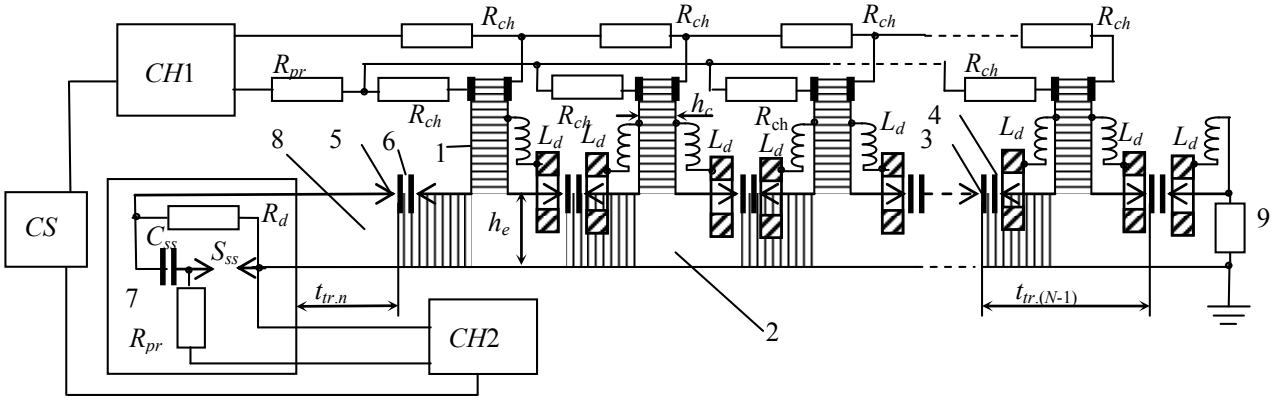

Fig. 1. Circuit of installation with generator of pulse voltages with a step-like peaking of the pulse front

In Fig. 1 pre-charged to voltage U_{main} sections of the power line and capacitive storages are shaded; N is the number of cascades; 1 – capacitive storage of a cascade with capacitance C_{st}, which can be a long line with distributed parameters; 2 – power line – broadband homogeneous long line with distributed parameters with distance he between direct and reverse current conductors with wave impedance z_e; 3 – cascade discharger; 4 – capacitance (C_{gap}) between the discharge gap electrodes 3; 5 – starting discharger of the GPVCP; 6 – capacitance ($C_{gap.o}$) between the discharge gap electrodes 5; 7 – starting system (device); 8 – long transmission line with wave impedance Z_n=Z_e between the device 7 and the starting discharger 5; 9 – load with impedance Z_{load}; $t_{tr.n}$ and $t_{tr.k}$ are the times of the electromagnetic wave traveling along the line 8 and between two adjacent cascade dischargers, respectively; k is the number of the cascade (k = 1, 2,…, N); h_c is the length of the discontinuity in the live current conductor, into which (discontinuity) the capacitive storage of the k-th cascade is connected. R_{pr}=1 MΩ, R_{ch}=3.2 kΩ, R_d=1440 Ω, L_d≈0.5 μH.

Both *CH*1 and *CH*2 chargers are assembled according to the Cockcroft multiplication scheme [6] and are powered by step-up transformers fed with an adjustable AC voltage from the *CS* control system. Starting device 7 contains a ceramic capacitor K15-10 with of 10 nF (C_{ss}) and a two-electrode spark gap S_{ss}, triggered by overvoltage (for self-breakdown).

In GPVCP, on which experiments were conducted, there are 5 cascades. Capacitive storage of cascades C_{st}=3×10^{-9} F are made in the form of low-resistance strip lines (which can be considered as flat capacitors when charged) from foil-coated glass-fiber laminate, 0.45 m in height and width of coatings, and with dielectric thickness h_c = 5 mm.

The power line of this GPVCP is made in the form of a real strip line with a distance between the forward and reverse current conductor h_e=50 mm [2]. The return current line is a brass sheet 1 m long, 0.4 m wide, 1 mm thick. It has a sheet of plexiglass 8 mm thick. The remaining space between the forward and reverse conductor is filled with air at atmospheric pressure.

The general view of a five-cascade pulse voltage generator with a step-like exacerbation of the front of the generated pulses, on which experiments are performed, is shown in Fig. 2.

Dischargers of cascades are of trigatron type with air filling at atmospheric pressure. Each of the two electrodes of the discharger is made in the form of a metal plate fixed to a plexiglass support, 5 mm thick, in which 10 holes are made at equal distances from each other. In these holes are inserted 10 needle electrodes connected in a short time with the corresponding capacitive storage plate of the GPVCP cascade and through the inductance L_d≈0.5 μH – with the plate.

Inter-electrode gaps in the dischargers are regulated along the length. Such a design of the dischargers provides a uniform electric field in them when the GPVCP cascades are charged and the field is sharply unhomogeneous during discharge. Therefore, when the GPVCP is discharged, spark channels are formed only between the corresponding two needle electrodes located on the same axis. In each of the cascade dischargers can be formed in the discharge from 1 to 10 sparks.

Fig. 2. General view of the GPVCP

The load 9 (Fig. 1) during the experiments was varied: it was carried out in the form of 10 resistors TBO-10 with nominal resistance of 560 Ω each (measured value of resistance was from 580 to 630 Ω), in the form of one working chamber with water, three working chambers with water. Load resistors and working chambers were connected to the corresponding tip electrodes of the 10-channel output gap of the GPVCP.

The experimental setup works as follows. With the help of the *SC* control system, capacitive storage of the GPVCP cascades is charged through *CH*1, and then the capacitive storage C_{ss} of the starting system is charged through *CH*2 before the S_{ss} self-breakdown. The charge level is controlled by kilovoltmeters C-196.

Pre-capacitive storage 1 of cascades of the generator are charged to the voltage U_{main} (Fig. 1). In general, charging can be either rectified voltage or an impulse voltage. After preliminary charging, the only discharger on which there is no «on standby» voltage U_{main} is the spark gap at the output of the GPVCP, it is also the discharger of the last *N*-th cascade. After charging the cascade from the start device 7 to the start-up discharger 5, a voltage pulse with an amplitude U_{ivp} is provided along the line 8 on the generator, providing the time of its switching $t_{sw.0}$ and the duration of the front $t_{f.0}$ of the generated pulse by a shorter time $2t_{tr.0}$ of the double path of the electromagnetic wave between the starting discharger of the first cascade. The dischargers of the GPVCP are triggered sequentially, starting from the starting one, triggered by the control pulse from the start-up system, and ending with the output discharger with the shortest switching time.

The beginning of the fall of the impulse voltage on the load of the GPVCP generator immediately after the voltage rise on it to the value A_N [2]:

$$A_N = \left(NU_{main} + 2U_{ivp}\right)\frac{Z_{load}}{Z_{load} + Z_e}, \qquad (1)$$

or

$$A_N = 2A_{N-1}\frac{Z_{load}}{Z_{load} + Z_e}, \qquad (2)$$

where Z_{load} is the load impedance ensured by the fact that possible reflections from the trigger device 7, which can lead to a slow increase in the voltage amplitude on the load up to $2\times A_N$, are compensated by the discharge of the cascade capacitors, and also because the start device is separated from the GPVCP proper by the transmission line 8 with the corresponding time The path of an electromagnetic wave along it. Number of cascades in this GPVCP $N = 5$.

In according with (1) at U_{main}=6 kV, U_{ivp}=12 kV, Z_{load} = 50 Ω, Z_e=50 Ω A_N=(5×6+2×12)×50/(50+50)= = 27 kV.

Results of investigations. Investigation of the pulse characteristics at different loads of the GPVCP was carried out using a low-resistance resistive voltage divider connected to the load of the generator, a recording C7-19 oscilloscope with 5 GHz bandwidth and a broadband coaxial cable with Z_c 50 Ω impedance connecting the shielded low-voltage divider arm to the input of oscilloscope through an attenuator of 20 dB. The oscilloscope was located in the measuring cabin, which protects it from electromagnetic interference.

Resistance of high-voltage divider arm R_1 = 560 Ω – one of the load resistors TBO-10 in the GPVCP, the resistance of the low-voltage arm R_2 = 3 Ω is collected from the parallel-connected resistors TBO-0,5 (Fig. 3). The low-voltage divider arm and the matching resistor R_3= 50 Ω are located in a shielding metal case of a cylindrical shape with a flange connected shortly with the generator's return current. The cable is connected to the low-voltage divider arm using a coaxial connector.

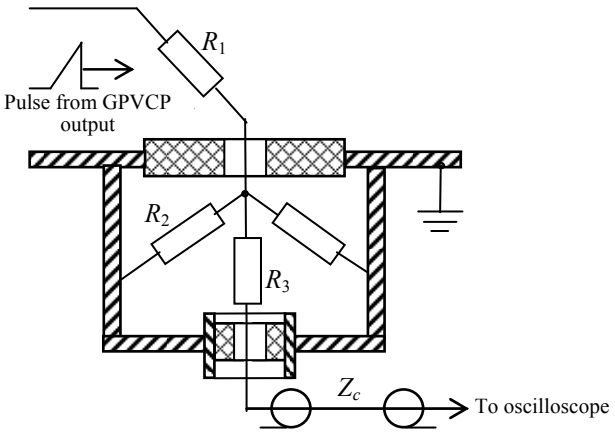

Fig. 3. Circuit of the resistive divider on the GPVCP output

Taking into account the fact that the input impedance of the oscilloscope C7-19 is 50 Ω, the divider division factor $K_d = [(R_1+R_2)/R_2]\times(R_3+Z_c)/Z_c$ = = [(560+3)/3]×(50+50)/50 ≈ 375 (Ω). Between the input of the oscilloscope C7-19 and the end of the cable with the connector, an attenuator 20 dB was inserted, which attenuates the incoming signal by a cable 10 times.

Therefore, the total division factor $K_{d\ total}$≈3750. The sensitivity of the oscilloscope CS7-19 is 1.6 V/div = = 1.6 V/cm.

The output multichannel discharger of the GPVCP at the amplitude of the charging voltage of the high-voltage capacitive storage of the control system, which exceeds twice the amplitude of the charging voltage of the main storages of the GPVCP cascades, stably operates in the 9-10 channel mode (10 is the maximum possible number of discharge channels in the discharger). This mode when the GPVCP operates on a resistive load in the form of ten TBO-10 resistors with a nominal resistance 560 Ω each is illustrated in Fig. 4. After the formation of ten channels in the output discharger, all ten load resistors are connected in parallel.

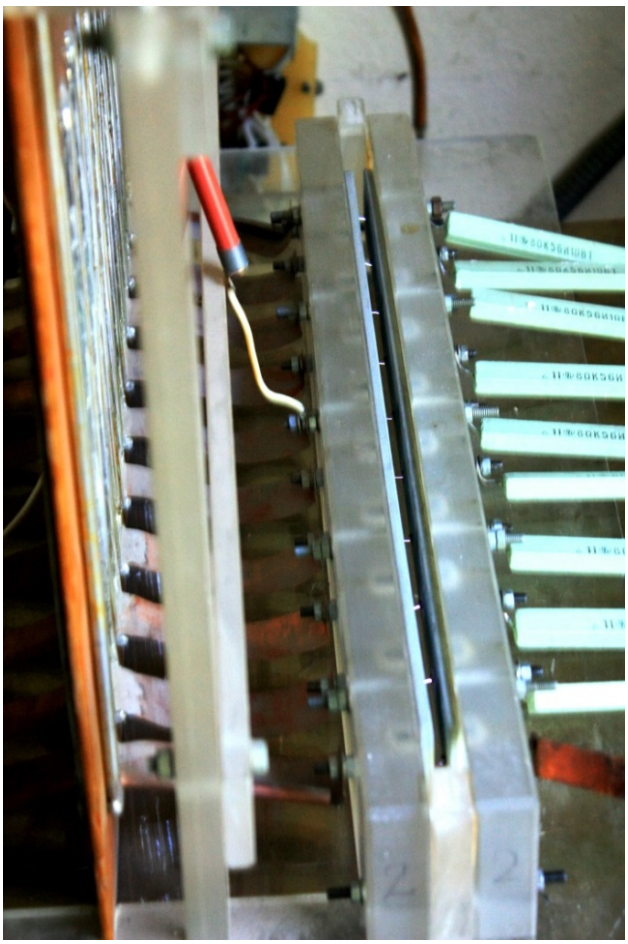

Fig. 4. Photo of the multichannel spark discharge in the GPVCP output

We note that the brightness of the discharge channels is approximately the same, which indicates that the current is uniformly distributed over the discharge channels. Oscillograms of pulses with nanosecond fronts on the GPVCP load in the form of TBO-10 resistors, one working chamber, and three working chambers are obtained. The shape of the pulses on the load is close to trapezoidal, which is illustrated in Fig. 5.

From the oscillograms in Fig. 5 it can be seen that the pulse front contains two parts: the first (initial) steep part and the second (closer to the top) more sloping. This indicates that in the GPVCP spark gap in this particular regime, there is not a complete, partial exacerbation of the front of the pulses being formed. Because of the presence of the sloping part, the total duration of the front of the t_f pulses is approximately $t_f \approx 20$ ns. The gently sloping part of the pulse front also occurs due to reflections of electromagnetic waves caused by the triggering of dischargers, from various inhomogeneities in the GPVCP power line and in the launch system. The pulse duration along the base is approximately 80 ns, the amplitude is 18 kV. This is 1.5 times less than the calculated amplitude given above.

The smaller values of the experimentally obtained amplitude, in comparison with the calculated amplitude, are explained by the lengthening of the front due to its incomplete aggravation by cascade dischargers, inadequate matching of the wave resistance of the GPVCP power line with its resistive load, resulting from this undesirable voltage reflections in the GPVCP and a fairly rapid discharge of capacitive storage devices GPVCP.

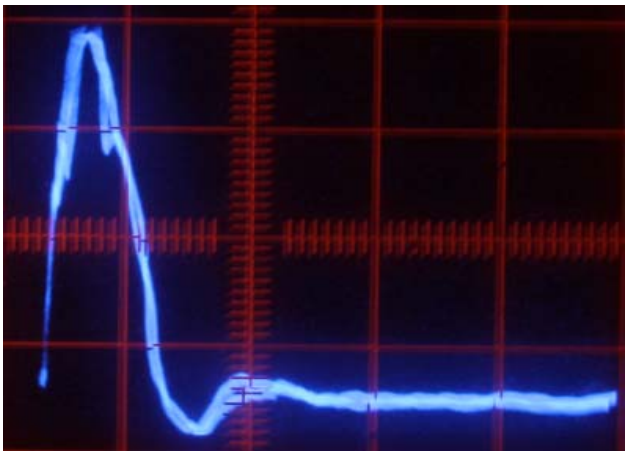

Fig. 5. Oscillograms (two oscillograms are superimposed) of the voltage pulses on the load in the form of 10 TBO-10 resistors 560 Ω: the division by the time axis is 100 ns/div, in the process axis 6 kV/div

The oscillogram in Fig. 6 illustrates the shape of the voltage on the load in the form of one working chamber and five TBO-10 resistors at 560 Ω.

From the oscillogram in Fig. 6 it follows that the pulse front duration is approximately 2.5 ns, and the amplitude is 12 kV. The amplitude decreased due to the fact that the load became more low-impedance after connecting the working chamber with water (see also formula (1)). The ring-shaped body of the working chamber is made of PTFE, and the metal electrodes forming the bottom and the chamber cover have flat linings of food grade stainless steel for contact with the food product inside the chamber.

The working volume of the working chamber filled with water has a disk shape with diameter D = 90 mm and height h = 15 mm. With a specific volume resistivity of water ρ = 10 Ω × m, the active resistance R_w of water in the working chamber is $R_w=\rho h/(\pi D^2/4) = 10\times0.015/(3.14\times0.09^2/4)\approx23.6$ Ω.

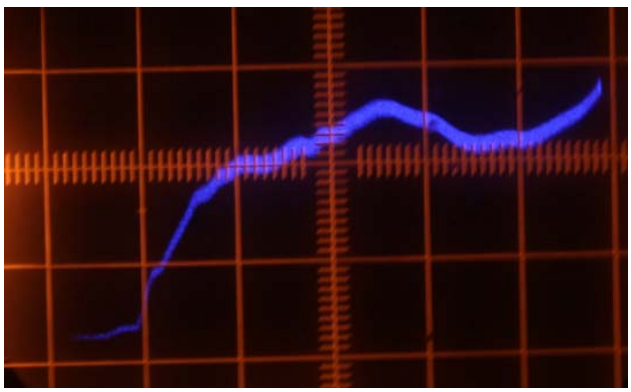

Fig. 6. Oscillogram of the front part of the voltage pulse on the load of the GPVCP in the form of one working chamber, connected in parallel with five load resistors TBO-10; the division by the time axis is 2.5 ns/div, in the process axis – 6 kV/div

In connection with the decrease in the load resistance capacitive cascade storages began to discharge faster, which in turn led to a decrease in the amplitude. At the same time, the contribution of the non-rapid part to the pulse front time on the load decreased significantly, and the front was shortened to ≈2.5 ns.

When three working chambers are connected as a load (see Fig. 7), the voltage amplitude on them becomes even smaller (see Fig. 8) than on one working chamber.

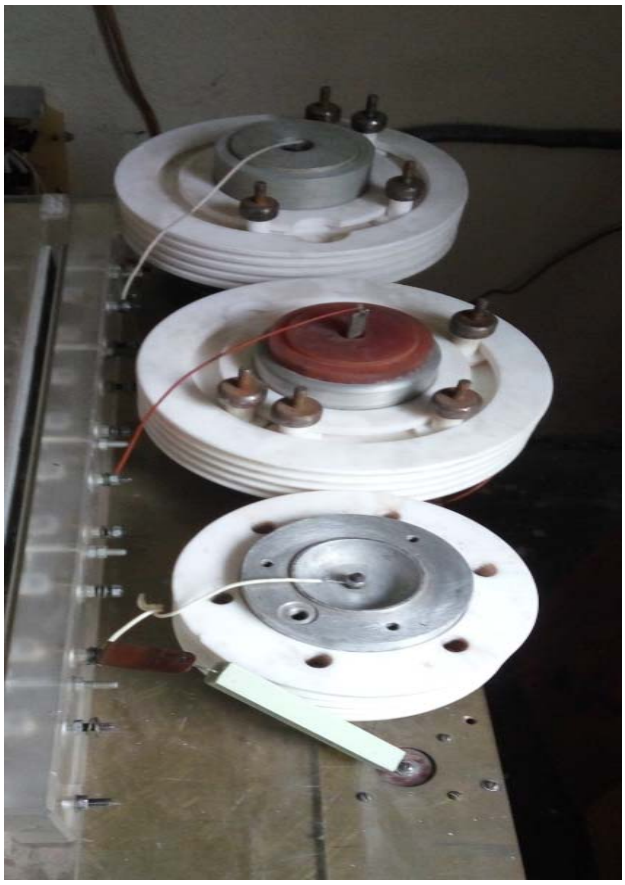

Fig. 7. GPVCP load as three working chambers with water

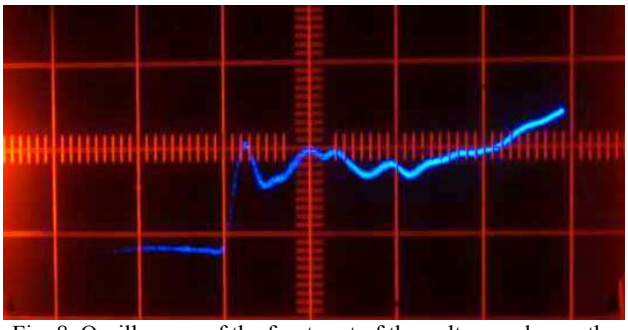

Fig. 8. Oscillogram of the front part of the voltage pulse on the load of the GPVCP in the form of three working chambers connected in parallel with each other and with a load resistor TBO-10; the division by time axis is 2.5 ns/div, in the process axis – 6 kV/div

From the oscillogram in Fig. 8 it follows that the duration of the pulse front on the load is about 1 ns, and the amplitude is about 8 kV.

To increase the intensity of the pulsed electric field in the working chambers and the voltage on them without extending the front of the pulses, it is necessary to increase the charging voltages of the capacitive storage devices from the charging devices *CH*1 and *CH*2, thus increasing the gaps in the GPVCP dischargers accordingly.

The possibility shown experimentally (see Fig. 8) of obtaining in several working chambers, connected in parallel, the voltages, and consequently also the strengths of the pulsed electric field with a record short front (about 1 ns), opens up the prospect of reducing the specific energy consumption for microbiologically disinfecting treatment of water-containing food products, increasing the shelf life of these products without impairing their consumer value. And, consequently, the prospect of industrial application of GPVCP.

Conclusions.

1. A method is proposed for shortening the front of pulses in working chambers for inactivating microorganisms processing food products by using pulse-voltage generators in accordance with the Arcadyev-Marx scheme in the regime of a step-by-step exacerbation of the pulse front.

2. The front of duration t_f ≈1 ns of pulses on the GPVCP load in the form of three parallel working chambers with water, the active resistance of each of which is less than 50 Ω was experimentally obtained. Such a short duration of the pulse front confirms that generators - GPVCP are promising for microbiologically disinfecting treatment of water-containing food products (inactivation of microorganisms in products).

3. The stable 9-10 channel mode of the output of the five-cascade generator – GPVCP – is debugged.

4. The pulses on the load are measured with a low-resistance resistive voltage divider, as a transmission line a broadband coaxial cable is used, connected to a recording device - an oscilloscope C7-19 with bandwidth of 5 GHz.

5. Working chambers made in the form of an annular body made of fluoroplastic and metal electrodes forming the bottom and the chamber cover having flat linings of food stainless steel for contact with the food product inside the working volume are used. The chambers were filled with water.

6. High-voltage pulses on the GPVCP load of about 50 Ω or less have a trapezoidal shape with base duration of no more than 80 ns, experimentally obtained pulse amplitudes on the load – up to 18 kV. As the load resistance decreases, the amplitude of the pulses decreases, and the duration of the front and pulses is generally shortened. The shortening of the front occurs as a result of the fact that the sloping (slow) part of the pulse front, which is due to reflections of electromagnetic waves caused by the operation of the dischargers, from various inhomogeneities in the GPVCP power line and in the launch system, is removed partially or fully by an accelerated discharge of capacitive cascade storages to a load with reduced resistance.

REFERENCES

1. Mesiats G.A. *Impul'snaia energetika i elektronika* [Pulsed power and electronics]. Moscow, Nauka Publ., 2004. 704 p. (Rus).

2. Boyko N.I. Generator on Arcadyev-Marx scheme in the mode with peaking of the pulse front in its cascades for food disinfecting. *Tekhnichna elektrodynamika. Tem. vypusk «Problemy suchasnoyi elektrotekhniky»*, 2000, part 6, pp. 94-97. (Rus).

3. Barbosa-Canovas G.V., Gongora-Nieto M.M., Pothakamury U.R., Swansson B.G. *Preservation of Foods with Pulsed Electric Fields*. − Washington, San Diego, Academic Press Publ., 1999. − 200 p. **doi: 10.1016/b978-0-12-078149-2.x5000-**

4. Jasim Ahmed, Hosahalli S. Ramaswamy, Stefan Kasapis, Joyce I Boye. *Novel Food Processing: Effects on Rheological and Functional Properties*. CRC Press Publ., 2016. 510 p. *Chapter 11. Pulsed Electric Fields for Food Processing Technology* by Maged E.A. Mohamed and Ayman H. Amer Eissa. 2012. pp. 275-306. **doi: 10.5772/48678.**

5. Boyko N.I., Makogon A.V. *Sposib obrobky ridyn i tekuchykh produktiv* [The method of treatment liquids and fluid products]. Patent UA, no. 113592, 2017. (Ukr).

6. Beier M., Bek V., Meller K., Tsaengl V. *Tekhnika vysokikh napriazhenii: teoreticheskie i prakticheskie osnovy primeneniia* [Technics of high voltages. Theoretical and practical application bases]. Moscow, Energoatomizdat Publ., 1989. 555 p. (Rus).

Received 08.06.2017

M.I. Boyko[1]*, Doctor of Technical Science, Professor,*
A.V. Makogon[1]*,*
[1] National Technical University «Kharkiv Polytechnic Institute», 2, Kyrpychova Str., Kharkiv, 61002, Ukraine,
phone +380 57 7076245,
e-mail: qnaboyg@gmail.com

How to cite this article:
Boyko M.I., Makogon A.V. Generator on Arcadyev-Marx scheme with peaking of the pulse front in its cascades for food disinfecting. *Electrical engineering & electromechanics*, 2017, no.4, pp. 49-54. **doi: 10.20998/2074-272X.2017.4.08.**

UDC 621.315.2 **doi: 10.20998/2074-272X.2017.4.09**

V.M. Zolotaryov, Yu.P. Antonets, S.Yu. Antonets, O.V. Golik, L.A. Shchebeniuk

ONLINE TECHNOLOGICAL MONITORING OF INSULATION DEFECTS IN ENAMELED WIRES

In this paper the authors used non-destructive technological monitoring of defects insulation enameled wire with poliimid polymer. The paper is devoted to the statistical method for processing, comparison and analysis of results of measurements of parameters of insulation of enameled wire because of mathematical model of trend for application in active technological monitoring is developed; the recommendations for parameters of such monitoring are used. It is theoretically justified and the possibility of determination of dependence of the error on the velocity of movement of a wire for want of quantifying of defects in enameled insulation by non-destructive tests by high voltage. The dependence of average value of amount of defects for enameled wire with two-sheeted poliimid insulation in a range of nominal diameter 0.56 mm is experimentally determined. The technological monitoring purpose is to reduce the quantifying defects of enameled insulation. References 10, figures 5.
Key words: **enameled wire, poliimid insulation, defects of insulation, technological monitoring, tests by voltage.**

Представлены результаты неразрушающего технологического контроля количества дефектов в изоляции эмаль провода на основе полиимидного полимера. Рассмотрено применение статистического анализа результатов измерения показателей контроля с помощью математической модели тренда для использования результатов в активном технологическом контроле. Предложены рекомендации для практического использования параметров функции тренда для контроля гарантированного уровня бездефектности изоляции методами статистики предельных значений. Параметром тренда является скорость уменьшения (или увеличения) длины провода с заданной дефектностью в течение технологического цикла. Теоретически показана и подтверждена измерениями возможность количественной оценки тенденции изменения дефектности эмальизоляции для провода ПЭЭИДХ2 – 200 с двухслойной полиимидной изоляцией номинальным диаметром 0,56 мм в течение технологического цикла. Определение количественной оценки тенденции изменения дефектности эмаль изоляции позволяет также выделить и количественно оценить случайную ошибку технологического процесса – суммарную ошибку результатов технологического контроля, которая является количественной характеристикой случайной составляющей стабильности технологического процесса и обусловлена большим количеством причин, каждой из которых можно пренебречь по сравнению с суммой. Библ. 10, рис. 5.
Ключевые слова: **эмаль провод, полиимидная изоляция, дефектность изоляции, технологический контроль, испытания напряжением.**

Problem definition. The enamel wire based on polyimide synthetic copolymers with a temperature index of 200 °C has high electrical and mechanical properties of insulation [1, 2]. The introduction of such innovative types of cable and wire products into production allows to provide the highest modern level of electrical, mechanical strength and heat resistance of the winding insulation of windings of electric machines and apparatuses - mass production of electric machinery.

To manufacture such wires, modern automatic lines with high velocities (up to 1000 m/min) and deep catalytic annealing of enamel lacquers are used [2]. The development of such products, innovative for a specific manufacturer, requires the application of an operational technological control system that ensures the liquidity of products at the reached level of technical parameters. At the same time, control and analysis of the dispersion of the main technical parameters of the products are basic information for the implementation of the principle of continuous quality improvement in accordance with ISO 9001: 2015.

The problem for a specific manufacturer is the development and implementation of non-standard technical and organizational solutions for technological control, with mandatory binding of the technical parameters to the achieved level of production technology. There is a contradiction between the relatively high cost of innovative products, the production of which is based on the use of modern advanced technologies and materials, on the one hand, and the need to organize technological control of the dispersion of technical parameters in the process of a continuous automatic technological cycle that requires additional costs on the other.

The task, at first glance, seems to be one that does not have a solution for the producers in the period of development of products known in the world, but innovative for them. An example is the well-known concept of «Six Sigma» («6σ») [3]. In it, the main criterion of product quality is its homogeneity, which is quantitatively reflected by the generally accepted characteristic of the spread of parameters - their root-mean-square deviation σ. The indicator of homogeneity used in marketing is the ratio of the range of admissible values of the main parameter to the experimentally determined value of σ. The concept of «Six Sigma Methodology» is a demonstration of the manufacturer's achievements in the quality industry, but does not contain a methodology for ensuring these achievements.

The presented example shows that the contradiction between the relatively high cost of innovative products and the need for additional costs to organize technological control of the innovative process of its production is one of the main problems of technological development of the enterprise. And the more the technological cycle is automated, the more this problem becomes actual. At the same time, its solution requires the adoption of non-standard technical and technological solutions, since there is a significant theoretical and technical difference between the tasks of acceptance and current technological control [4]. The problem of the organization of active technological control is conceptual for a modern, mass production-oriented, development and automation company.

Analysis of literature. Since this problem is closely related to the economic component of mass production, it was proposed in [1] to resolve the contradictions between the relatively high cost of production and the price factor, as a criterion for liquidity for wires with polyimide insulation, by reducing the level of breakdown voltage requirements agreed with the consumer. In our opinion, the introduction of a spectrum of technical requirements for the same products significantly expands the range of applicable technical requirements. This, at least, blurs the ranges of acceptable values for the parameters of the same product, complicates the relationship between the manufacturer and the customer of the product, but does not solve the problem of applying effective technological control.

The first conceptual works devoted to the tasks of current technological control are dated to the beginning of the 60s of the 20th century. And their result is formulated in [5]: «Unlike the acceptance control, where the degree of suitability of ready-made batches of products is determined, current monitoring should ensure the normal course of the technological process.» This means that in the very formulation of the issue of technological control, the possibility of changes in the technological process and the need for rapid detection and quantification of such changes are laid. Theoretically, this means that each regular result obtained during technological control is an element of a different, unknown statistical array. Therefore, the statistical procedure for processing the results of technological control requires the development of an algorithm for processing and presenting the results; Algorithm of decision making. The above general concept of technological control [4] is relevant. Its specific implementation in automated and high-speed continuous technological cycles of modern cable production requires, in addition to almost instantaneous efficiency (on-line mode) [2, 3, 5] solutions to a number of problems: scientific and technical.

Scientific problems are caused by the following.

Measuring the variance of a technical parameter in the production process by the method of obtaining and presenting the results is mediated and relative. The classical (canonical) measurement model can not be applied to these measurements, since it requires the fulfillment of three conditions [3]:

– the measurement time is unlimited;

– the measured value keeps the true value unchanged during the entire measurement cycle;

– all the factors affecting the result are precisely defined.

At least the first two conditions can not, in principle, be met when measuring the dispersion of a technical parameter in a specific task of the current process control. Therefore, in this case, only a statistical model is acceptable, in which the measured quantity is a sequence of values that give information about the current state of the measurement object. In this case, the true value of the quantity may remain undefined at a given interval of the measurement process [2].

Therefore, in each continuous technological process, it is necessary to develop a statistical model of a specific technological control process, which includes: a statistical model of the process of measuring variance of parameters, an algorithm for processing and presenting the results.

Technical problems are caused by the fact that on the basis of the analysis of the influence of the components of the technological process on the formation of the electrophysical parameters of the product, the following are need:

1) the choice of operations, which are decisive for ensuring the quality of products;

2) selection of measured parameters, which are decisive for ensuring product quality;

3) determining process tolerances for the selected parameters;

4) determining the periodicity of measurements and the minimum sample size.

In this case, it is necessary to divide the trend of the change in the control parameter as a function of the technological time and the random error of the technological process. This separation can be performed according to a known statistical trend model with an error (only the error is a random variable) for a number of observations of the values of the quantity x [7]:

$$x_i = f(t_i) + \delta_i, \quad (1)$$

where t_i is the deterministic variable, which is the technological time; $f(t_i)$ is the deterministic function (trend of the technological process); σ_i is the random variable (random component of process stability).

World manufacturers of equipment for enamel wires based on polyimide synthetic copolymers [3] use modern highly efficient systems for continuous statistical monitoring of the specific number of defects (*er*) of insulation *on-line* for current process control. The number of defects is the number of places in which the current through the insulation exceeds the established one.

Discrete current measurement through insulation under the influence of high DC voltage is provided by the EFHP system from MAG-ECOTESTER Company [3]. Statistical indices of the number of insulation defects

recorded for each coil are stored on magnetic media for further analysis. This is an example of modern technological control, in which the manufacturer decides on the criteria for making technological decisions.

The goal of the work. Assessment of **the guaranteed level of defect-free of insulation** of enamel wires insulated with polyimide copolymers on the basis of separation:

- trend of the technological process - a significant deterministic change in the results of technological control during the technological process;

- statistical **error** of the technological process - the total error in the results of technological control, which is a quantitative characteristic of the random component of the stability of the technological process.

Main results.

The results of measuring the number of wire defects during the manufacturing process for 24 hours show the presence of two different periods with a continuous automated process. A significant difference in the dynamics of defectiveness changes during these periods indicates that in the technological cycle it is necessary to distinguish the periods of run-in (increased but rapidly decreasing insulation defects at the beginning of the cycle) and normal insulation (insulation defect is stable).

Consideration of the results of control of imperfection of the enamel wire as a single statistical array is possible by choosing the appropriate function for the trend, in this case exponential (Fig. 1,*a*). However, a significant difference in the dynamics of defect change during the periods of run-in and normal insulation causes a significant difference in the estimation of the statistical error of the control (Fig. 1,*b*). Therefore, to solve the set task: the development of a method for **estimating the guaranteed level of insulation defectiveness**, the data array is divided into a deterministic linear function $f(t_i)$ (trend: solid line) and a random value δ_i in accordance with the trend model with error (1) in [7] (see Fig. 2).

The representation of the results of the control of the imperfection of the enamel wires with two statistical sets (Fig. 2) shows that the random component (process error) in the period of normal insulation is stable and can be quantified and its average value in this case is 10 % of the average number of defects for the entire period of observations. It is this quantity that is a quantitative estimate of random deviations in the technological process and should be subject to statistical control in the system for ensuring product homogeneity.

At the same time, the trend of the number of defects in the period of normal insulation, as it is determined by a deterministic function, should be subject to analysis for technologists, since it is **the trend of the number of defects in the period of normal insulation** that determines the criterion for the optimal duration of the continuous technological cycle. In this case, there is a weak positive trend: an increase in the number of defects (2 ± 1) defects per hour, which allows determining the time of the optimal duration of the continuous technological cycle.

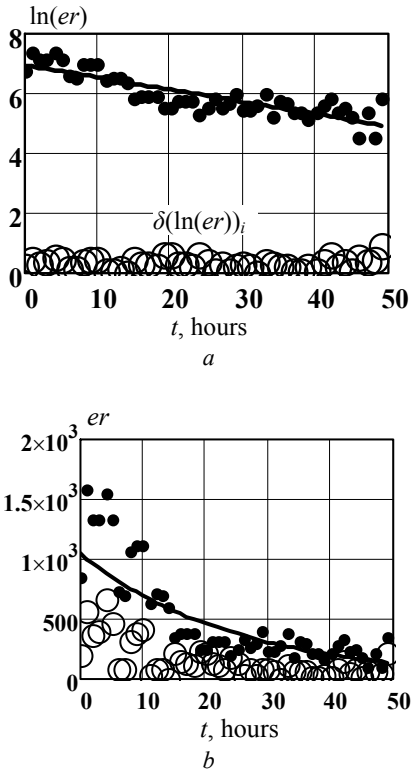

Fig. 1. Separation of the data sets on the number of defects on the coil (black dots) on - the deterministic function $f(t_i)$ (trend: solid line exponential function) and random value δ_i (empty points) using various mathematical separation procedures

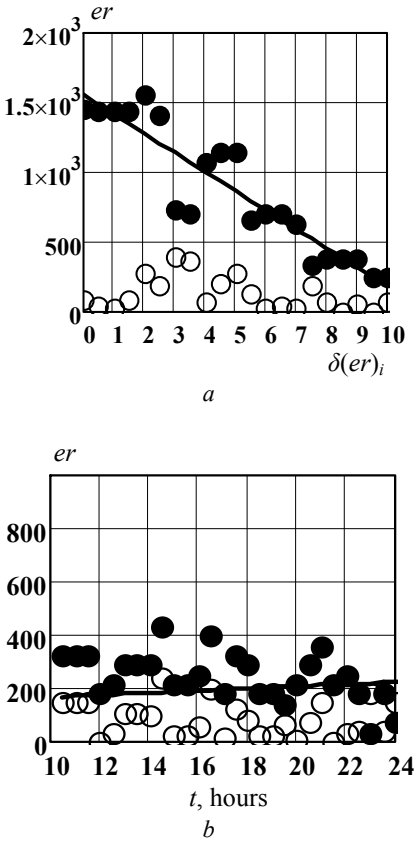

Fig. 2. Separation of data sets on the number of defects on the coil (black dots) on - the deterministic linear function $f(t_i)$ (trend: solid line) and random value δ_i (empty points) for two periods in a continuous automatic manufacturing process: the first (*a*) run-in period and the subsequent (*b*) normal insulation period

A different situation exists in the period of run-in. The data in Fig. 2,*b* show the need for technical solutions, first of all, to reduce the period of run-in. The quantitative criterion is the negative coefficient of the trend. In this case, minus (125 ± 7) defects per hour. The undoubted task of the technologist is to ensure the increase of this parameter in absolute terms by half.

The trend of a change in the values of the controlled parameter during a continuous technological cycle is characteristic not only for the defectiveness of insulation. Fig. 3 shows the results of a relative change in the diametric thickness of the enamel insulation $\delta\Delta$ in the continuous process of manufacturing 60 coils of the enamel wire.

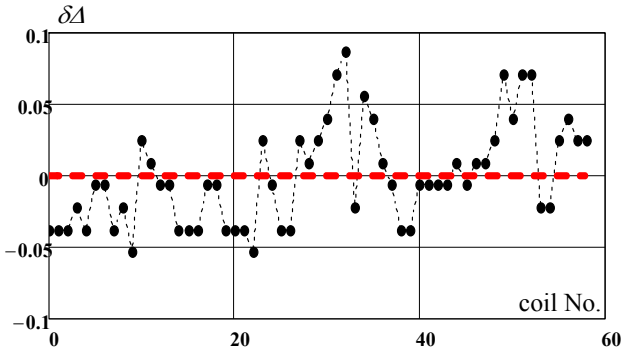

Fig. 3. The relative change in the diametric thickness of the enamel insulation $\delta\Delta$ in the continuous process of manufacturing the enamel wire ПЭЭИДХ2-200-МЭК with diameter of 0.56 mm

It is also obvious that there is a trend, so the standard variance of a parameter includes both its random spread (statistical error) and the influence of the parameters of the deterministic component (trend). In this case, the trend of the insulation thickness is due to the technological drawing of the copper wire, which is permissible (less than 0.5 % of the diameter), but affects the thickness of the enamel insulation.

Only when the trend parameters and its cause are determined (the duties of the process engineer) can the control of the variance of the controlled parameter be controlled, for this, a unified method for estimating the random component of the variance of the parameter should be used in mass production.

Dispersions of the rated parameters of the wire can be determined after it is manufactured (first of all, the variance of the breakdown voltage), therefore such control under production conditions remains largely passive.

In the EFHP system [3], the test results are displayed on-line on the monitor, the results are stored on magnetic media (system advantage). However, in production practice, these results are not used as quantitative indicators. To assess the guaranteed level of fault-free insulation, it is necessary to distinguish a random error of technological control. To this end, a unified estimation of the random component of the coil parameter dispersion should be used after the determination of the deterministic trend and the probability of the appearance of the maximum number of defects on the coil is estimated (see Fig. 4).

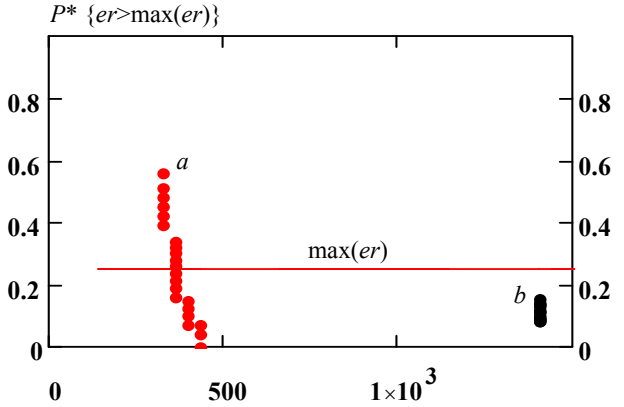

Fig. 4. Dependence of the probability of exceeding the maximum number of defects on the coil on the maximum number of defects detected (at length of 3600 m) as an estimate of the guaranteed level of homogeneity of the enamel insulation, obtained by limiting the distribution of maximum values during the periods of run-in (increased but rapidly decreasing insulation defect at the beginning of the continuous technological cycle *a*) and normal insulation (insulation defect is stable for a long time *b*): it can be seen that the use of the mathematical apparatus of the limit values allows you to clearly distinguish between the technological and the running period of the normal course of the process

The mathematical procedure of highlighting the trend of the process allows you to organize an active control of the random component of defectiveness (process error). Using the statistical procedures of discrete interval models [2], the current technical decision regarding the variance of the defectiveness of each regular wire coil during the whole technological cycle is evaluated, analyzed and accepted.

For example, when controlling the diameter of the enamel wire D, a statistical procedure is used to estimate the maximum probability $P_{\max}$ of the output of the controlled parameter ΔD beyond the limits of the range $\dot{E}\ldots\dot{E}$, defined as the sum of the corresponding probabilities of the parameter output for one-sided boundaries [4]. Moreover, the probability of a controlled parameter ΔD going beyond the lower limit is taken with a minus:

$$P_{\max i} = \sup(P_{\max i}) - \inf(P_{\max i}); \quad (2)$$

$$\sup(P_{\max i}) = [\sup(\Delta D_{i\cdot 2};\ \Delta D_{i\cdot 2-1}]^2/\{[\sup(\Delta D_{i\cdot 2};\ \Delta D_{i\cdot 2-1}]^2 + [\dot{E} - 0{,}5(D_{i\cdot 2-1} + D_{i\cdot 2})]^2\}; \quad (3)$$

$$\inf(P_{\max i}) = [\inf(\Delta D_{i\cdot 2};\ \Delta D_{i\cdot 2-1}]^2/\{[\inf(\Delta D_{i\cdot 2};\ \Delta D_{i\cdot 2-1}]^2 + [\dot{E} - 0{,}5(D_{i\cdot 2-1} + D_{i\cdot 2})]^2\}; \quad (4)$$

where D is the wire diameter; $\dot{E}$ is the upper technological diameter limit; $\dot{E}$ is the lower technological diameter limit; $\Delta D_{i\cdot 2}$ is the difference between the current diameter in sample No. $i\cdot 2$ and the average value of the diameter determined during the technological cycle (i: measurement No.):

$$\Delta D_{i\cdot 2} = D_{i\cdot 2} - (i)^{-1} \cdot \sum D_k,\ k = 1 \ldots i. \qquad (5)$$

Value $[\sup(\Delta D_{i\cdot 2};\ \Delta D_{i\cdot 2-1}]^2$ в (3) is the square of the largest current change in diameter in the sample No. $i\cdot 2$ towards the upper technological boundary. Value $[\inf(\Delta D_{i\cdot 2};\ \Delta D_{i\cdot 2-1}]^2$ in (4) is the the square of the largest current change in diameter towards the lower technological boundary.

Fig. 5 shows the results of testing the diameter (*a*) of enamel wire with polyimide insulation in a continuous technological cycle and a control map of the maximum probability of a diameter exit beyond the limits of the range *Ė…Ė* (*b*) determined in accordance with (2) - (5).

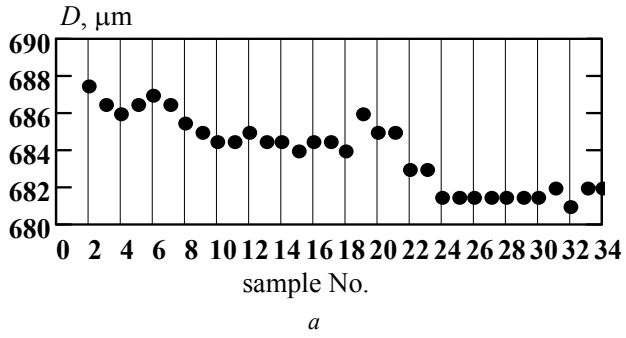

a

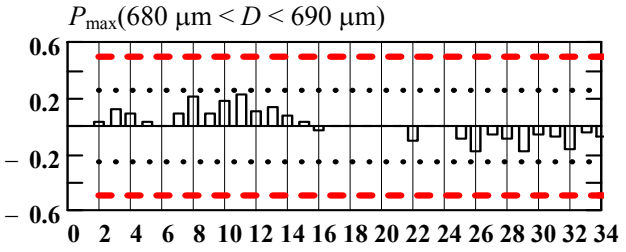

b

Fig. 5. The results of testing the diameter (*a*) of the enamel wire in the continuous technological cycle and a control card for the maximum probability of a diameter outlet beyond the limits of the regulatory range (*b*)

Comparison of Fig. 5,*a* and Fig. 5,*b* indicates the informative nature of the technological control of the maximum probability P_{max} of the parameter output beyond the limits of the specified two-sided range:

1) the control chart reflects the period of technological stability during which P_{max} does not exceed the absolute value of 0.25 (dotted line) - the level of the greatest sensitivity of the control to an increase in the deviation from the mean;

2) the control chart also reflects a stable tendency to reduce the values of the control parameter, which allowed to determine the cause of the reduction trend *D*, - the increase in the drawing of the conductor during the technological cycle.

The selection of ***the trend*** of the technological process makes it possible to estimate the quantitatively non-random trend of the controlled parameter change, as a result of **definable technological causes**. Without such an assessment, the very concept of technological control does not make sense, since it excludes feedback in the organization of such control. In addition, the selection of ***the trend*** of the technological process makes it possible to assess the accidental error of technological control, which is caused by the total influence of many such factors, the influence of each of which can be neglected in comparison with the sum.

The need to use the procedure for dividing the array of technological control data into deterministic and random components is due to the fundamental difference between the tasks of acceptance and technological control. This fundamental difference was noted by specialists [4]. The task of technological control is to ensure the possibility of active correction of the technological process, which is impossible without the identification of **definable technological causes** of the trend of the controlled parameter.

Conclusions.

1. The **guaranteed level of defect-free insulation** of enamel wires insulated with polyimide copolymers was evaluated. The probability that the maximum number of defects fixed at length of 3600 m is not more than 1400 during the run-in period, and 400 defects at length of 3600 m during the normal insulation period, is more than 80 %.

2. The statistical procedure for dividing the array of technological control data into a deterministic (trend) and random component (statistical error of the technological process) was developed and used in the organization of technological control of the defectiveness of a double-insulated cable with polyimide copolymers. The selection of a trend makes it possible to estimate the quantitatively non-random trend of a controlled parameter change, as a result **of definable technological causes**.

3. The trend of the number of defects in the period of normal insulation (Fig. 2,*b*) is weak positive: an increase in defectiveness (2 ± 1) defects per hour. Evaluation of the defectiveness trend in this period can be used to determine the time of the optimal duration of a continuous technological cycle.

4. During the run-in period, the negative trend coefficient (in this case, minus (125 ± 7) the number of defects per hour) was used to estimate the duration of run-in and to control the measures to cut it down by half.

5. The allocation of the random component allows quantifying the error of the technological process, the reduction of which requires an integrated approach, called in the world practice by the Deming method [10]. The random component (error of the technological process) during the normal insulation is stable, its average value in this case is 10 % of the average number of defects for the entire observation period.

REFERENCES

1. Zelenetsky Yu.A. About the improvement of technical documentation for enameled wires. *Cables and wires*, 2013, no.5, pp. 19-23. (Rus).

2. Shchebeniuk L.A., Antonets S.Yu. Statistical method purpose is the reduce of quantifying defects of enameled wire. *Bulletin of NTU «KhPI»*, 2012, no.23, pp. 166-169. (Ukr).

3. Golik O.V. Quantifying of defects for enameled wire with two-sheeted poliimid isolation by tests by high voltage. *Ukrainian metrological journal*, 2009, no.1, pp. 15-18. (Rus).

4. Golik O.V. Statistical procedures for two-sided limit of a controlled parameter in the process of production of cable and wire products. *Electrical Engineering & Electromechanics*, 2016, no.5, pp. 47-50. (Rus). **doi: 10.20998/2074-272X.2016.5.07.**

5. Gnedenko B.V., Belyaev Yu.O., Solovjev A.D. *Matematicheskie metody v teorii nadezhnosti* [Mathematical methods in theory of reliability]. Moscow, Nauka Publ., 1965. 524 p. (Rus).

6. Kuznetsov V.P. *Interval'nye statisticheskie modeli* [Interval statistical models]. Moscow, Radio i sviaz' Publ., 1991. 352 p. (Rus).

7. Tutubalin V.N. *Statisticheskaia obrabotka riadov nabliudenii* [Statistical analysis of observation series]. Moscow, Znanie Publ., 1973. 64 p. (Rus).

8. Andrianov A.V., Andrianov V.K., Bykov E.V. About the statistics of pin-hole damages of winding wires and inter-turn short-circuits in windings. *Cables and wires*, 2013, no.5, pp. 28-31. (Rus).

9. Technical Report IVA Laboratories: Breakdown voltage. – classified: October 2007. − p. 18.

10. Mary Walton. *The Deming Management Method*. Foreword by W. Edward Deming. New York: NY 10016 Copyright, 1986. 262 p.

Received 11.05.2017

V.M. Zolotaryov[1], *Doctor of Technical Science, Professor,*
Yu.P. Antonets[1], *Candidate of Technical Science,*
S.Yu. Antonets[2], *Postgraduate Student,*
O.V. Golik[2], *Candidate of Technical Science, Associate Professor,*
L.A. Shchebeniuk[2], *Candidate of Technical Science, Professor,*
[1] Private Joint-stock company Yuzhcable works,
7, Avtogennaya Str., Kharkiv, 61099, Ukraine,
phone +380 57 7545312,
e-mail: zavod@yuzhcable.com.ua, antonets@yuzhcable.com.ua
[2] National Technical University «Kharkiv Polytechnic Institute»,
2, Kyrpychova Str., Kharkiv, 61002, Ukraine,
тел/phone +380 57 7076544,
e-mail: unona928@gmail.com, agurin@kpi.kharkov.ua

How to cite this article:
Zolotaryov V.M., Antonets Yu.P., Antonets S.Yu., Golik O.V., Shchebeniuk L.A. Online technological monitoring of insulation defects in enameled wires. *Electrical engineering & electromechanics*, 2017, no.4, pp. 55-60. **doi: 10.20998/2074-272X.2017.4.09.**

UDC 621.311 **doi: 10.20998/2074-2X.2017.4.10**

Y.I. Sokol, Yu.A. Sirotin, T.S. Iierusalimova, O.G. Gryb, S.V. Shvets, D.A. Gapon

THE DEVELOPMENT OF THE THEORY OF INSTANTANEOUS POWER OF THREE-PHASE NETWORK IN TERMS OF NETWORK CENTRISM

Purpose. Information technologies allow multidimensional analysis of information about the state of the power system in a single information space in terms of providing network-centric approach to control and use of unmanned aerial vehicles as tools for condition monitoring of three-phase network. Methodology. The idea of energy processes in three independent (rather than four dependent) curves vector-functions with values in the arithmetic three-dimensional space adequately for both 4-wire and 3–wire circuits. The presence of zero sequence current structural (and mathematically) features a 4-wire scheme of energy from a 3-wire circuit. The zero sequence voltage caused by the displacement of the zero voltage phases. Offset zero in the calculations can be taken into account by appropriate selection of the reference voltages. Both of these energetic phenomena with common methodical positions are described in the framework of the general mathematical model, in which a significant role is played by the ort zero sequence. Results. Vector approach with a unified voice allows us to obtain and analyze new energy characteristics for 4–wire and 3–wire circuits in sinusoidal and non-sinusoidal mode, both in temporal and frequency domain. Originality. Symmetric sinusoidal mode is balanced, even with non-zero reactive power. The converse is not true. The mode can be balanced and unbalanced load. The mode can be balanced and unbalanced voltage. Practical value. Assessing balance in network mode and the impact of instantaneous power on the magnitude of the losses, will allow to avoid the appearance of zero sequence and, thus, to improve the quality of electricity. References 9, figures 3.

Key words: **network-centric technology, instant power, zero sequence, neutral.**

Обеспечение сетецентрического подхода к режиму управления трехфазной сетью и оценка сбалансированности режима сети с учетом влияния мгновенной мощности на величину потерь даст возможность исключить появление нулевой последовательности и, тем самым, повысить качество электроэнергии. Библ. 9, рис. 3.

Ключевые слова: **сетецентрическая технология, мгновенная мощность, нулевая последовательность, нейтраль.**

Introduction and problem definition. Compatibility problems of different types of generation require concentration of efforts on the integration of energy clusters, which must be balanced by primary energy resources with the interaction of the subjects of production, transmission and consumption of electric energy. When comparing the properties of traditional hierarchical and innovative network-centric control systems for the operation modes of a three-phase network, the main advantages of the latter include the use of irregular subsystems (subsystems with variable structure and a changing set of functions) and the use of information in real time. However, this requires the reorganization of not only the attached local power systems, but also the entire set of distributed energy objects [1].

Solving the problem complicates the presence of weak and at the same time extensive information and management connections in large areas [2].

Modern information technologies allow multidimensional analysis of information on the state of the power system in a single information space under the conditions of providing a network-centric approach to the control and use of unmanned aerial vehicles as a means of monitoring the state of a three-phase network [3].

Reactivity, asymmetry and non-sinusoidal mode of consumption for a number of consumers are caused by technological reasons and have a long-term nature, which is the reason for the appearance of pulsations of instantaneous power (IP), which causes additional losses of electricity and contributes to the emergence of dangerous resonance phenomena during operation of a three-phase network [4].

Analysis of recent investigations and publications. At asymmetric voltage, the problem of minimizing losses and creating a balanced power supply regime becomes multi-criteria. Improvement of methods of compensation and load symmetrization with asymmetric voltage requires further development of the theory of power [5].

The goal of investigations. Development of methods of the theory of instantaneous power in the presence of an asymmetric load in the network-centric control of the operating modes of a three-phase network.

Main materials of investigations. In a 4-wire system, the IP is defined as the sum of four pairwise products of instantaneous values (IV) currents and voltages. By the first Kirchhoff law, only three linear currents (out of four) are independent (free) quantities, and IP is invariant with respect to the choice of the reference point (RP) simultaneously for 4 voltages. Such an invariance of the IP leads to the fact that among 4 voltages (three phase voltages and neutral voltage) only three values of the voltages are independent (free).

RP voltage voltages, with respect to which the zero sequence of the phase voltage vector is «0», is called an *artificial point* of grounding (APG). The choice of the APG for the section ‹*a*, *b*, *c*, *n*› makes 4 voltage values conditionally four-dimensional. This leads to the complication of the mathematical description of energy processes and requires an unjustified application of the technique of Lagrange multipliers [6].

The choice of neutral as the voltage RP does not change the value of IP. In this case, the IP clearly depends only on three independent phase voltages and three independent linear currents. This allows us to consider the energy processes (current and voltage) in a 4-wire system

by three-dimensional and completely determined three phase values of the cross section of three phases ‹*a*, *b*, *c*› depending on time - by three curves (3-waveforms): $x_a = x_a(t)$, $x_b = x_b(t)$, $x_c = x_c(t)$. The curves of the considered process in three phases determine the radius vector $x(t)=[x_a(t)\ x_b(t)\ x_c(t)]^{\bullet}$ with values in the 3-dimensional space $X^{(3)}$ (3-dimensional curve $x(t) \in X^{(3)}$, abbreviated 3-curve).

Here $X^{(3)}$ is the arithmetic space of three-dimensional real vectors (matrix-columns) with the operations:

– scalar product (SP):

$$(x,y) = x^{\bullet} y = \begin{bmatrix} x_a & x_b & x_c \end{bmatrix} \cdot \begin{bmatrix} y_a \\ y_b \\ y_c \end{bmatrix} = x_a y_a + x_b y_b + x_c y_c \,; \quad (1)$$

– vector product (VP):

$$x \times y = \begin{bmatrix} x_b y_c - x_c y_b \\ x_c y_a - x_a y_c \\ x_a y_b - x_b y_a \end{bmatrix} = \\ = \begin{bmatrix} x_b y_c - x_c y_b - x_c y_a - x_a y_c - x_a y_b - x_b y_a \end{bmatrix}. \quad (2)$$

Vectors are orthogonal if their scalar product is zero:

$$x \perp y \Leftrightarrow (x,y) = 0 \,. \quad (3)$$

Vectors are parallel (collinear) if their vector product is zero:

$$x \parallel y \Leftrightarrow x \times y = 0 \,. \quad (4)$$

The representation of energy processes by three independent (and not four dependent) curve vector-valued functions with values in the arithmetic 3-dimensional space $X^{(3)}$ is adequate both for 4-wire, and for 3-wire circuits.

Analysis of energy processes in a 4-wire network. A vector approach from a single point of view makes it possible to obtain and analyze new energy characteristics for both 4-wire and 3-wire circuits, both in sinusoidal and non-sinusoidal mode, both in the time and frequency domain, mathematically considering 3-wire power supply circuit as a special case of a 4-wire power supply circuit.

Instant power and unbalanced mode. At each moment of time, the local state of the energy processes in the three-phase section ‹*a*, *b*, *c*› is characterized by vectors of instantaneous current and voltage values:

$$u(t) = \begin{bmatrix} u_a(t)\ u_b(t)\ u_c(t) \end{bmatrix}^{\bullet}, \\ i(t) = \begin{bmatrix} i_a(t)\ i_b(t)\ i_c(t) \end{bmatrix}^{\bullet}. \quad (5)$$

When considering a 4-wire circuit, we assume that the voltages are measured with respect to the neutral. The definition of the norm of a vector in a 3-dimensional space $X^{(3)}$ at each instant of time determines the norm of the vector of the IV of current and voltage:

$$\left|u(t)\right| = \sqrt{u^{\bullet}(t)\,u(t)} = \sqrt{u_a(t)^2 + u_b(t)^2 + u_c(t)^2} \,; \quad (6)$$

$$\left|i\right| = \left|i(t)\right| = \sqrt{i^{\bullet}(t)\,i(t)} = \sqrt{i_a(t)^2 + i_b(t)^2 + i_c(t)^2} \,. \quad (7)$$

The standard (scalar) IP is defined as the sum of pairwise products of IV of current and voltage of three phases:

$$p(t) = u_a(t) i_a(t) + u_b(t) i_b(t) + u_c(t) i_c(t) = \frac{dW}{dt} \quad (8)$$

and characterizes the energy transfer rate $W=W(t)$ in this section. As follows from (1), at each instant of time it is equal to the SP of vectors (5):

$$p(t) = (i,u) = i^{\bullet} u = \begin{bmatrix} i_a(t)\ i_b(t)\ i_c(t) \end{bmatrix} \cdot \begin{bmatrix} u_a(t) \\ u_b(t) \\ u_c(t) \end{bmatrix}. \quad (9)$$

Assuming that the processes (5) are T-periodic, that is, $u(t+T)=u(t)$ и $i(t+T)=i(t)$, we can correctly determine the mean IP and isolate the variable component:

$$P = \overline{p} = \frac{1}{T} \int_{\tau}^{\tau+T} p(t) d(t), \\ p(t) = \overline{p} + \widetilde{p}(t), \quad (10)$$

where $\tau \geq 0$ is the arbitrary number.

If the MM does not have a variable (pulsating) component $\widetilde{p}(t) \equiv 0$, then the mode is balanced [7]. In general case $\widetilde{p} = p(t) - \overline{p} \neq 0$ and the mode is unbalanced. Symmetric sinusoidal mode is balanced, even with non-zero reactive power. The converse is not true. The mode can be balanced even with an asymmetric load. The mode can be balanced even with asymmetric voltage.

Vector IP and instantaneous power equation. The product of the norms of the vectors (5) determines the apparent IP of the energy mode:

$$s(t) = \left|u(t)\right| \cdot \left|i(t)\right| = u(t) \cdot i(t) \,. \quad (11)$$

In the 3-dimensional space $X^{(3)}$, for any pair of vectors, the Cauchy-Schwarz inequality [8] holds, which for the vectors (5) gives the implication:

$$\left|i(t)^{\bullet} u(t)\right| \leq \left|i(t) u(t)\right| \Rightarrow \left|p(t)\right| \leq s(t) \,. \quad (12)$$

We introduce the vector IP as the VP of vectors (5) of currents and voltages [8]:

$$q(t) = i(t) \times u(t) = \\ = \begin{bmatrix} \underbrace{i_b u_c - i_c u_b}_{q_a} & \underbrace{i_c u_a - i_a u_c}_{q_b} & \underbrace{i_a u_b - i_b u_a}_{q_c} \end{bmatrix} = \\ = \begin{bmatrix} q_a\ q_b\ q_c \end{bmatrix}^{\bullet}. \quad (13)$$

The pairwise SP of vectors (5) form a Gram matrix (2×2):

$$G(i,u) = \begin{bmatrix} i^{\bullet} i & i^{\bullet} u \\ i^{\bullet} u & u^{\bullet} u \end{bmatrix} = \begin{bmatrix} i^2(t) & p(t) \\ p(t) & u^2(t) \end{bmatrix}. \quad (14)$$

The positive values on its main diagonal are equal to the squares of the norms of the vectors (5) of the voltages and currents: $u^{\bullet}u=|u(t)|^2=u^2(t)$, $i^{\bullet}i=|i(t)|^2=i^2(t)$. The determinant of the Gram matrix is equal to the square of the norm of the VP of vectors of the IV of currents and voltages – to the scalar square of the vector of the IP (13):

$$\det\left[G(i,u)\right] = \begin{vmatrix} i^{\bullet} i & i^{\bullet} u \\ i^{\bullet} u & u^{\bullet} u \end{vmatrix} \equiv \underbrace{\left[i \times u\right]^{\bullet}}_{q(t)} \underbrace{\left[i \times u\right]}_{q(t)} = \left|q(t)\right|^2 . \quad (15)$$

The geometric meaning of the determinant of the Gram matrix: «the square of the area of the parallelogram, which is formed by the vectors of voltage $u=u(t)$ and the current $i=i(t)$» is illustrated in Fig. 1.

The area of such an «instantaneous» parallelogram is:

$$q(t)=\left|q(t)\right|=\left|u(t)\right|\cdot\left|i(t)\right|\sin\varphi(t)=s(t)\sin\varphi(t)\,, \quad (16)$$

where $\varphi(t)$ is instantaneous angle between vectors of the IV of current and voltage in the arithmetic 3-dimensional space $X^{(3)}$ at time t.

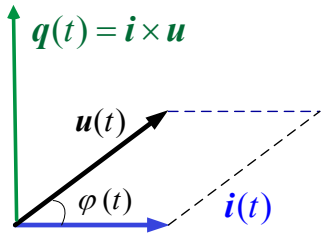

Fig. 1. Vector of current, vector of voltage and vector IP

The area of the parallelogram is zero if generating its vectors are parallel (collinear) $u(t)\|i(t)$ when the apparent power is equal to IP. Therefore, the norm of VP of the current $i=i(t)$ and the voltage $u = u(t)$ can be interpreted as an inactive IP. To emphasize this interpretation, the standard (scalar) IP will be called the active IP. The expansion (15) is invariant under the permutation of the vectors i and u, but $i\times u= -u\times i$. Here the vector (inactive) IP is determined according to (13).

The opposite choice is made in the «*pq*-theory» and leads to an error [9]. Note that the vectors i, u, $i\times u$ form a right triple.

The Cauchy inequality (12) at each moment is quadratically complemented to equality by the determinant of the Gram matrix [8]:

$$\underbrace{\left(i^{\bullet}i\right)}_{i^2(t)}\cdot\underbrace{\left(u^{\bullet}u\right)}_{u^2(t)}=\underbrace{\left(i^{\bullet}u\right)^2}_{p^2(t)}+\underbrace{\left[i\times u\right]^{\bullet}\left(i\times u\right)}_{q(t)}. \quad (17)$$

The identity (17) gives the power equation for instantaneous powers and is illustrated in Fig. 2:

$$s^2(t)=p^2(t)+q^2(t)\,. \quad (18)$$

In the triangle of instantaneous powers (Fig. 2), two legs correspond to active and inactive instantaneous powers. If the inactive IP is due to $\sin\varphi(t)$, then the active MM is due to $\cos\varphi(t)$:

$$p(t)=u^{\bullet}i=\underbrace{\left|u\right|\left|i\right|}_{s(t)}\cdot\underbrace{\frac{u^{\bullet}i}{\left|u\right|\left|i\right|}}_{\cos\varphi(t)}=s(t)\cdot\cos\varphi(t)\,. \quad (19)$$

The angle in the power triangle $\varphi(t)$ is equal to the angle introduced earlier between the vectors of current $i = i(t)$ and voltage $u = u\,(t)$.

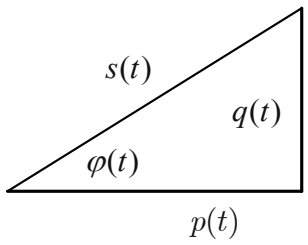

Fig. 2. Instantaneous power triangle

If the active IP (8) characterizes the efficiency of the energy mode, the vector IP (13) characterizes the energy mode losses.

Unbalanced and balanced mode. Like (10) in the vector IP, we can select vector components - a constant and a variable:

$$\overline{q}=\frac{1}{T}\int_{\tau}^{\tau+T}q(t)d(t),\quad \widetilde{q}(t)=q(t)-\overline{q}\,. \quad (20)$$

The mode in which the vector IP does not have a variable component $\widetilde{q}=\widetilde{q}(t)\equiv 0$ will be called the balanced mode [7].

The mode is really balanced if the vector IP (inactive IP) is identically equal to zero:

$$q(t)\equiv 0\Leftrightarrow\left(\overline{q}(t)\equiv 0\right)\&\left(\widetilde{q}(t)\equiv 0\right). \quad (21)$$

Thus, the mode is really balanced ($q(t)\equiv|q(t)|\equiv 0$) if at each moment (identically) the vectors (5) are parallel:

$$q(t)\equiv\left|q(t)\right|\equiv 0\quad\Leftrightarrow\quad y(t)\cdot u(t)=i(t)\,. \quad (22)$$

The scalar quantity $y(t)$ (has the conductivity dimension) need not be a constant and the power factor is, in general, less than 1.

Current and voltage of the 0-sequence. In a 4-wire circuit with an asymmetrical load, the neutral current is not zero (the zero sequence (ZS) current is non-zero). It is the presence of the ZS current that is structurally (and mathematically) different from the 4-wire power supply circuit from the 3-wire circuit. The voltage ZS is due to the phase angle shift. The zero offset in the calculations can be taken into account by the appropriate choice of the voltage reference point. Both these energy phenomena are described from the same methodological positions within the framework of a general mathematical model in which an essential role is played by the ZS unit vector (a vector with a unit norm)

$$e_0=\frac{1}{\sqrt{3}}\left[1\quad 1\quad 1\right]^{\bullet},\quad \left|e\right|=1\,. \quad (23)$$

The expansion of the 3-dimensional vector $x=[x_a\ x_b\ x_c]^{\bullet}\in X^{(3)}$ along the ZS unit vector determines the representation of the 3-dimensional vector by two mutually orthogonal components

$$x=\underbrace{\left(x^{\bullet}e_0\right)e_0}_{x_0}+\underbrace{e_0\times\left[x\times e_0\right]}_{x_!}=x_0+x_!;\quad \left(x_0\perp x_!\right), \quad (24)$$

where «×» is the symbol of the vector product.

In the expansion (24), the first component:

$$x_0=\left(x^{\bullet}e_0\right)e_0=\underbrace{\frac{x_a+x_b+x_c}{3}}_{\hat{x}}\cdot\begin{bmatrix}1\\1\\1\end{bmatrix}=\hat{x}\cdot\begin{bmatrix}1\\1\\1\end{bmatrix} \quad (25)$$

is the vector projection of the vector $x=(x_a,\ x_b,x_c)$ to the 0-unit (23) and is equal to the 0-component of this vector.

The coordinates of the vector (25) are the same and equal to the average value of the 3-phase quantities:

$$\hat{x}(t)=\left(x_a(t)+x_b(t)+x_c(t)\right)/3\,. \quad (26)$$

Component without 0-component (double vector product):

$$x_!=e_0\times\left[x\times e_0\right] \quad (27)$$

is an orthogonal complement of the component (25) to the full vector (and does not contain 0-component). This component will be called the 0-balanced component.

Vector product of the vector by 0-unit on the left:

$$e_0 \times x = \frac{1}{\sqrt{3}}\begin{bmatrix} x_c - x_b \\ x_a - x_c \\ x_b - x_a \end{bmatrix} = \frac{1}{\sqrt{3}}\begin{bmatrix} 0 & -1 & 1 \\ 1 & 0 & -1 \\ -1 & 1 & 0 \end{bmatrix} \cdot \begin{bmatrix} x_a \\ x_b \\ x_c \end{bmatrix} \quad (28)$$

can be represented using a skew-symmetric matrix

$$K = \frac{1}{\sqrt{3}}\begin{bmatrix} 0 & -1 & 1 \\ 1 & 0 & -1 \\ -1 & 1 & 0 \end{bmatrix} \quad (29)$$

in the form:

$$e_0 \times x = K \cdot x\,. \quad (30)$$

The vector product on the left and on the right is distinguished by the sign. Product on the right:

$$y \times e_0 = \frac{1}{\sqrt{3}}\begin{bmatrix} y_b - y_c \\ y_c - y_a \\ y_a - y_b \end{bmatrix} = \underbrace{\frac{1}{\sqrt{3}}\begin{bmatrix} 0 & -1 & 1 \\ -1 & 0 & 1 \\ 1 & -1 & 0 \end{bmatrix}}_{K^\bullet} \cdot \begin{bmatrix} y_a \\ y_b \\ y_c \end{bmatrix} \quad (31)$$

$$y \times e_0 = K^\bullet \cdot y \quad (32)$$

is equivalent to multiplying by the transpose matrix $K^\bullet = -K$.

For the second component (27) of the expansion (24) we have:

$$x_! = \underbrace{[e_0 \times x]}_{K \cdot x} \times e_0 = \underbrace{K \cdot x \times e_0}_{K^\bullet K \cdot x} = \underbrace{K^\bullet K}_{D_!} \cdot x = D_! \cdot x\,. \quad (33)$$

In the matrix form, the components of the expansion (24) are written as:

$$x_0 = D_0 \cdot x, \quad x_! = D_! \cdot x\,. \quad (34)$$

Matrices:

$$D_0 = \frac{1}{3}\begin{bmatrix} 1 & 1 & 1 \\ 1 & 1 & 1 \\ 1 & 1 & 1 \end{bmatrix}, \quad D_! = \frac{1}{3}\begin{bmatrix} 2 & -1 & -1 \\ -1 & 2 & -1 \\ -1 & -1 & 2 \end{bmatrix} \quad (35)$$

determine the projector D_0 on the unit vector of the 0-sequence and the projector $D_!$ on a 2-dimensional subspace of three-dimensional vectors orthogonal to 0-unit:

$$L_!^{(2)} = \left\{ x \in X^{(3)} : x^\bullet e_0 = 0 \right\} \subset X^{(3)}\,. \quad (36)$$

The vector $x=D_!\cdot x$ is 0-balanced. By the equivalence of the assertions:

$$x \perp e_0 \quad \Leftrightarrow \quad x_0 = 0 \quad \Leftrightarrow \quad x = D_! \cdot x = x_! \quad (37)$$

an alternative description of the 2-dimensional subspace (36) of three-dimensional 0-balanced vectors is valid (without the 0-sequence)

$$L_!^{(2)} = \left\{ x \in X^{(3)} : x = D_! \cdot x \right\}. \quad (38)$$

of 2-dimensional subspace (36) as the set of 3-dimensional vectors that do not change under the influence of the matrix $D_!$.

The matrices (35) satisfy the following conditions:

– the square of the matrix coincides with the matrix itself (the idempotency property)

$$D_0^2 = D_0, \quad D_!^2 = D_!\,; \quad (39)$$

– the product of matrices is equal to zero (orthogonality):

$$D_0 D_! = 0\,; \quad (40)$$

– the sum of the matrices gives an orthogonal decomposition of the unit third-order matrix

$$D_0 + D_! = \begin{bmatrix} 1 & 0 & 0 \\ 0 & 1 & 0 \\ 0 & 0 & 1 \end{bmatrix}. \quad (41)$$

The orthogonal decomposition (24) is valid at each instant of time, i.e. (24) is identically satisfied for the 3-dimensional curve:

$$x(t) \equiv x_0(t) + x_!(t) \equiv D_0 x(t) + D_! x(t)\,. \quad (42)$$

Since the above formulas are identically satisfied for 3-dimensional curves (valid at each instant of time), then, in order not to overload the formulas, the dependence on time will not be indicated. In particular, for the 3-current and voltage curves (5), we write the expansion (42) (obviously not indicating the time dependence) as (Fig. 3):

$$i = \underbrace{D_0 i}_{i_0} + \underbrace{D_! i}_{i_!} = i_0 + i_!; \quad u = \underbrace{D_0 u}_{u_0} + \underbrace{D_! u}_{u_!} = u_0 + u_!\,. \quad (43)$$

The voltage (potential difference) is a relative value that depends on the RP. From the representation (43) for the voltage vector, it follows that with the change in the voltage RP, only the ZS of the voltage vector u_0 changes, and 0-balanced component of the vector $u_!$ does not change.

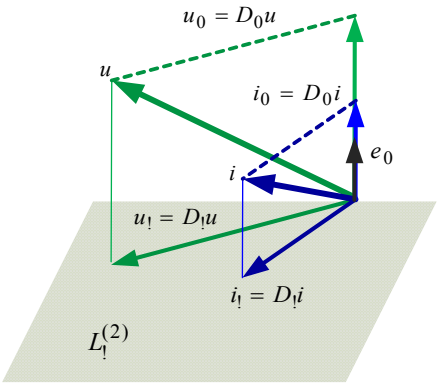

Fig. 3. Orthogonal decomposition of vectors of voltage and current along the ZS in a 4-wire circuit

The vector of phase voltages $u_!=D_!\cdot u$ is 0-balanced and (at each instant of time) is equal to the voltage vector, all phase components of which are measured relative to the APG.

All three coordinates of the voltage vector of 0-sequences

$$u_0 = D_0 u = (\hat{u}_a(t), \hat{u}_b(t), \hat{u}_c(t))^\bullet \quad (44)$$

are the same:

$$\hat{u} = (u_a(t) + u_b(t) + u_c(t))/3 \quad (45)$$

and equal to the voltage difference between neutral and APG. If the voltage is symmetrical, then it does not contain ZS, in this case the APG coincides with the neutral.

Conclusions. The network-centric technology of three-phase network management is the idea of integrating all forces and means in a single space, which allows increasing the efficiency of their application to the destination. One of the components of this process is the estimation of the balance of the network mode and the

influence of IP on the amount of losses, will make it possible to eliminate the occurrence of the zero sequence and, thereby, to improve the quality of electricity.

REFERENCES

1. Sokol Y.I., Gryb O.G., Shvets S.V. Network centrism optimization of expeditious service of elements of the power supply system. *Electrical engineering & electromechanics*, 2016, no.3, pp. 67-72. (Rus). **doi: 10.20998/2074-272X.2016.3.11.**

2. Sokol Y.I., Gryb O.G., Shvets S.V. The structural and parametrical organization of elements of a power supply system in the conditions of network centrism. *Electrical engineering & electromechanics*, 2016, no.2, pp. 61-64. (Rus). **doi: 10.20998/2074-272X.2016.2.11.**

3. Shvets S.V., Voropai U. G. Mariechantal aspects of the use of unmanned aerial vehicles. *Bulletin of Kharkiv Petro Vasylenko National Technical University of Agriculture*, 2016, no.176, pp. 33-34. (Ukr).

4. *Sirotin Iu.A., Ierusalimova T.S.* Instantaneous and integral power equations of nonsinusoidal 3-phase processes. *Electrical engineering & electromechanics*, 2016, no.1, pp. 69-73. **doi: 10.20998/2074-272X.2016.1.13.**

5. Zhezhelenko I.V., Saenko Yu.L. *Voprosy kachestva elektroenergii v elektroustanovkakh* [Issues of power quality in electrical installations]. Mariupol, PSTU Publ., 1996. 173 p. (Rus).

6. Willems J.L, Ghijselen J.A. The relation between the generalized apparent power and the voltage reference. *Energia elettrica*, 2004, vol.81, pp. 37-45.

7. Shidlovskii A. K., Mostovyak A.G., Moskalenko A.G. *Uravnoveshivanie rezhimov mnogofaznykh tsepei* [Balancing the modes of multiphase circuits]. Kiev, Naukova Dumka Publ., 1990. 181 p. (Rus).

8. Korn G., Korn T. *Spravochnik po matematike dlia nauchnykh rabotnikov i inzhenerov* [Mathematical handbook for scientists and engineers]. Moscow, Nauka Publ., 1973. 832 p. (Rus).

9. Peng F.Z., Lai J.S. Generalized instantaneous reactive power theory for three-phase power systems. *IEEE Transactions on Instrumentation and Measurement*, 1996, vol.45, no.1, pp. 293-297. **doi: 10.1109/19.481350.**

Received 17.05.2017

Y.I. Sokol[1]*, Doctor of Technical Science, Professor, Corresponding Member of the National Academy of Science of Ukraine,*
Yu.A. Sirotin[1]*, Doctor of Technical Science, Professor,*
T.S. Iierusalimova[1]*, Candidate of Technical Science,*
O.G. Gryb[1]*, Doctor of Technical Science, Professor,*
S.V. Shvets[1]*, Candidate of Technical Science, Associate Professor,*
D.A. Gapon[1]*, Candidate of Technical Science, Associate Professor,*
[1] National Technical University «Kharkiv Polytechnic Institute», 2, Kyrpychova Str., Kharkiv, 61002, Ukraine,
phone +380 57 7076551,
e-mail: Ierusalimovat@mail.ru, dima12345ml@mail.ru, se55sh32@gmail.com

How to cite this article:
Sokol Y.I., Sirotin Yu.A., Iierusalimova T.S., Gryb O.G., Shvets S.V., Gapon D.A. The development of the theory of instantaneous power of three-phase network in terms of network centrism. *Electrical engineering & electromechanics*, 2017, no.4, pp. 61-65. **doi: 10.20998/2074-272X.2017.4.10.**

UDC 621.316 **doi: 10.20998/2074-272X.2017.4.11**

K.A. Starkov, E.N. Fedoseenko

IMPROVED ALGORITHM FOR CALCULATING COMPLEX NON-EQUIPOTENTIAL GROUNDING DEVICES OF ELECTRICAL INSTALLATIONS TAKING INTO ACCOUNT CONDUCTIVITY OF NATURAL GROUNDINGS

Purpose. The method of natural concentrated groundings substitution by the set of electrodes taking them into account in the algorithm of electric characteristics calculation for complicated grounding connections of electric installation is offered. An equivalent model as a set of linear electrodes is chosen in accordance with two criteria: leakage resistance and potentials on the ground surface. Methodology. We have applied induced potential method and methods for computing branched electrical circuits with distributed parameters. Results. We have obtained the algorithm for calculating complex non-equipotential grounding connections, which makes it possible to obtain refined values of the potential distribution in the electric stations and substations with outdoor switchgear. Originality. For the first time, we have taking into account the conductivity of natural concentrated grounds by a set of vertical and horizontal electrodes based on equivalent electrical characteristics applied to a two-layer ground. Practical value. The using of the proposed calculation algorithm in the electric grids of JSC «Kharkivoblenergo» made it possible to determine the values of the potential distribution at short circuit in electrical substation taking into account the influence of the conductivity of natural concentrated groundings. References 9, figures 1.

Key words: **natural concentrated groundings, substitution, induced potential method, the potential distribution, a two-layer ground model.**

Цель. Целью статьи является разработка алгоритма расчета электрических характеристик неэквипотенциальных заземляющих устройств электроустановок с учетом большого числа естественных сосредоточенных заземлителей, а также собственных активных и реактивных сопротивлений горизонтальных заземлителей. Методика. Проведены теоретические исследования с использованием метода наведенных потенциалов, методов конечных разностей для расчета электрического поля простых заземлителей в земле с двухслойной структурой и последовательного применения метода наведенных потенциалов и методов расчета разветвленных электрических цепей с распределенными параметрами. Результаты. Получен алгоритм расчета сложных неэквипотенциальных заземляющих устройств, позволяющий получить уточненные значения распределения потенциала на территории электроустановки. Научная новизна. Новые положения, по сравнению с известными решениями, состоят в учете проводимости естественных сосредоточенных заземлителей совокупностью вертикальных и горизонтальных электродов, обоснованной по равнозначным электрическим характеристикам применительно к двухслойной модели электрической структуры земли. Практическое значение. Использование предложенного алгоритма расчёта в электрических сетях АК «Харьковоблэнерго» позволили определить значения распределения потенциалов при КЗ на электрической подстанции с учетом влияния проводимости естественных сосредоточенных заземлителей. Скорректированные таким образом результаты расчета дадут более точную информацию о величинах нормируемых параметров по заземляющим устройствам действующих электроустановок. С помощью предложенного алгоритма могут быть получены уточненные значения падения напряжений по заземляющим устройствам при КЗ, а, следовательно, рассчитаны напряжения, воздействующие на изоляцию кабелей вторичных цепей, – параметры, нормируемые по условиям электромагнитной совместимости. Библ. 9, рис. 1.

Ключевые слова: **природные сосредоточенные заземлители, электрическая подстанция, метод наведеного потенциала, распределение потенциала, двухслойная модель земли.**

Introduction. The characteristics of grounding devices (GD) of electrical installations with open distribution devices directly determine the electromagnetic situation at power facilities. The natural concentrated groundings, due to the large contact surface with the ground, equalize the potential in the GD nodes and, thereby, unload the horizontal artificial and natural groundings. Therefore, their detailed accounting in solving the problem of calculating the electrical characteristics of complex non-equipotential GD is mandatory, since it affects the level of electromagnetic interference.

The calculation of the electrical characteristics of non-equipotential groundings is based on the consistent application of the induced potential method and methods for calculating branched electrical circuits with distributed electrical parameters. Using the capabilities of this algorithm for calculating complex GD involves the replacement of natural concentrated groundings (reinforced concrete bases and foundations) with a set of vertical and horizontal electrodes whose diameters are taken to be the same as those of the corresponding artificial electrodes. At the same time the uniformity of the calculated forms of all the GD electrodes is achieved.

The method of calculating a complex combined grounding can be based on the condition of its equipotentiality, and on the condition of non-equipotentiality, i.e. taking into account the longitudinal resistance of the horizontal electrodes. Modern

computational capabilities make it possible to implement an algorithm for calculating non-equipotential complex combined groundings as a universal one.

Analysis of recent investigations and publications. The mathematical model of the non-equipotential GD of a substation located in a two-layer soil proposed in work [1] is based on the main provisions of the joint representation of the GD in the general case as a complex electric circuit and creating a steady electric field in the ground. Additionally into account the change in the current density flowing from the horizontal electrodes, linearly and their arbitrary arrangement is taken into account. However, the impact on the formation of electrical characteristics of the GD of electrical installations, which can have natural concentrated groundings is not taken into account in this work not taken into account.

The calculation algorithm based on a unified mathematical model and simultaneously taking into account both the non-uniformity of the potential distribution with respect to the object's GD and the process of current flow from the grounding to the ground are realized in the form of the «Contour» software package [2]. The proposed mathematical model, judging from the construction of the algorithm, does not take into account the nonlinear dependence of the distributed parameters of the horizontal electrodes on the current flowing through them.

In work [3] various methods of calculation of resistance of various groundings in homogeneous and two-layer models of electric structure of the earth are considered. The obtained results are compared with the corresponding formulas of the finite element method, which are considered as reference ones. In work [3] it was noted the need to find the best approximations in the course of calculating the resistance of a complex GD, especially for the case of a multilayer ground model.

The main idea of the method [4] consists in a joint consideration of the GD in the general case as a complex electric circuit and creating a steady electric field in the ground. According to this method, vertical elements are represented by lumped parameters, and horizontal ones are represented by distributed parameters that are nonlinearly dependent on the current flowing through them.

An analysis of the expressions given in [4] shows that they do not cover all possible variants of arrangement of elements of complex GD with respect to a two-layer soil model. The form of the representations of these expressions reflects those limitations in the geometry part of the computational model of GD that are adopted in the algorithm that implements the expressions. According to [4], in the design of complex GD structures, reinforcing skeletons of reinforced concrete bases (natural concentrated groundings) should be replaced by a combination of vertical and horizontal electrodes, taking into account the capabilities of known algorithms for the calculation of groundings. It should, however, be noted that the calculated set of replacement electrodes in this case is not based on equivalent electrical characteristics.

The goal of the work is the improvement of the algorithm that implements a mathematical model based on joint consideration of the GD as a complex electric circuit and creating steady electric field of current in the ground, by taking detailed account of the natural concentrated groundings of the open distribution devices of high voltage electrical installations.

A method of complex GD calculation. The basis for the algorithm for calculating complex non-equipotential GD of electrical installations taking into account the conductivity of natural groundings is the method of calculating GD taking into account the longitudinal resistance of horizontal elements [4]. This method is developed for the case when the GD contains, along with horizontal and vertical elements. Under horizontal elements, the longitudinal resistance of which is taken into account, the parts of the grounding, enclosed between two adjacent nodal points (the points at which two or more elements intersect and converge) are understood and which are constructively the electrodes of the grounding grid. As a node, you can take any point located on the horizontal part of the grounding [4]. When replacing reinforced concrete pedestals and racks with a combination of vertical and horizontal linear electrodes, the longitudinal resistance of the last elements is not taken into account.

The initial model of a complex earth electrode is determined by the assumptions in accordance with [4]:

1) within a given complex grounding plane, those horizontal elements whose longitudinal resistance is taken into account have homogeneous (within the element) distributed specific parameters, i.e. per unit length: longitudinal active resistances, inductance and transverse conductance of current spreading;

2) the values of the transverse conductivity of the elements also depend on their longitudinal parameters, which in turn, when using elements of steel, are a nonlinear function of the current passing through them;

3) there is no effect on the distributed parameters of the grounding of the electromagnetic field of the single-phase grounding fault current passing through the air lines;

4) vertical elements and those horizontal elements whose longitudinal resistance is not taken into account are ideal lumped;

5) there may be several «setting» points within the grounding, i.e. points directly electrically connected to the external electrical circuit (the «setting» is the nodal points of the grounding directly connected to the neutral transformers or autotransformers, and the point at which the phase of the power line is closed in the design emergency mode);

6) with the design single-phase closure through the setting node points, the driving currents (steady-state values of the single-phase ground fault current and the

currents «returning» to the system through neutral transformers and autotransformers) pass.

In accordance with the requirements for the straightness of the grounding electrodes, the following method for taking into account the natural conductivity of the current spreading from the reinforcement of reinforced concrete groundings is proposed to realize the capabilities of this calculation algorithm. Let's imagine a natural concentrated grounding as an equivalent set of linear electrodes, for example, so that these electrodes are located on the outline of a natural grounding. In particular, the reinforcing frame of the footrests is replaced by a set of vertical electrodes, the dimensions and location of which is determined by the corresponding geometric characteristics of the pedestal stand, and the set of horizontal electrodes – in accordance with the geometric characteristics of its plate. The set of replacement electrodes is located in the ground with a layer-by-layer homogeneous electrical structure, as well as a simulated natural concentrated grounding. Further to the indicated set of electrodes, one can apply the induced potential method [4] to solve the electric field problem as a complex GD and determine the values of the flow resistance and the potentials of points on the surface of the ground.

Replacement of natural concentrated groundings. The polyfunctionality of the GD of electrical installations with voltages above 1 kV of a network with a solidly grounded or effectively grounded neutral has led to the necessity of rationing several parameters of the GD - or touch voltage or resistance of the GD [5]. In this regard, we accept two criteria for the equivalence of the replacement circuit for natural concentrated GD by a set of linear electrodes: the approximation in resistance and the approximation of the potentials of points on the surface of the earth. In this case, as initial data for estimating the sufficiency of the approximation, we take the results of solving the boundary-value problem for the Laplace equation with reference to the model of a natural concentrated grounding in a limited volume of the ground. The sufficiency of the approximation achieved in the process of building up replacing linear electrodes is estimated as follows:

by resistance

$$\xi_R = \left| \frac{R_{s,e} - R_{p,\mathrm{m}}}{R_{p,\mathrm{m}}} \right| \le \xi_{R,\lim}; \qquad (1)$$

by potentials of points

$$\xi_\varphi = \frac{1}{n} \sum_{i=1}^{n} \left| \frac{\varphi_{i,s,\mathrm{e}} - \varphi_{i,p,\mathrm{m}}}{\varphi_{i,p,\mathrm{m}}} \right| \le \xi_{\varphi,\lim}, \qquad (2)$$

where $R_{s,e}$, $R_{p,m}$ are the resistance to the spreading of the set of electrodes and the approved model, respectively; $\varphi_{i,s,e}$, $\varphi_{i,s,e}$ are the potential on the earth's surface of a set of electrodes and the approved model, respectively; n is the number of points on the earth's surface.

Variants of substitution of natural concentrated groundings (reinforced concrete racks and footrests) with the calculated set of linear electrodes were obtained by the method described earlier using ξ_R- и ξ_φ-criteria, and presented in [6, 7].

Calculation expressions for mutual and intrinsic resistances. The proposed method of taking into account the natural conductivity of current spreading from the reinforcement of reinforced concrete natural groundings may require the use of expressions for mutual and intrinsic resistances with respect to horizontal electrodes located in the lower layer of a two-layer earth model. Necessity in these expressions will appear when the reinforcing frame of the footrunners is replaced, the slab of which is located at a depth of about 3 m, a set of vertical and horizontal electrodes.

The calculation expressions for the mutual and intrinsic resistances are derived from the general formula for the mutual resistance R_{qg} between two electrodes with the indices g and q located in the conducting half-space with respect to the electrodes whose cross-sectional dimensions are hundreds of times smaller than their length [4], i.e .

$$R_{qg} = \frac{1}{l_q l_g} \int\limits_{(l_q)} \int\limits_{(l_g)} f'_{0q}(Q) f'_{0g}(G) \Psi_{QG} dl_Q dl_G , \qquad (3)$$

where l_q and l_g is the length of electrodes; $f'_{0q}(Q)$ and $f'_{0g}(G)$ is function of the non-uniformity of the linear current density along the electrode length; Ψ_{QG} is the proportionality function between the current flowing out into the conducting half-space from the vicinity of the point G, and the potential induced by this current at the point Q.

As a result of the derivation according to (3), the following expressions are obtained: the mutual resistance of two horizontal electrodes located in the lower layer and parallel to each other; mutual resistance of two horizontal electrodes located in the lower layer and perpendicular to each other; the mutual resistance of two horizontal electrodes, in the case where one electrode is located in the upper layer, the second - in the lower layer; mutual resistance of two horizontal crossed at right angles electrodes located in the upper and lower layer; the mutual resistance of the horizontal electrode located in the lower layer, and the vertical electrode crossing the interface of the layers.

The correctness of the expressions is confirmed by comparing the results of the test calculations by them and the expressions given in [4] for the location conditions of the horizontal electrode(s) in the upper layer and the initial data corresponding to the position of the electrode(s) at the interface of the layers. The calculated expressions for the mutual and intrinsic resistances of the electrodes were published in [8] and, together with previously published ones, encompass all possible combinations of the arrangement of the electrodes in the

calculation of complex GD with allowance for natural concentrated groundings.

Algorithm for calculating a complex non-equipotential GD. The obtained models of natural concentrated groundings in the form of a set of linear vertical and horizontal electrodes are introduced into the algorithm for calculating a complex non-equipotential GD, which we take as the initial one. These elements, along with artificial linear earth conductors, participate in the current distribution of the GD. In this case, the longitudinal resistance of the horizontal electrodes, replacing the natural groundings, is not taken into account. At an industrial frequency, the electric field of the current leaving the earth electrode into the ground can be considered as stationary. In this case, the current distribution between the equipotential bond elements is determined by a system of linear algebraic equations (SLAE) [4]:

$$\varphi_G = \sum_{p=1}^{n} \alpha_{mp} I_p , \quad \text{at } m = \overline{1,n} \tag{4}$$

where n is the number of grounding elements; α_{mp} is the mutual resistance of GD elements with indices m and p (at $m \neq p$) and the intrinsic resistance of elements with identical indices; I_p is current flowing into the ground from the p-th element; φ_G is the potential of the grounding (equipotential).

In this case we have SLAE (5) analogous to SLAE with proper and mutual potential coefficients in the system of charged bodies [9].

According to [4], in the case of a non-equipotential grounding, the SLAE in matrix form has the form:

$$AI_0 = U , \tag{5}$$

where A is the matrix of mutual and intrinsic resistances of elements; I_0 is the matrix-column of complex values of currents flowing from the elements of a complex grounding to the earth; U is the matrix-column of complex values of the voltages of elements (for horizontal elements, the average of the values of the voltage at the beginning and the end of the element is taken, and for the vertical elements, the voltage of the node point with which it is connected).

The complex values of the voltages of the GD elements are related to the values of the driving currents and to the parameters of a complex nonlinear electrical circuit simulating the original GD, without taking into account the natural groundings. We express this connection by the method of nodal voltages in matrix form (all nodes starting from the reference one, which we take as the «ground» – zone of the zero potential, are numbered from zero to q) [4]:

$$YU_{nodal} = I_{set} , \tag{6}$$

where Y is the square matrix of total conductivity of circuits; U_{nodal} is the matrix-column of nodal voltages; I_{set} is the matrix-column of setting currents.

In accordance with [4], the calculation of a complex electric circuit replacing a multielement GD is reduced to joint solution of two matrix equations (5) and (6). Taking into account the fact that the parameters of horizontal elements are nonlinearly dependent on the current flowing through them, equation (6) is nonlinear. Vertical elements of the GD are replaced by concentrated conductances on the ground; also those horizontal elements are replaced whose longitudinal resistance is not taken into account.

At the next stage of the calculation algorithm, the horizontal elements whose longitudinal resistance is taken into account are replaced by equivalent U-shaped circuits with lumped parameters (Fig. 1).

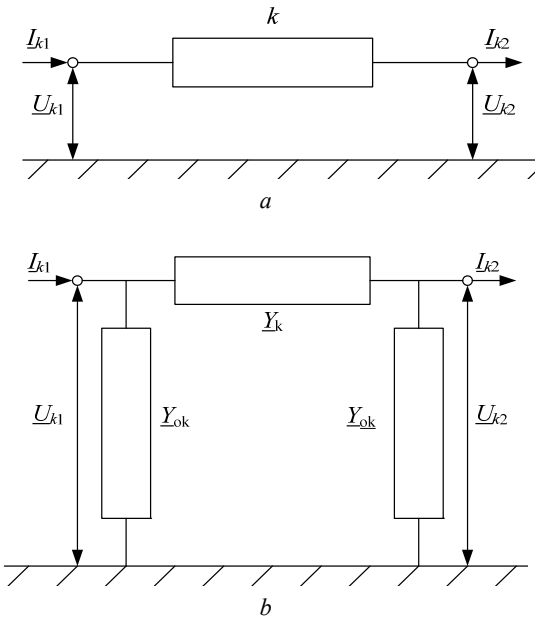

Fig. 1. Horizontal k-th element with distributed parameters r, L, g (*a*) and its equivalent U-shaped equivalent circuit (*b*)

The relationship of the lumped parameters of the U-shaped equivalent circuit of the k-th horizontal element ($\underline{Y}_k$ and $\underline{Y}_{0k}$) with its distributed parameters is known [6]:

$$\begin{aligned} \underline{Y}_k &= 1 \big/ \underline{Z}_{wk} \operatorname{sh} \underline{\gamma}_k l_k ; \\ \underline{Y}_{0k} &= \left(\operatorname{ch} \underline{\gamma}_k l_k - 1 \right) \big/ \underline{Z}_{wk} \operatorname{sh} \underline{\gamma}_k l_k , \end{aligned} \tag{7}$$

where $\underline{Z}_{wk}$ is the wave impedance; $\underline{\gamma}_k$ is the propagation coefficient.

The quantities included in the formulas for the wave impedance $\underline{Z}_{wk}$ and the propagation coefficient $\underline{\gamma}_k$ are the specific impedance of the element and the specific total transverse conductivity g_k. The specific total longitudinal resistance of the horizontal electrode is determined by the active resistance and inductance, the latter having two components: the external L_{ext}, caused by the magnetic field outside the electrode, and the internal L_{int}, connected with the magnetic field inside the electrode. The internal inductance L_{int} is calculated as a function of the magnetic permeability of the electrode

steel μ_k which is determined from the main magnetization curve at a given effective value of the magnetic field strength at the electrode surface. The magnetic permeability of the steel of the element μ_k depends nonlinearly on the current I_k passing through the k-th element. The external inductance of L_{ext} is determined on the basis of the well-known Pollachek formula. Conductivity

$$g_k = G_k l_k^{-1},$$

and G_k is determined by the method of the induced potential.

For the first approximation or the first iteration [4], the grounding is assumed to be equipotential and the numerical values of the solution vector of the matrix equation (4) are found. Further, the transverse conductivities G of all horizontal and vertical elements of the grounding are determined; at the first iteration, we assume that all the conductivities under consideration are of an active nature.

Further, given a certain initial value of the magnetic permeability of the electrode steel μ, we determine the distributed longitudinal parameters of the horizontal elements of the grounding grid and the parameters of their equivalent U-shaped replacement circuits. The solution of the matrix equation (6) for given reference currents makes it possible to obtain numerical values of the node voltages and calculate the currents in all branches of the equivalent circuit for the complex GD.

At the second approximation [4], the voltages in the nodes and currents in the branches of the grounding's equivalent circuit calculated in the first approximation are used as additional initial data, namely, the grounding is represented as non-equipotential - the SLAE has the form (5), and the above current values allow to clarify the magnetic permeability of the electrode steel μ. For this refinement, the values of μ we use the mean between the current values at the beginning and at the end of each horizontal element with distributed longitudinal parameters. The solution of system (3) with respect to currents in complex form allows us to further determine the values of the total transverse conductivities of all elements; these conductivities have reactive components which is formally connected with the presence of phase shifts with respect to each other at the node voltages at the first iteration. Further by using μ and G, the distributed longitudinal parameters of those horizontal elements of the grounding, whose longitudinal resistance is taken into account, are determined, etc.

In the part of determining the voltage before touching the given points on the ground and the input resistance of the GD, the calculation is performed in a known manner [4].

The obtained solution of currents in all branches of the equivalent circuit of the complex GD gives values of the currents flowing along the horizontal elements of the GD as average between the current values at the beginning and at the end of each horizontal element with distributed longitudinal parameters. As a result of this is adding to the algorithm for calculating complex non-equipotential GD of electrical installations the solution of the problem of determining the level of electromagnetic compatibility.

The sufficiency of the approximation achieved is estimated by the ξ-criterion:

$$\xi = \frac{1}{q}\sum_{j=1}^{q}\left|\frac{U_{jo}^{(n-1)} - U_{jo}^{(n)}}{U_{jo}^{(n)}}\right| \le \xi_{\lim}, \qquad (8)$$

where (n) is the upper index indicating the number of last iteration; q is the number of nodes of the grounding's equivalent circuit; U_{jo} is the voltage module of the j-th node with respect to the reference one.

Conclusions.

The necessity of taking into account the influence of natural concentrated groundings during the formation of electrical characteristics of complex non-equipotential GD of electrical installations by means of their equivalence by a set of vertical and horizontal electrodes is justified.

The calculation expressions for the mutual and intrinsic resistances of horizontal electrodes of complex non-equipotential GD located in the lower layer of the two-layer ground model that encompass all possible combinations of their location and provide for the calculation of natural concentrated groundings are obtained.

The use of the proposed algorithm for calculating the potential distribution at short-circuit at the substation in the electric networks of JSC «Kharkivoblenergo» taking into account the influence of the conductivity of natural concentrated groundings, made it possible to ensure the optimal normalization of the parameters of the operating electric installations due to more accurate determination of the touching voltage.

Expressions for calculating the values of voltage drops on the GD at short circuit are determined, which allow to estimate the level of voltages affecting the insulation of secondary circuit cables, which is necessary for normalizing their parameters according to the electromagnetic compatibility conditions.

REFERENCES

1. Link I.Yu., Koliushko D.G., Koliushko G.M. A mathematical model is not an equipotential ground grids substation placed in a double layer. *Electronic modeling*, 2003, vol.25, no.2, pp. 99-111. (Rus).

2. Matveev M.V., Kuznetsov M.B., Lushchishin A.R. Evaluation of the electromagnetic environment in the power station and substations engineering. *Vesti v elektroenergetike*, 2005, no.2, pp. 1-8. (Rus).

3. Katsanou V.N., Papagiannis G.K. *Substation grounding system resistance calculations using a FEM approach*. IEEE Bucharest PowerTech, Jun. 2009. **doi: 10.1109/PTC.2009.5282044.**

4. Burgsdorf V.V., Yakobs A.I. *Zazemlyayushchie ustroystva elektroustanovok* [Grounding device of electrical installations]. Moscow, Energoatomizdat Publ., 1987. 400 p. (Rus).

5. *Pravila ulashtuvannya elektroustanovok. Rozdil 1. Zagal'ni pravila. Glava 1.7. Zazemlennya i zakhisni zakhodi vid urazhennya elektrichnim strumom* [Rules of the device electroinstallations. Chapter 1. General rules. Grounding and protective measures against electric shock]. Kyiv, Minenergovugillya Ukrayiny Publ., 2011. 72 p. (Ukr).

6. Fedoseenko E.N. Minchenko A.A. The substitution option of natural concentrated grounds, such as concrete pole armature, by the calculated set of electrodes. *Eastern-European Journal of Enterprise Technologies*, 2006, vol.3, no.6(24), pp. 81-84. (Rus).

7. Minchenko A.A., Fedoseenko E.N. Taking into account the natural conductivity of current spreading with concrete pole armature for calculation complicated grounding connections by the set of vertical electrodes. *Bulletin of NTU «KhPI»*, 2006, no.28, pp. 96-100. (Rus).

8. Fedoseenko E.N. Finding of mutual and own resistances of vertical and horizontal electrodes for complicated grounding connections in a double layer ground. *Bulletin of NTU «KhPI»*, 2006, no.34, pp. 84-91. (Rus).

9. Demirchian K.S., Neiman L.R., Korovkin N.V., Chechurin V.L. *Teoreticheskie osnovy elektrotekhniki: V 3-kh t. Uchebnik dlia vuzov. Tom 2* [Theoretical bases of electrical engineering. In 3 vols. Vol.2.]. St. Petersburg, Piter Publ, 2003. 576 p. (Rus).

Received 25.04.2017

K.A. Starkov[1]*, Candidate of Technical Science,*
E.N. Fedoseenko[2]*, Senior Instructor,*
[1] JSC «Kharkivoblenergo»,
149, Plekhanovskaia Str., Kharkiv, 61037, Ukraine,
phone +380 57 7401268,
e-mail: ptu1@obl.kh.energy.gov.ua
[2] National Technical University «Kharkiv Polytechnic Institute»,
2, Kyrpychova Str., Kharkiv, 61002, Ukraine,
phone +380 57 7076977,
e-mail: fedosejenko@gmail.com

How to cite this article:
Starkov K.A., Fedoseenko E.N. Improved algorithm for calculating complex non-equipotential grounding devices of electrical installations taking into account conductivity of natural groundings. *Electrical engineering & electromechanics*, 2017, no.4, pp. 66-71. **doi: 10.20998/2074-272X.2017.4.11.**

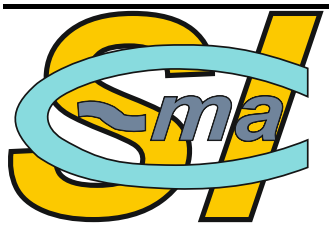

МІЖНАРОДНИЙ СИМПОЗІУМ
ПРОБЛЕМИ ЕЛЕКТРОЕНЕРГЕТИКИ, ЕЛЕКТРОТЕХНІКИ ТА ЕЛЕКТРОМЕХАНІКИ (SIEMA'2017)

INTERNATIONAL SYMPOSIUM
PROBLEMS OF ELECTRIC POWER ENGINEERING, ELECTRICAL ENGINEERING AND ELECTROMECHANICS (SIEMA'2017)

Шановні колеги!
Оргкомітет Симпозіуму має честь запросити Вас і зацікавлених співробітників Вашої установи прийняти участь у ювілейному XX Міжнародному симпозіумі «Проблеми електроенергетики, електротехніки та електромеханіки» (SIEMA'2017), який відбудеться 26 - 27 жовтня 2017 р. за адресою: НТУ «ХПІ» (електротехнічний корпус) вул. Кирпичова, 2, м. Харків, 61002, Україна.
У симпозіумуі приймуть участь:
- завідувачі кафедр, що ведуть підготовку фахівців за спеціальністю 141 Електроенергетика, Електротехніка і Електромеханіка, а також провідні викладачі ВНЗ України та інших країн;
- представники науково-дослідних організацій, що займаються проблемами, пов'язаними з електроенергетикою, електротехнікою і електромеханікою;
- представники підприємств – розробників електричних машин, апаратів та інших електротехнічних пристроїв;
- представники підприємств – споживачів електроустаткування;
- представники проектних організацій;
- представники комерційних організацій електротехнічного профілю.

Учасникам симпозіуму надається можливість опублікувати доповіді. Публікації будуть видані як спеціальний випуск Вісника Національного технічного університету «ХПІ» та в журналі «Електротехніка і електромеханіка» (EIE), що входять до Переліку фахових видань ВАК України та індексується у наукометричних базах (Index Copernicus, РІНЦ, тощо), а журнал EIE, починаючи з 2017 р., індексується у Web of Science Core Collection.
Учасники можуть виступити на пленарному засіданні та на засіданнях секцій.

СЕКЦІЇ СИМПОЗІУМУ
1. Теоретична електротехніка.
2. Електричні машини.
3. Електричні апарати.
4. Сильні електричні і магнітні поля.
5. Електроізоляційна і кабельна техніка.
6. Передача електричної енергії.
7. Електромагнітна сумісність.
8. Автоматизація та кібербезпека енергетичних систем

Детальнішу інформацію стосовно Симпозіуму та умов участі у ньому можна отримати на сайті кафедри «Електричні апарати»: web.kpi.kharkov.ua/ea

З повагою до Вас
Голова оргкомітету Ректор НТУ «ХПІ»

Професор Є.І. Сокол

Координатор симпозіуму
Професор Б.В. Клименко

Телефони для довідок:
(057) 707 62 81, 050 653 49 82, 096 987 20 85
Факс: (057) 707 66 01.
E-Mail: varshamova.i.s@gmail.com,
korolelgn@gmail.com

Dear Colleagues,
the Organizing Committee of the Symposium has the honor to invite you and interested employees of your institution to participate in the anniversary XX International Symposium «Problems of Electric Power Engineering, Electrical Engineering and Electromechanics» (SIEMA'2017) which will take place on 26th – 27th of October, 2017 at the NTU «KhPI» (Electrical Engineering Building), Kyrpychova Str. 2, Kharkiv, UA-61002.
In the Symposium will take part:
- Heads of Departments conducting training in the specialty 141 Electric Power Engineering, Electrical Engineering and Electromechanics as well as leading University Professors from Ukraine and other countries;
- representatives of research institutions dealing with problems related to Electric Power Engineering, Electrical Engineering and Electromechanics;
- representatives of enterprises - developers of electric machines, apparatus and other electrical equipment;
- representatives of enterprises - consumers of electrical equipment;
- representatives of design institutions;
- representatives of commercial institutions of electrical engineering profile.

Participants of the Symposium will have the opportunity to publish their papers. Papers will be published as a special issue of the Bulletin of the NTU «KhPI» and in the Journal «Electrical Engineering & Electromechanics» (E&E) which are included in the list of professional editions of the Higher Attestation Commission of Ukraine and indexed in scientometric databases (Index Copernicus, RSCI, etc.), and the E&E Journal since 2017 is indexed in the Web of Science Core Collection.
Participants can make presentations at the plenary and sectional sessions.

SYMPOSIUM SECTIONS
1. Theoretical electrical engineering.
2. Electric machines.
3. Electrical apparatus.
4. High electric and magnetic fields.
5. Electrical insulating and cable engineering.
6. Transmission of electric energy.
7. Electromagnetic compatibility.
8. Automation and cybersecurity of power systems.

More detailed information regarding the Symposium and conditions of participation can be found on the site of the Department for Electric Apparatus: web.kpi.kharkov.ua/ea

Sincerely yours,
Head of the Organizing Committee

Rector of the NTU «KhPI» Professor Ye.I. Sokol

Symposium Coordinator
Professor B.V. Klymenko

Contact:
phone (+380) 57 707 62 81, (+380) 50 653 49 82,
(+380) 96 987 20 85, fax: (+380) 57 707 66 01.
E-Mail: varshamova.i.s@gmail.com,
korolelgn@gmail.com